NANYANG
TECHNOLOGICAL
UNIVERSITY

DESIGN AND ANALYSIS OF OPTICAL PACKET SWITCHING SYSTEMS WITH MULTICAST CAPABILITY

HUANG QIRUI

SCHOOL OF ELECTRICAL & ELECTRONIC ENGINEERING

2011

DESIGN AND ANALYSIS OF OPTICAL PACKET SWITCHING SYSTEMS WITH MULTICAST CAPABILITY

HUANG QIRUI

2011

Design and Analysis of Optical Packet Switching Systems with Multicast Capability

Huang Qirui

School of Electrical & Electronic Engineering

A thesis submitted to the Nanyang Technological University
in fulfillment of the requirement for the degree of
Doctor of Philosophy

2011

Statement of Originality

I hereby certify that the work embodied in this thesis is the result of original research and has not been submitted for a higher degree to any other university or institution.

黄启睿 07-June-2011

Huang Qirui Date

Summary

Optical fiber communication has developed so rapidly during the last decades that it has become the backbone of today's communication systems. To take advantage of the huge bandwidth of optical fiber links, optical packet switching systems have been proposed and investigated intensively. However, most of the existing optical packet switches cannot effectively support multicast applications. To address this problem, this thesis is focused on optical multicast packet switching. Several optical multicast packet switches are proposed and their performances are studied in detail.

Motivated by the good scalability and less complexity, a wavelength-routed multicast packet switch utilizing multicast modules is proposed and investigated. The switch allows copies of a multicast packet to be made in multiple timeslots to reduce packet contention and then to be switched to desired outputs. Furthermore, a packet scheduling technique is designed for contention resolution for the proposed switch. Performance evaluation is carried out to study the feasibility of the multicast switch. It is shown that the switch can achieve an acceptable multicast packet loss probability with a few multicast modules. Despite that, since a multicast module cannot store two or more multicast packets from the same input of the switch due to wavelength collision, it has a low utilization. To eliminate this restriction, an improved scheme is then designed by modifying the multicast modules in the switch. Investigation on traffic performance shows that the improved scheme can considerably reduce packet

loss probability for the switch without adding more multicast modules. Nevertheless, this kind of switch can only handle a small proportion of multicast traffic.

To overcome the performance deterioration caused by a large volume of multicast traffic, a novel wavelength-routed multicast packet switch with a shared fiber delay lines (FDLs) buffer is then proposed. This switch allows both unicast and multicast packets to share a set of FDLs for buffering, and more importantly, a multicast packet can be replicated in multiple timeslots by multi-wavelength conversion in conjunction with the shared FDLs buffer. Traffic performance evaluation and complexity discussion show that the proposed switch can not only effectively reduce the performance deterioration caused by the increase of multicast traffic, but also exhibit much simpler configuration than other proposals for optical packet multicasting.

Furthermore, a multi-wavelength broadcast-and-select packet switch and its multicast traffic performance are comprehensively investigated. The switch enables to concurrently transmit multiple optical packets to the same output fiber of the switch and employs a multi-timeslot replication scheme to reduce the multicast packet contention. An analytical model of the switch is developed for traffic performance investigation and then verified by simulation. Results show that with the multi-timeslot replication, the switch can achieve a much better traffic performance, which is unaffected by the multicast traffic ratio. Scalability analysis reveals that the switch with more wavelengths per fiber can achieve a given packet loss probability with a lower power loss.

Acknowledgement

Four years did it take me to complete the Ph. D. studies, yet without the help and support of the following people, I would never have been here to make it at all. I would like to express my gratitude to them at the completion of this dissertation.

First of all, I would like to thank my supervisor, Professor ZHONG Wen-De for offering me the opportunity of pursuing Ph. D. degree under his supervision in the School of Electrical and Electronic Engineering at Nanyang Technological University (NTU), Singapore. During the four years' studies in NTU, Prof. Zhong continuously taught me a lot of research skills with his brilliant knowledge and profound insight in optical communications and networks, which would benefit me throughout my future career and life. Numerous discussions with Prof. Zhong inspired me with fruitful ideas and improvement for my Ph. D. research. This dissertation would not have been possible without his guidance, support and encouragement.

For over four years now I have been a member of the Network Technology Research Centre (NTRC), where I have made many friends, though some of them moved away after the completion of their contracts or assignments. I generally thank all past and present members of NTRC for being great colleagues to work with, and in particular thanks to Professor Shum Ping, Ms. Koh Lee Min, Ms. Wu Wenyu, Ms. Ma Lin, Mr. Chong Lui Tat, Mr. Poh Khoon Yong, Dr. Tang Ming, Dr. Liu Ning, Dr. Xu Zhaowen, Dr. Sun Jian, Dr. Yu Xia, Dr. Zhao Luming, Dr. Zhang Feng, Dr. Ouyang Chunmei,

Dr. Lam Quo Huy, Dr. Luo Zhengqian, Ms. Sona Hassani, Mr. Lin Rongping, Mr. Li Yihui, Mr. Zhou Junqiang, Mr. Wang Zixiong, Mr. Zhang Han, Ms. Wu Xuan, Ms. Xiong Fei and Mr. Wang Dawei for their kind support to the completion of this dissertation. I shall also acknowledge Dr. Fu Songnian for showing me the world of physical-layer research and sharing his in-depth knowledge on laboratory experiment. I appreciate the interesting discussions and friendship with every NTRC member.

It is really lucky for me to be able to know many researchers and experts who gave me countless help and assistance to my Ph. D. research. It is a pleasure to express my gratitude to Dr. Ni Yan at the Eindhoven University of Technology, who not only sent me her dissertation and papers, but also gave me so many valuable suggestions to improve my research work. Next to that, I am grateful to Prof. Ken-ichi Kitayama and Prof. Chinlon Lin for their insightful comments on some of my papers and helping me with my postdoctoral research career. I am also thankful to Prof. Yaohui Jin, Prof. Zhaohui Li, Dr. Naoya Wada, Dr. Sander Lars Jansen, Dr. Juan Jose Vegas Olmos, Dr. Giampiero Contestabile and all the other names that I cannot list exhaustively, for their selfless help to me.

Special thanks go to two of my best friends, Dr. Xia Ming at Institute of Information and Communications Technology (NICT), Japan and Dr. Hu Jia at the University of Bradford, United Kingdom, for their fruitful comments and advices on my research work. I did learn a lot from their expertise on communication networks and simulation tools. I heartily cherish the pleasant time we spent together in Wuhan, China during my Master studies.

Last, but by no means least, I am greatly indebted to my parents for their constant encouragement. Words cannot express my gratitude to my wife, Zheng Wenjing. Her love, support and all the sacrifice she has made are giving me courage and wisdom to overcome all the difficulty in my Ph. D. studies and life.

Table of Contents

List of Figures

List of Tables

List of Acronyms

Abbreviations	Full Expressions
AM	Amplitude Modulation
AOLS	All-Optical Label Switching
ASE	Amplifier Spontaneous Emission
ATM	Asynchronous Transfer Mode
AWG	Arrayed Waveguide Grating
BER	Bit Error Rate
BS	Broadcast-and-Select
CW	Continuous Wave
CWDM	Coarse Wavelength Division Multiplexing
DFB	Distributed Feed Back
DFG	Difference Frequency Generation
DPSK	Differential Phase Shift Keying
DQPSK	Differential Quadrature Phase Shift Keying
DSF	Dispersion-Shifted Fiber
DWDM	Dense Wavelength Division Multiplexing
EAM	Electro-Absorption Modulator
EDFA	Erbium-Doped Fiber Amplifier
ER	Extinction Ratio

FBG	Fiber Bragg Grating
FDL	Fiber Delay Line
FIFO	First-In-First-Out
FM	Frequency Modulation
FWC	Fixed Wavelength Converter
FWM	Four-Wave Mixing
GMPLS	Generalized Multi-Protocol Label Switching
HDTV	High Definition Television
HOL	Head-Of-Line
IQ	Input Queue
IM	Intensity Modular/Modulation
LD	Laser Diode
$LiNbO_3$	Lithium Niobate
MEMS	Micro-Electro-Mechanical System
MPLS	Multi-Protocol Label Switching
MUX	Multiplexer
MWC	Multi-Wavelength Conversion
MZI	Mach-Zehnder Interferometer
NPS	Nonlinear Polarization Switching
NRZ	Non-Return-to-Zero
OADM	Optical Add/Drop Multiplexer
OBS	Optical Burst Switching
OCDMA	Optical Code Division Multiplexing Access
OCS	Optical Circuit Switching

ODL	Optical Delay Line
O/E/O	Optic-Electronic-Optic
OFS	Optical Flow Switching
OLS	Optical Label Switching
OPA	Optical Parametric Amplifier
OPS	Optical Packet Switching
OPSN	Optical Packet Switched Network
OXC	Optical Cross Connect
OQ	Output Queue
OSNR	Optical Signal-to-Noise Ratio
OTN	Optical Transport Network
PC	Polarization Controller
PLP	Packet Loss Probability
PM	Phase Modulation
PRBS	Pseudo Random Binary Sequence
QoS	Quality of Service
RAM	Random Access Memory
ROADM	Reconfigurable Optical Add/Drop Multiplexer
RR	Round-Robin
RZ	Return-to-Zero
SDH	Synchronous Digital Hierarchy
SOA	Semiconductor Optical Amplifier
SONET	Synchronous Optical Network
SPM	Self Phase Modulation

TDM	Time Division Multiplexing
TSI	Time Slot Interchange
TST	Time-Space-Time
TW	Traveling Wave
TWC	Tunable Wavelength Converter
VOA	Variable Optical Attenuator
VoD	Video-on-Demand
VoIP	Voice-over IP
VOQ	Virtual Output Queue
WBC	Waveband Converter
WC	Wavelength Converter
WDM	Wavelength Division Multiplexing
WSS	Wavelength Selective Switch
XAM	Cross Absorption Modulation
XGM	Cross Gain Modulation
XPM	Cross Phase Modulation

Chapter 1
Introduction

1.1 Background and Motivation

Fiber optical communication has been developed so rapidly during the last decades that it has become the backbone of long-haul communication networks. Optical networking provides a good solution to various communication systems by its nature of huge bandwidth, high data rates and transparency in data formats. **Figure 1-1** illustrates the evolution of optical transport networks (OTN) [1]. In the first generation optical communication systems, the main function of optical layer was only responsible for data transmission over optical fiber links. At each network node, optical data must be converted to electronic data for routing and switching, and then reconverted back to optical domain and transmitted to next node, and these processes repeat along all the intermediate nodes [1-3]. Next to that, wavelength switching/routing functions were realized in optical networks though optical add-drop multiplexers (OADMs) and optical cross connects (OXCs). Current optical core networks deploy mostly optical circuit switching (OCS) or point-to-point wavelength channels. Generally, OCS is easy to implement and suitable for the wavelength-based services. However, since the switching granularity of OCS is of wavelength level and

the switching speed is usually at the millisecond range, it cannot support many packet-based services in the current Internet. The optical burst switching (OBS) offers smaller granularity than OCS but mainly relies on complex control mechanism in electrical domain [4]. Future backbone networks should be able to serve a layer that includes packet-based networks like the Internet, which may have a highly dynamic connection pattern with significant portion of traffic between networks nodes. The next generation optical communication networks may evolve towards the integration of packet-based services and optical networks by providing packet switching in the optical layer [5].

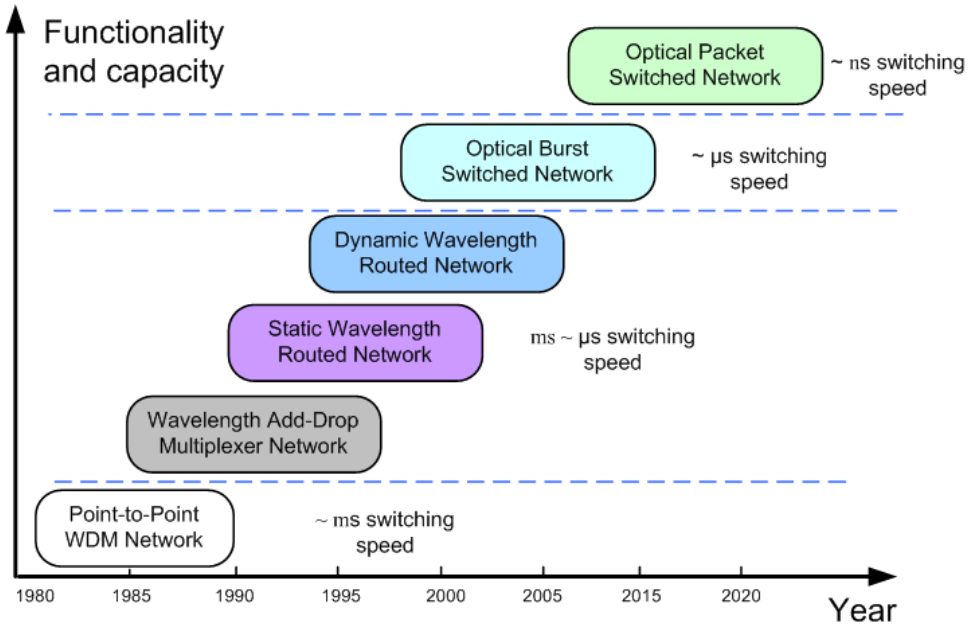

Figure 1-1: Evolution of optical transport networks

During recent years, we have witnessed the fast developments of various enabling technologies for optical transmission such as wavelength division multiplexing (WDM), erbium-doped fiber amplifier (EDFA), advanced modulation formats, optical dispersion compensator, etc [6]. With the advent of these technologies, the

transmission capacity of optical core network has been expanded up to 10 Tbit/s range over a single strand of optical fiber [7-9]. Such huge transmission capacity, however, does not bring in a great revolution for optical packet-based networks since the packet switching and routing is still performed electronically in current optical networks [10-12], while the throughput of current high-performance electronic packet switches/routers is just around 1 Tbit/s range [13]. The severe mismatch between transmission capacity and switching throughput resulted in a large bandwidth waste in optical networks. To alleviate this problem, optical packet-switched network was proposed and usually regarded as the ultimate solution for the next generation optical networks.

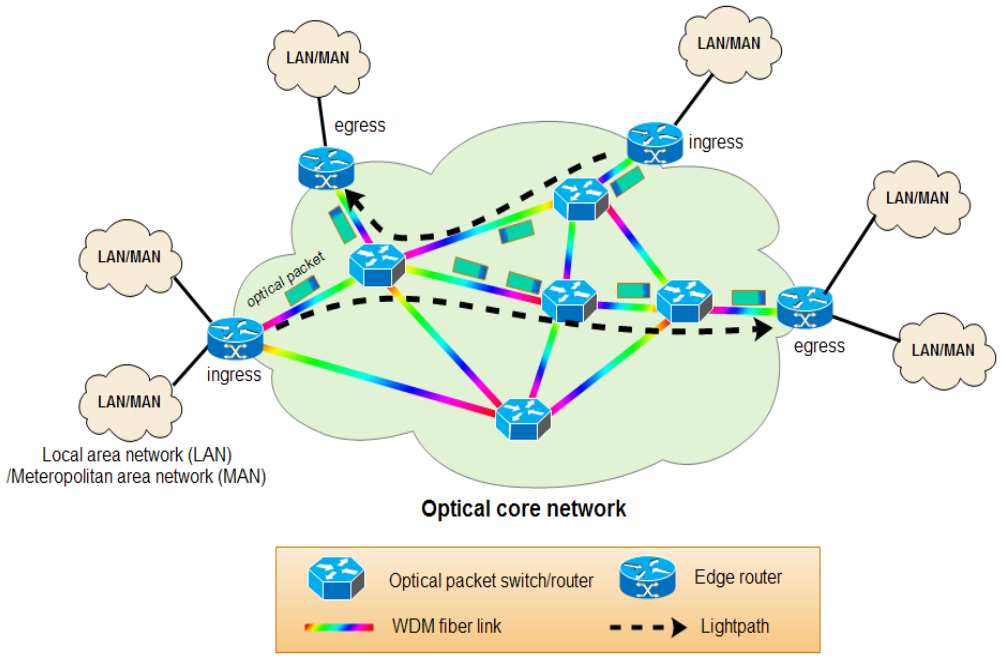

Figure 1-2: Optical packet-switched network paradigm

In an optical packet-switched network, as depicted in **Figure 1-2**, the low data-rate (several 100 Mbps) packets from source LANs/MANs would be aggregated and

converted into high data-rate (up to 40 Gbps and beyond) optical packets by the edge routers at ingress nodes for fiber transmission. Each optical packet consists of a payload and a header that is used for switching/routing decision at switching nodes (or optical packet switches/routers) along its light path. At each switching node, the incoming optical packets are processed all-optically, and the packets might be converted into different wavelengths to travel to the next node. The packet signals remain in the optical domain until they reach destination egress edge routers, where they are demultiplexed into low speed data for electronic processing and delivery at their end users via local networks. Optical packet switch is an indispensable part in optical packet-switched network. It would remove expensive O/E/O equipments, and provide ultrafast switching speed to respond to the fast changing of service flow and transparency in data rate and format, which are important characteristics for future optical networks supporting various formats of data [14-16]. However, all-optical optical packet switching is currently still immature. Electronic header processing is considered for most of the proposed optical packet switches.

With continuous development of the Internet, many multicast applications such as Internet protocol television (IPTV), video conferencing, video-on-demand, multi-party online games are rapidly growing. According to the market report of the Multimedia Research Group [17], as shown in **Figure 1-3**, the number of global IPTV subscribers will grow from 26.7 million in 2009 to 81 million in 2013, with a compound annual growth rate of 32%. In terms of service revenue, as shown in **Figure 1-4**, the global IPTV market will grow from $6.7 billion in 2009 to $19.9 billion in 2013, with a compound annual growth rate of 31%.

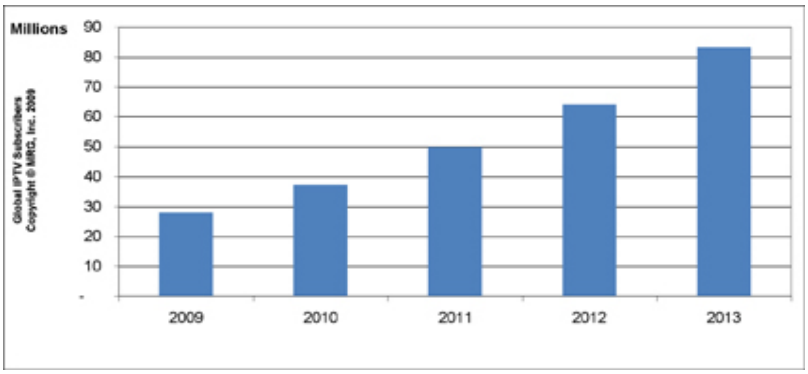

Figure 1-3: Global IPTV subscriber forecast (Source: Multimedia Research Group, Inc. May 2009)

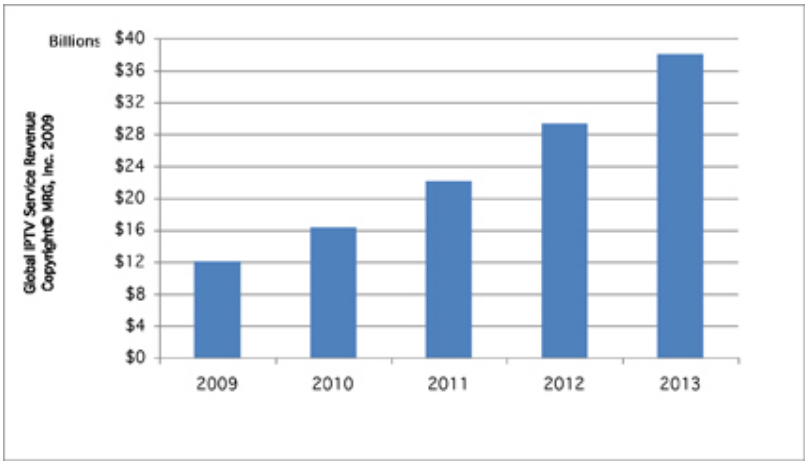

Figure 1-4: Global IPTV service revenue (Source: Multimedia Research Group, Inc. May 2009)

As the multicast traffic is growing continuously and rapidly, the challenge for the current optical core networks to deliver a large volume of multicast traffic lies in that the traditional optical packet switches/routers designed for unicast applications need a lot of network resources such as optical transmitters, optical buffers and fiber links to perform multiple unicast operations, which would incur tremendous impact on the operation cost and complexity of the networks. Therefore, there is a strong need to

integrate multicast capability into optical packet switches for effectively supporting those multicast traffic, reducing the cost and complexity of the optical core networks [18].

1.2 Objectives

Currently, most of the existing optical packet switches do not have the multicast capability, and cannot be directly extended to support multicast traffic. To integrate multicast capability into an optical packet switch, considerable efforts are required in the aspects of switch architecture design, packet scheduling techniques, physical and traffic performance modeling and analysis. The research of this thesis aims to solve the technical challenges of integrating multicast capability into an optical packet switch. The main objectives of the work are:

- To propose novel switch architectures that are capable of optical multicast packet switching with low packet loss probability, small delay, and high throughput up to terabit per second range.

- To devise suitable wavelength division multiplexed photonic packet buffers that can handle optical multicast packets efficiently. In order to implement multicast in an optical packet switch, it is extremely important to resolve packet contention. This issue can be addressed by exploiting well-designed buffer structures in conjunction with advanced packet scheduling techniques.

- To investigate both physical optical performance (such as crosstalk, bit-error-rate, and spectral characteristic) and traffic performance (such as packet loss

probability and delay) of the multicast-capable optical packet switches proposed in this project.

- To investigate ultrafast and high capacity multi-wavelength multicast-capable optical packet switches. Most of the existing optical multicast packet switches only consider packet switching with a single wavelength on each input/output fiber, which do not take advantage of the abundant wavelength resource to resolve contention. This study will investigate the performance of multi-wavelength optical multicast packet switches, providing a guideline for the practical implementation of optical multicast packet switches.

1.3 Major Contributions of the Thesis

The original contributions of this thesis are listed as follows:

- A wavelength-routed multicast packet switch utilizing multicast modules is proposed and investigated. With the help of multicast modules, the switch allows the copies of a multicast packet to be made in multiple timeslots to reduce packet contention and to be switched to desired outputs without going through any more tunable wavelength converters. In addition, a packet scheduling technique is designed for contention resolution for the switch. Simulation results show that the switch can achieve a low multicast packet loss probability with a few multicast modules. (Chapter 3)
- In order to further enhance the performance of the wavelength-routed multicast packet switch utilizing multicast modules, an improved scheme is presented by modifying the multicast modules. Results show that the improved scheme can

considerably reduce multicast packet loss probability without adding more multicast modules, thus saving the implementation cost for the switch. (Chapter 3)

- A novel wavelength-routed multicast packet switch with shared fiber delay lines (FDLs) buffer is proposed. The switch allows both unicast and multicast packets to share a set of fiber delay lines for buffering, and more importantly, a multicast packet can be replicated in multiple timeslots by means of multi-wavelength converters and the shared buffer, which owns higher efficiency in reducing multicast packet contention. A packet scheduling technique is also designed to resolve packet contention for the switch. Results show that the switch can not only effectively avoid the performance deterioration caused by the increase of multicast traffic, but also indicate an efficient and cost-effective solution to optical packet multicasting. (Chapter 4)

- A multi-wavelength broadcast-and-select packet switch is proposed. The switch enables to concurrently transmit multiple optical packets to the same output fiber of the switch. A contention resolution scheme, which is referred to as the multi-timeslot replication, is employed in the switch. Using the multi-timeslot replication, the copies of a multicast packet are allowed to be made in multiple timeslots to avoid output contention rather than in a single timeslot (Chapter 5).

- For traffic performance investigation, an analytical model of the multi-wavelength broadcast-and-select packet switch is developed and then verified by simulation. Both analytical and simulation results show that the multi-wavelength broadcast-and-select packet switch can achieve much better multicast performance than the single wavelength multicast packet switch. Moreover, the advantages of the multi-timeslot replication scheme in enhancing traffic performance for the switch are confirmed by simulation. (Chapter 5)

1.4 Organization of the Thesis

The rest of the thesis is organized as follows:

Chapter 2 reviews the key technologies of optical packet switching such as optical switching fabrics, contention resolutions, synchronization and header processing. The existing proposals for optical packet multicasting are discussed in terms of their advantages and challenges.

Chapter 3 investigates a wavelength-routed multicast packet utilizing multicast modules. The physical performance such as bit-error-rate, optical signal-to-noise-ratio, and spectral characteristic of the multicast module are examined. A packet scheduling techniques is designed to assist contention resolution for the switch. To enhance the traffic performance, a cost-effective improved scheme is further developed by modifying rather than adding multicast modules in the switch. The traffic performances of the switch before and after the modification are both evaluated and discussed.

Chapter 4 proposes a new wavelength-routed multicast packet switch with a set of fiber delay lines as shared buffer for both unicast and multicast packets. Also, a packet scheduling technique is designed to assist the operation of the proposed switch. Both traffic performance and complexity of the proposed switch are extensively investigated by comparison with other multicast switches.

Chapter 5 presents a multi-wavelength broadcast-and-select packet switch incorporating a multi-timeslot replication scheme for contention resolution. An analytical model of the switch is developed to investigate its traffic performance in

terms of packet loss probability, mean delay and normalized throughput, and then verified through computer simulation. In order to examine the advantages of the multi-timeslot replication scheme in enhancing multicast performance, the traffic performances of the switch with and without this scheme are also discussed.

Finally, Chapter 6 concludes the thesis and gives recommendations for future research.

Chapter 2
Literature Review

2.1 Introduction

In this chapter, the development of optical switching technologies is briefly reviewed, where it is shown that the next generation optical networks will be evolved towards high-speed, large-capacity, packet-switched networks. Various optical switching fabric designs, contention resolution schemes as well as major concerns of optical packet switches are summarized. As a main focus of this thesis, we then show the significance of multicast in optical layer that have not yet been widely investigated in the scope of optical packet switching. Two primary schemes of realizing optical packet multicasting are discussed and compared in terms of their advantages and challenges.

2.2 Evolution of Optical Switching Technologies

During last decades, the field of telecommunication industry has experienced tremendous growth in transmission capacity thanks to widespread deployment of

wavelength division multiplexing technologies [19] . The appearance of the EDFA greatly boosts the transmission distance of fiber link. Using optical amplifiers together with transmission line optimization and spectral efficiency enhancement, 6Tbit/s transmission has been demonstrated over 6120km using Raman amplifiers in conjunction with differential phase shift key (DPSK) modulation technology [20], and the transmission speed of up to 10Tbit/s has been recently realized [21]. The transmission capacity will no longer be the primary issue for the future optical transport networks. On the other hand, however, most of the switching and routing functions are performed electrically, that is, the optical signal would experience expensive O/E/O equipment and the switching speed of a conventional electrical packet switch is still lagging far behind the transmission capability of optical fiber link. For instance, the switching capacity of the Cisco XR 12000 Series Router is only in the range of several 100Gbit/s [22].

To eliminate expensive O/E/O equipments and at the same time to enhance the throughput, optical circuit/wavelength switching (OCS) was early proposed and deployed in optical networks, where optical data switching is realized by optical cross connect (OXC) systems [23]. However, the main drawback of OXC is the low reconfiguration speed and the coarse switching granularity (wavelength level), which makes it not be suitable for the future optical packet-based networks. Optical burst switching (OBS) was proposed to offer smaller switching granularity for optical networks [24]. Generally OBS is a bufferless technique by setting up a connection and reserving end-to-end resource during the transmission of a burst that consists of a set of packets. Although OBS can achieve higher bandwidth utilization for optical

networks than OCS, it relies on complex computation and control mechanism in electrical domain, which makes it not compatible with the nature of the Internet.

With the development of all-optical signal processing technologies and advanced devices such as optical modulators, semiconductor optical amplifiers (SOAs), ultrafast optical switches, etc, optical packet switching (OPS) has been proposed and regarded as a long-term strategy that can remove the expensive O/E/O equipment and fully exploit the huge bandwidth of optical fiber and other optical components to improve the network capacity efficiency, functionality, and utilization [25-28]. Driven by the tendency of OPS, a number of projects and test-beds of optical packet switches have been proposed and demonstrated, for example, the prototype broadcast-and-select photonic ATM switch [29], and the Keys to Optical Packet Switching (KEOPS) project [30-32], the Wavelength Switched Packet Network (WASPNET) project [33, 34], the Data And Voice Integration over DWDM (DAVID) project [35, 36], the IRIS optical packet router [37], the LAbel SwApping employing optical logic Gates in NEtwork nodes (IST-LASAGNE) project [38, 39], and recent asynchronous burst variable-length optical packet switching prototype [40].

2.3 Overview of Optical Packet Switching

Optical packet switches can be divided into two categories according to the mode of operation: slotted (synchronous) and unslotted (asynchronous) [41]. In a slotted optical packet switch, all the incoming optical packets of fixed packet length are synchronous by timeslots and the length of each timeslot is equal to the packet length plus the guard

time of adjacent packets. The switch fabric is reconfigured during the guard time of each timeslot. For an unslotted optical packet switch, optical packets do not necessarily have the same size. Incoming packets can be switched immediately without being aligned in any timeslot and the switching operation can take place at any point of time. Also, an unslotted switch can avoid scheduling error caused by the synchronization distortion due to signal impairments in transmission link. That is, it has the advantage of flexibility. However, they require complex scheduling technique for avoiding packet contention compared with slotted switches.

Figure 2-1 shows the schematic diagram of a general optical packet switch with time slotted operation. At each input of the switch, a small portion of incoming optical signal is tapped and directed to the switch control units (synchronization control, switch control and header rewriting). The key divisions of an optical packet switch include: switching fabric, contention resolution, packet header processor, and packet synchronizer [28]. Until now, a number of technologies have been proposed to address various issues in these divisions of optical packet switches.

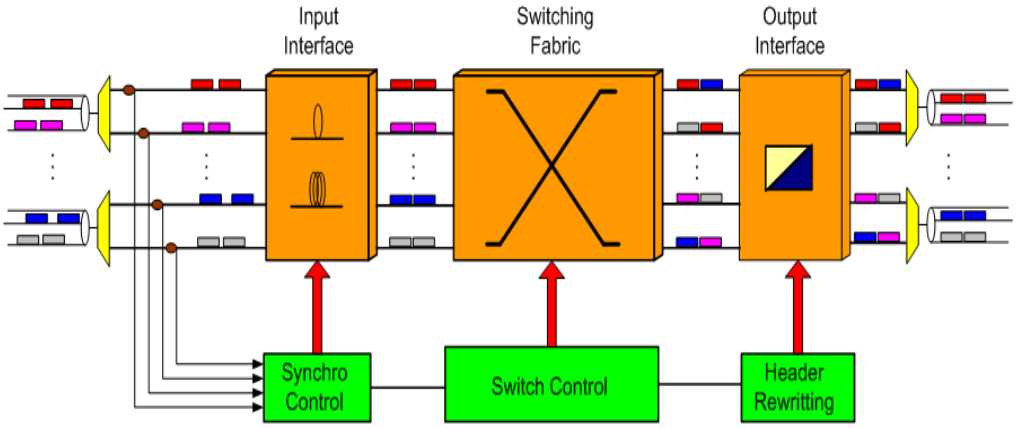

Figure 2-1: Schematic of a general optical packet switch with time slotted operation

2.3.1 Optical Switching Fabrics

The switching fabric is at the heart of an optical packet switch, because the choice of switching fabric weights greatly on the performance of an optical packet switch. The most important parameter of a switching fabric is its reconfiguration speed of switching operation. To match the high transmission speed of optical fiber link, an optical packet switch requires a fast reconfiguration speed in the order of nanosecond [27]. However, switching speeds of commercially available optical switches such as micro-electrical mechanical switches (MEMS) are just in the order of milliseconds, which are not suitable for OPS. Other important characteristics of a switching fabric include the ability of system upgrading, easy implementation, environmental reliability and cost-effectiveness. Currently, semiconductor optical amplifiers (SOAs) and electro-optic lithium Niobate ($LiNbO_3$) switches are two promising candidates for high-speed optical switching fabric. The SOAs have switching time in the order of a few nanoseconds and can be integrated on a chip [42]. In addition, they may be used for compensating for power loss of optical signal by virtue of their inherent amplification. One limitation of SOA is the amplified spontaneous emission (ASE) noise added to the signal. Electro-optic $LiNbO_3$ switches may offer subnanosecond switching time, while only medium-scale integration is possible for $LiNbO_3$ switches due to the relatively high insertion loss. Up to now, the most popular optical switching fabrics include the broadcast-and-select architecture, space switching architecture and wavelength-routed architecture.

The broadcast-and-select architecture has been extensively employed in optical packet switches thanks to its easy implementation and excellent traffic performance [29-32, 43, 44]. **Figure 2-2** shows a prototype broadcast-and-select photonic ATM switch

reported in [29]. It is composed of a star coupler and a WDM buffer placed at each output. The WDM buffer consists of a traveling-type timeslot selector and a wavelength-channel selector. In this switch, all the input optical signals are broadcasted to all the outputs by a star coupler, and then the WDM buffer placed at each output will select desired signals in appropriate timeslots by adjusting the optical gates in the timeslot selector and wavelength-channel selector. The studies in [29] have demonstrated stable operation and high throughput of this photonic ATM switch. However, this switch suffers from high power loss that is proportional to both of the switch size and number of FDLs used in each WDM buffer.

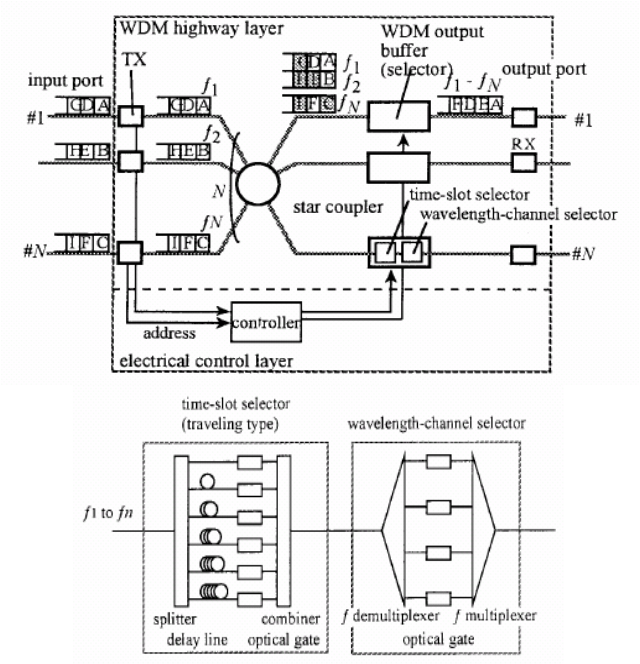

Figure 2-2: Architecture of the broadcast-and-select type photonic ATM switch (left) and its WDM output buffer (right) [29]

Space switching architecture has also been widely used in optical packet switches [45-49]. **Figure 2-3** shows the configuration of the Staggering switch in [49]. It

consists of a control unit, an $N\times M$ nonblocking space switch, an $M\times N$ space switch, and a set of M delay lines whose length vary from 0 to (M-1)T, where T is the duration of one timeslot. The $N\times M$ nonblocking space switch is used to provide input optical packets with access to appropriate delay lines such that no two or more packets arrive at the same input port of the $M\times N$ space switch concurrently, thereby packet contention can be avoided. Then, the $M\times N$ space switch will route the packets to their desired outputs. In this switch, the packets coming from the same input port may leave from their output ports in the reverse order, since they could be assigned to different delay lines. Ordered transmission can also be achieved by proper packet scheduling in the control unit. The main drawback of this switch architecture is that the packet scheduling for contention resolution would become too complicated to handle large switch size or high input line rate [49].

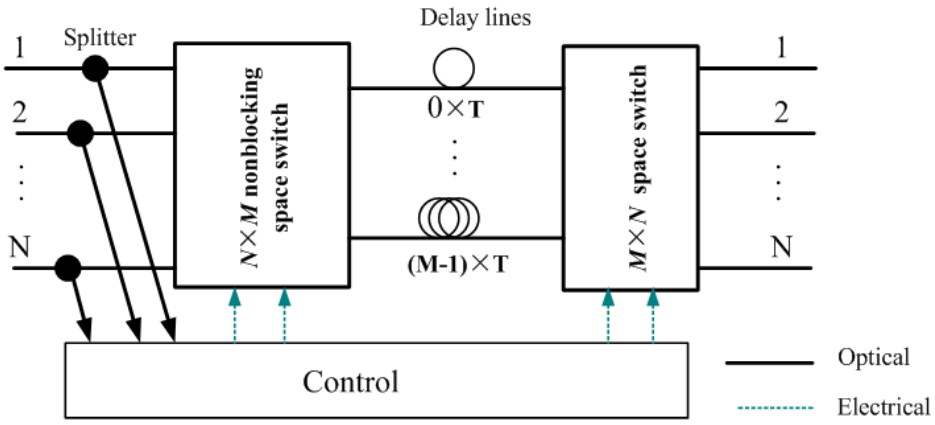

Figure 2-3: Configuration of the staggering switch [49]

Wavelength routing architecture provides an effective and scalable solution to the implementation of optical packet switches with large scalability [34, 50-58]. Refs [50, 51] proposed an input-buffered photonic packet switch using wavelength

routing-based buffer, as shown in **Figure 2-4**. It is composed of a scheduling section, a switching section and an electronical controller. The scheduling section consists of a set of N tunable wavelength converters (TWCs), two $K \times K$ arrayed wavelength gratings (AWGs) that are interconnected by a set of FDLs of different delay time. In the scheduling section, the incoming optical packets are given corresponding wavelengths by the TWCs so that they will be routed to the appropriate FDLs. It is interesting to note that the packet arriving at the *i*th input of the scheduling section will leave from the *i*th output of the scheduling section after it receives certain delay time according to its wavelength. In the switching section, the packets will be routed to their desired outputs by another set of TWCs in conjunction of the subsequent AWG. The novelty of this switch is that all the input packets can share the same wavelength routing-based buffer, which can also work as the output buffer by cooperating with an optical space switch to achieve an output-buffer photonic packet switch as illustrated in **Figure 2-5**.

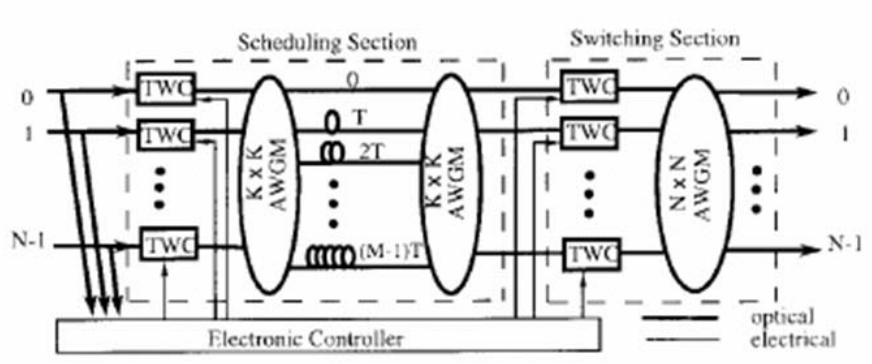

Figure 2-4: Schematic of an input-buffer photonic packet switch using the wavelength routing-based packet buffer [50]

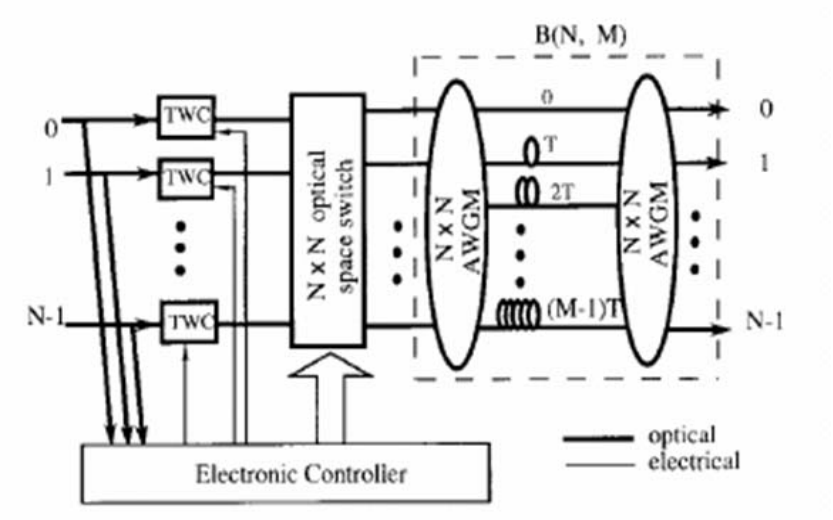

Figure 2-5: Schematic of an output-buffer photonic packet switch using the wavelength routing-based packet buffer [50]

2.3.2 Contention Resolutions

In a packet switch, contentions may occur when two or more packets from different inputs are destined for the same output simultaneously, which brings negative impact on the traffic performance of the switch as this might result in massive packet loss and latency, resulting in a low throughput. The contention resolution strategy must be carefully designed in accordance with the traffic pattern, switch architecture, and the type of buffer. In an electrical packet switch, packet contention can be resolved by using a store-and-forward scheme, by which the contending packets are kept in an electronic random access memory (RAM) until the desired output port becomes available. In an optical packet switch, however, due to the lack of mature optical RAM, the contention resolution is a major handicap for realizing all-optical packet switching. To address this issue, an optical packet switch can exploit time, space, and wavelength domains or a combination of them to avoid packet contention [28, 59-64].

In the time domain, packet contention in an optical packet switch can be avoided by using optical fiber delay lines (FDLs), which are usually regarded as the optical buffers, to provide different time delays for the contending packets so that they could be switched to the desired outputs asynchronously. The optical buffers can be basically categorized into two groups according to their operation [65]: traveling-type and recirculating-type. An typical traveling-type optical buffer, as shown in **Figure 2-6**, consists of an optical switch and a set of optical fiber delay lines whose lengths are equal to the multiple of one packet duration, and an optical coupler. A number of traveling-type optical buffers have been reported in [29, 50, 66-71]. Ref. [50] proposed an wavelength routing-based optical packet buffer based on the FDLs and AWGs, which could provide shared-buffering for multiple wavelengths packets. The main advantage of traveling-type optical buffer is that it can be easily operated in an optical packet switching system.

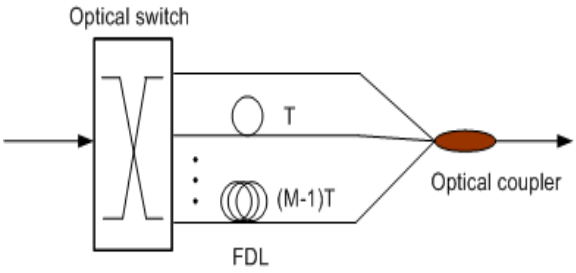

Figure 2-6: Traveling-type optical buffer based on FDLs

An recirculating-type optical buffer is generally composed of an optical coupler, optical amplifier and a fiber delay line forming a loop with one circulation time that is equal to one packet duration [65]. As shown in **Figure 2-7**, the optical amplifier is used to compensate for the transmission loss during each circulation. The

recirculating-type optical buffer can provide a buffering time equalling to the multiple of a packet duration with a single fiber delay line by circulating the optical packet in the delay line loop. Because of this advantage, the recirculating-type optical buffers have been attracting much attention of research [50, 51, 72-76]. However, the ASE noise induced by the optical amplifier will accumulate and substantially degrade the optical signal, which would limit the number of circulations of the optical signal in the buffer [77].

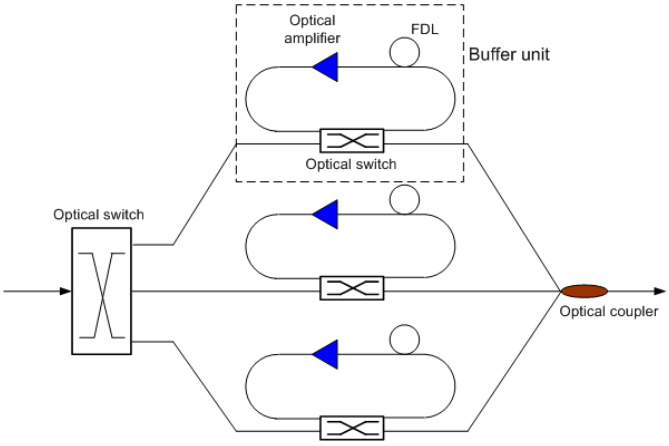

Figure 2-7: Recirculating-type optical buffer

The optical buffers based on FDLs are simple and widely available contention resolution for optical packet switching. However, since the FDLs are first-in-first-out (FIFO) queues with fixed delays, they still have many short-comings compared with the electronic RAM. Firstly, the delay time offered by the FDLs is pre-determined, hence it is impossible to retrieve a packet before a fixed duration of time. Secondly, a quite long optical medium or fiber may be required for providing a sufficient delay time to avoid collision for the contending packets, which also increases extra power penalty and system dimension [65]. In addition, the optical packet switch that employs FDLs for buffering strategy at the input side often suffers from the head-of-line (HOL)

blocking. Although output buffering strategy might avoid HOL blocking problem, it is quite difficult to implement output buffering in optical packet switch.

In space domain, deflection routing is often used to provide separate routes for the optical packets to avoid output contention [78-81]. In this approach, some optical packets may take long routes to their destined outputs, resulting in a long latency and signal quality degradation. Hence, this approach is only suitable for the switching nodes that have limited buffering capacity.

In addition, an optical packet switch can also utilize wavelength domain to resolve the problem of packet contention [82-87]. That is, two or more optical packets destined for the same output fiber of an optical packet switch can be transmitted simultaneously on different wavelengths without collision. In optical packet switches, wavelength converters are usually used to assign wavelengths to the contending packets. **Figure 2-8** illustrates the contention resolution without and with wavelength converters. Two optical packets, P1 and P2 destined for the same outlet, arrive simultaneously and have the same wavelength λ1. Without wavelength converters, a fiber delay line is required to store one of packets, whereas with converters, no fiber delay line is needed since one packet could be converted to another wavelength λ2. Besides, wavelength converters can also be used for wavelength routing or switching in conjunction with AWGs. Ref. [88] provided detailed discussion on various technologies for all-optical wavelength conversion. However, as wavelength converters are technologically complex and rather expensive, sharing of wavelength converters is more attractive [89].

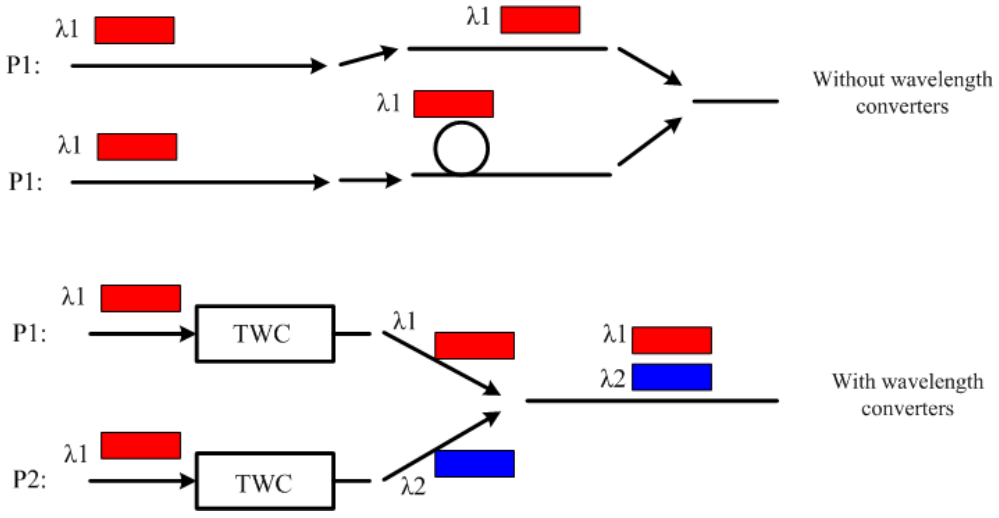

Figure 2-8: Illustration of contention resolution without and with wavelength converters

Depending on where packets are buffered or queued, packet switches are classified into three different categories including output-queued (OQ), input-queued (IQ), and combined input/output-queued switch architectures [90]. For an $N \times N$ output-queued switch, the switching speed is required to be N times data rate of input/output link, which is very difficult to be implemented in optics as the switching speed needs to be fast enough (a few nanoseconds) to accommodate the high data-rate of fiber links. In order to build large-scale optical packet switches, one approach is to employ input-queued architecture with advanced scheduling techniques [91].

The purpose of packet scheduling is to prevent multiple packets from contending the same output and to find an appropriate timeslot for each packet to be delivered. For a pure input-queued switch with first-in-first-out (FIFO) buffers, there is a head-of-line (HOL) blocking problem [90]. This happens when some of packets in the input queue are prevented from being delivering to a free output because of the packet ahead of it

in the same queue [90], which would limit the traffic performance of the switch to a great extent. Virtual output-queue (VOQ) schemes are able to overcome this problem: the input queues are organized into a set of virtual queues that store and forward the packets to the desired output of the switch [92-94]. Until now, many packet scheduling algorithms for optical packet switches have been proposed and widely studied [50, 51, 95, 96], most of which are mainly developed for unicast packets. Some multicast scheduling algorithms based on fanout splitting principle have been proposed in electronic packet switches, such as the TATRA algorithm [97], WBA [98], and integrated scheduling of unicast and multicast traffic [99], while these scheduling algorithms are too complex to be implemented in optics. An interesting multicast scheduling based on load-balanced operation in optical switch was reported recently [100]. It was showed that such load-balanced optical switch might achieve close-to-100% throughput, but it is only applicable in ring network.

2.3.3 Main Concerns in Optical Packet Switches

Since packet synchronization can greatly simplify the operation of packet contention resolution, header processing, and packet switching, most of the optical packet switches reported in the literature are synchronous. In synchronous optical packet switch, all incoming packet are required to be synchronized before they are switched in the switching fabric. Although there have been a number of testbeds and demonstrations of optical packet switching, optical packet synchronization is one of the concerns that restrict the commercial deployment of optical packet switches in optical transport networks. Ref. [101] proposed a general optical packet synchronizer that consists of a packet start recognizer and programmable delay line module. Once a

packet arrival is detected by the recognizer, the programmable delay line module will function to assign appropriate delay line for the packet to be synchronized. The KEOPS project in [32] utilized a bidimensional structure to realize the optical synchronizer as shown in **Figure 2-9**, which is composed of a number of stages including passive couplers, optically gated calibrated fiber delay lines, and electronics controller. A delay time with 3.2 ns resolution was achieved by implementing three stages of four delay lines [102]. In addition, an optical packet synchronizer using wavelength and space switching with a time resolution of 16 ns was demonstrated in [103], and finer time delay resolution could be achieved in this synchronizer by increasing the number of wavelengths without any significant increase in loss or crosstalk. Recently, a variable-length optical packet synchronizer based on SOA-based switches with fiber delays was reported, by which asynchronously arriving packets could be aligned to a local clock with a resolution of 853 ps and tuning range of 12.8 ns [104]. The progress on slow light effect also inspires an interesting method to achieve optical packet synchronization and buffering for OPS systems [105].

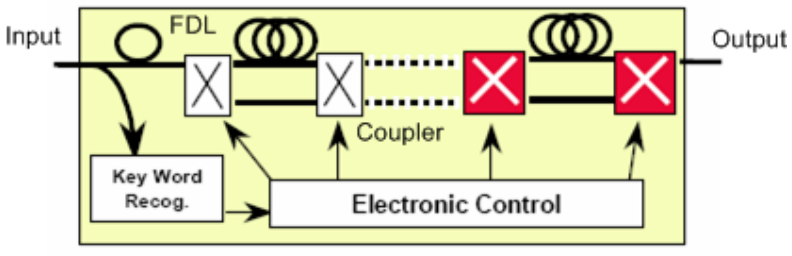

Figure 2-9: Optical packet synchronizer in KEOPS project [32]

Another challenge in optical packet switches is the all-optical packet header processing [106]. Optical packet header contains the information that is necessary for the switch to perform routing and switching functions to forward packets towards their

destinations. Additional information in the header may assist in traffic engineering and management in the network, though there is an overhead bandwidth that is required to transmit and process the packet headers. In an OPS system, the header of an optical packet should be well-designed such that it could be easily detached and attached from the optical data payload. Hence, the format of optical packet header is a crucial factor in determining the optical switch architecture [61]. **Figure 2-10** illustrates the definition of packet format used in the KEOPS project [32]. The packet duration is fixed at 1.646 μs, including 1.35μs payload, two guard time segments each of about 30 ns, and 180 ns header.

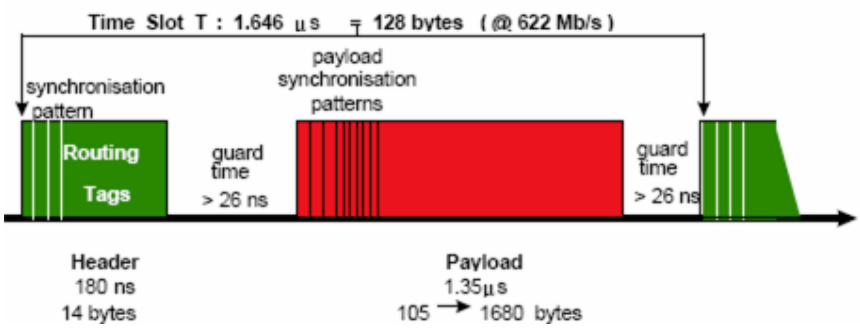

Figure 2-10: Packet format in KEOPS project [32]

Optical header processing includes header detachment and attachment using optical technology [61]. Major techniques for header processing in OPS can be categorized into:

1) Time domain technique. In this technique, header and payload of an optical packet are separated by a guard time and led by synchronization bits to facilitate clock recovery. The packet header replacement is to remove the old header and to attach a new one to the payload by time switching. Since the line rates for optical header can be much lower than those for optical payload, simple electronic circuit technology can

be applied to process the header and look up the routing table upon reading the header content using a burst-mode optoelectronic receiver [102, 107].

2) Subcarrier multiplexing (SCM) technique. In this technique, the header is carried by the subcarrier of the data payload on the baseband [108]. The header detachment can be easily realized by using an optical filter (such as an FBG) to extract the subcarrier, and then header rewriting can be achieved by replacing the old header with a new header on the subcarrier. A number of SCM techniques including double-sideband optical header technique [109-111], carrier suppression method [112], and single-side optical labeling with carrier suppression [113], have been widely studied.

3) Wavelength multiplexing technique. This technique uses a separate wavelength or multiple wavelength channels to provide a signaling channel for optical headers, which makes the header extraction and rewriting extremely simple to be implemented in optics [114, 115]. On the other hand, the accuracy of this technique is determined by the relative accumulated dispersion between the header and data payload. Furthermore, if there are multiple payloads launched at the same time, the wavelengths of headers may contend with each other.

4) Optical code-division multiple-access (O-CDMA) technique. Similar to the CDMA technique, O-CDMA employs a set of optical codes in the encoder for encoding optical header, which can be identified by a decoder with matching optical codes. Compared with the time domain header processing technique, the O-CDMA technique consumes less time in identifying optical header contents, which can help reduce the latency in optical packet switches. O-CDMA header encoding/encoding can be realized by utilizing parallel FBGs or compact AWGs [116-119]. 1.28 Tbit/s variable-length optical packet switching technology with 160 Gbit/s TDM data

payload on eight wavelength channels and O-CDMA headers has been experimentally demonstrated [120].

5) Orthogonal modulation technique. This technique employs orthogonal modulation formats for the header and the data, respectively [121]. For example, ON-OFF keying intensity modulated payloads with frequency shifted keying (FSK) [122], and ON-OFF keying intensity modulated headers with return-to-zero (RZ) differential phase-shift keying (DPSK) modulated payload headers [123], have been demonstrated. Other orthogonal modulation schemes include polarization modulations [124, 125], wavelength-shifted keying for plus position modulation [126] and embedded DPSK header in amplitude shift keying (ASK) payload [127].

2.4 Optical Packet Multicasting

Although optical packet switching was proposed two decades ago with the goal of eliminating expensive O/E/O conversion and offering transparency in data format, protocol, and line rate, most of the existing optical packet switches are only capable of unicast switching. With rapid deployment of the Internet, many multicast applications such as IPTV, HDTV, video conferencing, and VoD are continuously spreading all over the world [18, 128, 129]. To deliver a large volume of multicast traffic in optical transport networks, traditional optical packet switches/routers designed for unicast applications need a lot of network equipments such as optical transmitters, optical buffers and fiber interconnections to achieve multicasting, which incurs huge cost and operation complexity for the optical networks. To effectively support the increasing

multicast applications, it is extremely important to incorporate multicast capability into optical packet switches. Until now, optical multicast packet switches are mainly realized by two major schemes [130]: light splitting and multi-wavelength conversion. Various architecture designs, key technologies as well as challenges of these two schemes are reviewed in this section.

2.4.1 Light Splitting

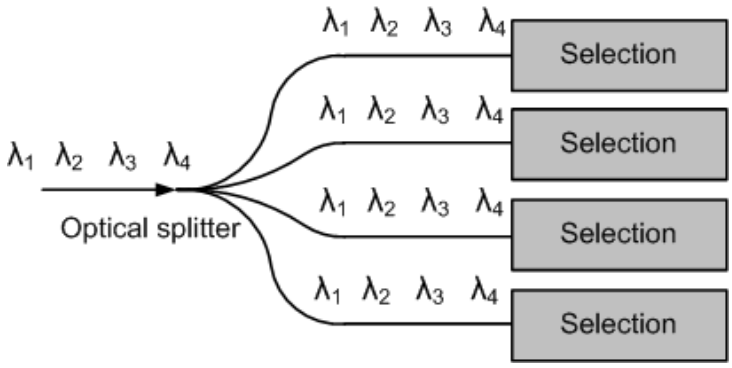

Figure 2-11: Light splitting scheme for packet multicasting

Optical packet multicast based on light splitting scheme can be realized by passive and active approaches. Several optical multicast packet switches based on passive light splitting have been proposed and studied in [29, 32, 131-134]. In the passive approach, as illustrated in **Figure 2-11**, the input optical signals are split into a group of copies by an optical coupler or splitter, and then coupled onto all the outputs of the switch; a fast wavelength selector is placed at each output to select the desire copy. A typical optical multicast packet switch based on passive light splitting is shown in **Figure 2-11**. The switch relies on the use of the broadcast-and-select architecture, wavelength

encoding and fast wavelength selector to achieve packet switching, and on the combination of optical fiber delay lines and fast optical gate switches to perform packet buffering. At the inputs of the switch, each incoming optical packet is assigned a corresponding wavelength to identify its input by a wavelength converter, and then fed into a set of fiber delay lines (FDLs) through a $1 \times K$ coupler for buffering. Each packet after being buffered by FDLs is broadcast by optical splitters to the subsequent optical gate switches, which are used for selecting the packets in appropriate timeslots and feeding them into the wavelength selectors at each output. The wavelength selectors will select desired packets according to their destined outputs. The advantages of the switch are easy implementation and excellent throughput. However, it requires a large number of optical gate switches and suffers from a high power loss due to the use of a lot of optical splitters or couplers. Thus the switches based on passive light splitting scheme have limited scalability. Recently, an interesting multicast-capable architecture based on wavelength-striped and light splitting technologies was demonstrated [135, 136], the results showed that the architecture could reduce hardware cost with a trade-off of increasing routing logic complexity.

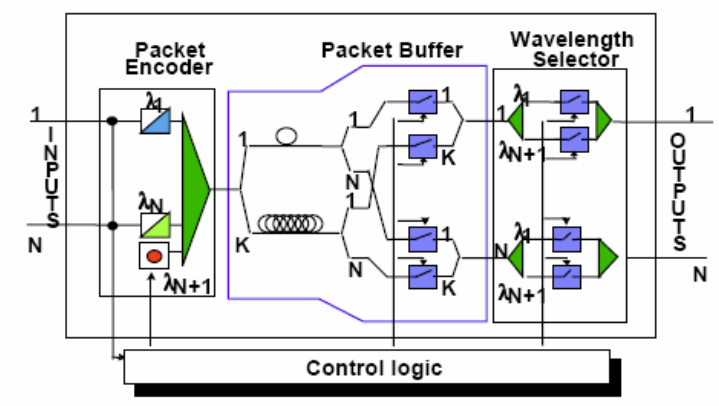

Figure 2-12: Optical multicast packet switch based on passive light splitting [32]

Optical packet multicasting without excess splitting loss can be realized using the active vertical coupler (AVC)-based optical switch matrix [75, 137-140]. The structure of optical switch matrix is shown in **Figure 2-13**. It consists of interconnected optical switch cells based on AVC. Each cell connects two passive waveguides that intersect each other perpendicularly. The principle of the switch is described as follows. In the ON state, carriers are injected into the selected switch cell, which would results in the reduction of refractive index of the active upper waveguide to match that of the lower waveguide to allow coupling. The input signal coupled up into the active layer is amplified, and reflected by a total internal reflection mirror cutting diagonally across the waveguide crosspoint, then coupled down to the output passive waveguide. In the OFF state, the input signal will pass through the cell along the input passive waveguide to the next cell.

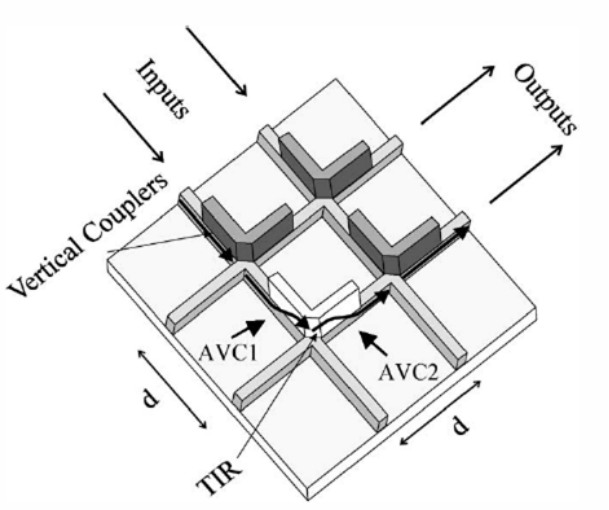

Figure 2-13: Structure of optical switch matrix based on active vertical coupler [140]

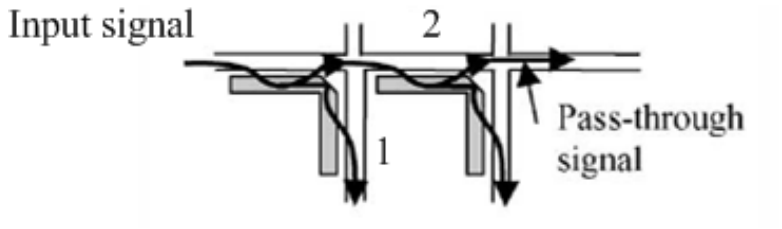

Figure 2-14: Optical multicast based on active vertical coupler (AVC) [140]

Lossless optical multicast can be realized by appropriately adjusting the injected carrier density rather than the perfect coupled point as illustrated in **Figure 2-14**, where the phase-matching condition is removed such that the input signal would be coupled onto waveguides 1 and 2, thereby a 1-to-2 optical multicast is achieved. However, this technology is still immature. Only small-scale optical multicast can be realized with current technology.

2.4.2 Multi-wavelength Conversion

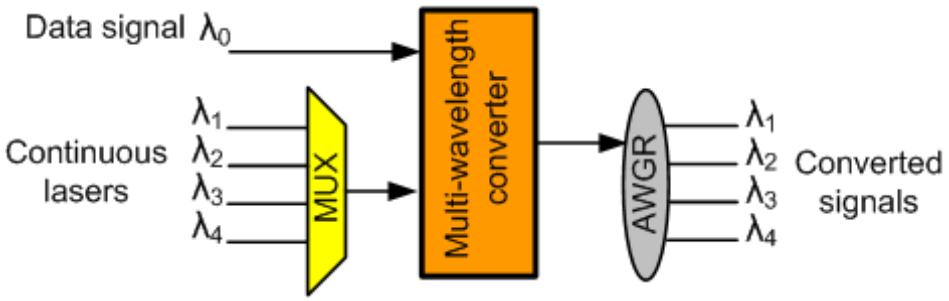

Figure 2-15: Multi-wavelength conversion scheme for packet multicasting

Another scheme to realize optical packet multicast is through multi-wavelength conversion, as shown in **Figure 2-15**, where an input optical signal is fed into a multi-wavelength converter with a group of continuous wave (CW) lasers. The optical

signal is replicated into multiple copies of different wavelengths simultaneously, and then routed to desired outputs by the subsequent AWG according to their wavelengths. Multi-wavelength conversion has enormous potential of transparent provisioning of data rates and formats, and more importantly, it can combine with wavelength switching and buffering technologies to achieve wavelength-routed optical multicast packet switches with less power loss and better scalability. Thus it has attracted much research interest in recent years. According to implementation mechanism, there are several types of multi-wavelength conversion technologies: four-wave mixing (FWM), cross gain modulation (XGM), cross absorption modulation (XAM), nonlinear polarization switching (NPS), and cross phase modulation (XPM).

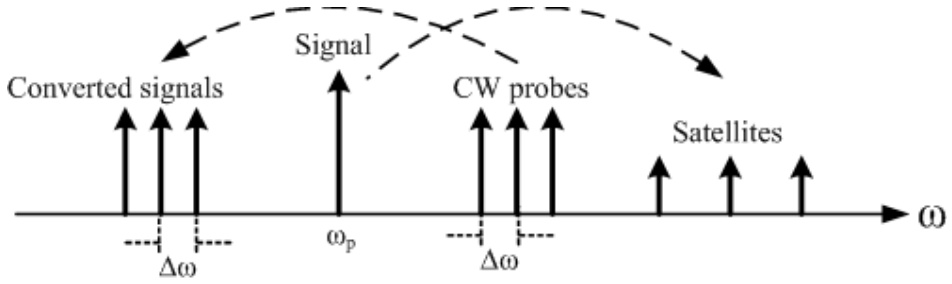

Figure 2-16: Multi-wavelength conversion based on first-order FWM

Multi-wavelength conversion by FWM can be realized if multiple probes are injected together with the data modulated signal into an SOA or a high-nonlinearity fiber [141-147]. According to the principle of first-order FWM, one-to-many multi-wavelength conversion can be achieved by placing the data modulated signal on the pump wavelength and using CW lasers as probe wavelengths [148], as illustrated in **Figure 2-16**. One-to-five multi-wavelength converter based on FWM in an SOA has been demonstrated at 10 Gbit/s with one input NRZ signal and three probes [145]. Recently, 40 Gbit/s multifunction optical format conversion with wavelength multicast

capability using nondegenerate FWM in an SOA was reported in [142]. Although the use of multiple probes in this approach can improve the conversion efficiency response of the SOA, the result of such multi-wavelength conversion relies on the alignment of input wavelengths and the phase matching conditions, which are difficult to achieve. Another FWM-based multi-wavelength converter was implemented using a dispersion-shifted fiber (DSF), but this method does not have much flexibility in wavelength [141, 144]. FWM effects in SOAs and nonlinear fibers have a number of distinct differences due to the different attributes of the physical media. To minimize the in-band crosstalk due to the high-order FWM products, the wavelengths, power levels and polarizations of both signal and pumps have to be properly adjusted. Recently, a scalable multicasting based on fiber optical parametric amplifier (FOPA) was reported to support 1-to-40 error free wavelength multicasting with 1-pump [149], and it could achieve 320-Gb/s multicasting in a single channel using a two-pump parametric amplifier [150].

The XGM in SOA is a practical way to achieve multi-wavelength conversion because of its characteristics of compactness, stability, and polarization independence [151-156]. As shown in **Figure 2-17** [155], when the input data signal is launched along with multiple continuous wave (CW) pumps into an SOA, the inverse pattern of input data would be achieved at all wavelengths of the CW pumps due to the XGM effect in SOA. After that, an optical filter or AWG is required to distinguish the converted signals from the input signal. However, this technique suffers from poor extinction ratio and waveform distortion related to the gain dynamics of SOA. In addition, it requires rather high input signal power to achieve gain saturation in an SOA. The maximum operational bit rate might become a bottleneck for this technique

due to the relatively long carrier recovery time of SOA [84], though lengthening the SOA chip could provide a temporary solution.

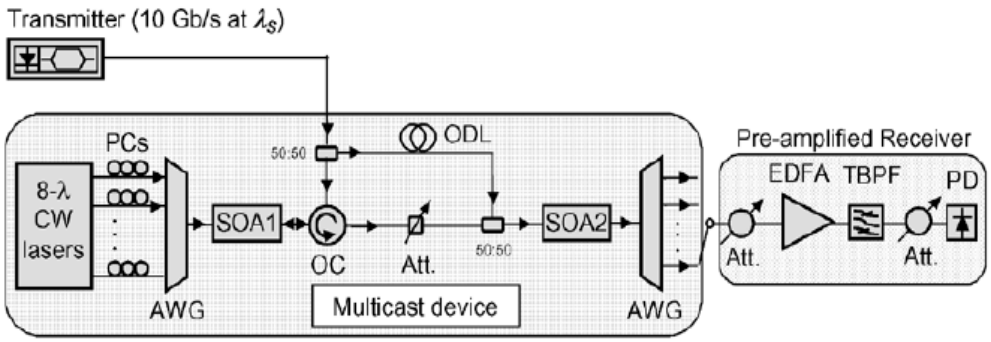

Figure 2-17: Multi-wavelength conversion based on XGM in SOA [156]

Multi-wavelength conversion can also be realized in an electroabsorption modulator (EAM) through cross absorption modulation (XAM). Several schemes of MWC for RZ signal at 40 Gbit/s based on XAM in a single EAM have been demonstrated [157-160]. XAM-based multi-wavelength conversion offers advantages such as compactness, integration, environmental stability, and stable conversion output. However, this scheme suffers from large insertion loss. A high input power of more than 10 dBm is generally required. Furthermore, insufficient XAM also results in low extinction ratio (ER) of converted signals, thus limiting low conversion efficiency.

Nonlinear polarization switching (NPS) in SOA is an alternative for high-speed multi-wavelength conversion [161-165]. This technology requires a single SOA, polarization-controlled input and CW pumps, and a polarization-controlled output to a polarization beam splitter (PBS). A data modulated signal produces a change of the effective refraction indices of the two orthogonal modes (transverse electric and transverse magnetic modes) in the SOA, such that these two modes experience a net

phase difference and then interfere with each other in the PBS. One-to-four MWC for NRZ data at 40 Gbit/s was achieved by NPS utilizing an SOA with high gain figure and fast saturated gain recovery time [165].

Cross phase modulation (XPM) in an SOA-based interferometer or optical fiber is a promising candidature for multi-wavelength conversion [166-175], by which the converted signal quality can be significantly improved. The Mach-Zehnder interferometer (MZI) structure is often used among all the interferometric structure, since it can be easily integrated by using optical waveguide, leading to a compact device for flexible applications. Multi-wavelength conversion based on the XPM in SOA-MZI has been explored and optimized by many schemes [170-175]. With an SOA-MZI, both inverted and non-inverted conversion can be achieved by means of XPM. However, there are also some limitations of this technology: a) the signal rate is limited due to the long gain recovery time of SOA; b) the maximum number of converted wavelengths is expected to be restricted by the narrow SOA gain spectrum; c) the efficiency of multi-wavelength conversion based on XPM in SOA extremely relies on the input signal power and the injection current of the SOA, which might be quite high to provide sufficient modulation depth of XPM. On the other hand, the XPM based on high-nonlinear fiber has potential for multi-wavelength conversion, and it can offer more bit-rate independent conversion. One-to-eight wavelength conversion was realized at the bite rate of 40Gbit/s [167]. And more than 20 channels of multi-wavelength conversion has been demonstrated with error-free operation at 10 Gbit/s [166]. However, due to the requirement of quite long nonlinear fiber, this technology is difficult to be integrated in comparison with SOA-based XPM. **Table**

2-1 summarizes the properties of multi-wavelength conversion technologies discussed in this section.

Table 2.1: Comparison of various multi-wavelength conversion techniques (IM: intensity modulation; PM: phase modulation; FM: frequency modulation)

Principle	Data format	Operation speed	Efficiency	ER improvement	Flexibility
FWM	IM, PM, FM	~Tb/s	low	~ 0 dB	non-inverted
XGM	IM	≤10G/s	limited	< 0 dB	inverted
XAM	IM	≤40G/s	low	< 0 dB	both
NPS	IM	≤40G/s	low	~ 0 dB	both
XPM	IM	≤40G/s	high	> 0 dB	both

2.5 Summary

This chapter first gave an overview of research in optical packet switching. Various architectures, key technologies as well as challenges for implementing optical packet synchronization, optical header processing, switching fabric, and contention resolution in optical packet switches were reviewed. As a special focus of this chapter, recent progress in optical packet multicasting technologies was summarized. Light splitting and multi-wavelength conversion are two primary schemes of implementing optical packet multicasting. The former is a simple way but requires a large number of optical components to perform the broadcast-and-select processing, which has much high power loss and implementation cost, thus limiting the scalability of switching systems. The latter achieves optical multicasting by converting an optical packet into multiple copies with different wavelengths and using a wavelength router to route them to desired outputs, which can achieve large scalability and is compatible with wavelength-routed optical networks. Various techniques of realizing multi-wavelength conversion via different mechanism in materials or optical components were discussed in terms of their advantages and challenges.

Chapter 3
Wavelength-Routed Multicast Packet Switch Utilizing Multicast Modules

3.1 Introduction

Wavelength conversion is a key functionality for network interoperability and scalability in future optical WDM networks [88]. It can be used to route wavelength channels or optical packets, resolve packets contention, and enable dynamic wavelength assignment for optical networks [176-178]. Currently, wavelength converters at 10~80 Gbit/s for various data formats are available [179-183], and successful experimental demonstration of 320 Gbit/s all-optical conversions have been reported recently [184-187]. Compared with other optical packet switches using crossbar space switches or Benes switches, wavelength-routed optical packet switches based on wavelength conversion technologies have been intensively explored as a potential candidate for OPS for years thanks to their nature of large scalability and small power loss as well as perfect compatibility with current WDM optical networks [28, 34, 50, 51, 188].

Most of wavelength-routed optical packet switches, however, are only capable of unicast switching. In order to integrate multicasting function in the wavelength-routed packet switches, one-to-many multi-wavelength conversion (MWC) has been proposed in recent years to realize wavelength-routed multicast packet switches [173, 174, 189, 190]. Compared with conventional OEO converters and single wavelength converters, a multi-wavelength converter can be realized in a single device, saving both implementation and operational costs and reducing system complexity [191]. Furthermore, multi-wavelength conversion provides more independency on bit rate, protocol, modulation formant, and many new applications [154]. However, in those existing multi-wavelength conversion based optical packet switches, the copies of a multicast are considered to be made only in a single timeslot, which is not efficient in solving packet collision.

In this chapter, an optical wavelength-routed multicast packet switch utilizing multicast modules is proposed [191-193]. In a multicast module, the copies of a multicast packet are allowed to be made in multiple timeslots to reduce packet contention. Furthermore, in order to enhance the packet loss performance of the switch, a cost-effective scheme is subsequently presented by modifying the multicast modules rather than adding more multicast modules [194]. The rest of this chapter is organized as follows. Section 3.2 describes the architecture and operation of the proposed wavelength-routed multicast packet switch utilizing multicast modules. The principle of the multicast module is explained in Section 3.3. In Section 3.4, a packet scheduling technique is designed to resolve output contention for both of unicast and multicast packets. Section 3.5 investigates the physical performance of the multicast module. The traffic performance evaluation of the proposed switch is conducted in Section 3.6.

In Section 3.7, the issues that might limit the traffic performance of the proposed wavelength-routed multicast packet switch are discussed, and an improved design is given for enhancing the traffic performance of the switch. Finally, Section 3.8 summarizes the work of this chapter.

3.2 Architecture and Operation

The schematic diagram of the wavelength-routed multicast packet switch utilizing multicast modules is depicted in **Figure 3-1**. It is composed of a demultiplexing stage, *m* sub-blocks (where *m* is the number of wavelengths per input/output fiber), and a multiplexing stage. The configuration and operation of each sub-block is identical. The switch is operated synchronously. That is, incoming packets (unicast or multicast packets) of fixed length arrive at the input fibers of the switch on a timeslot-by-timeslot basis. The operation of the switch is described as follows.

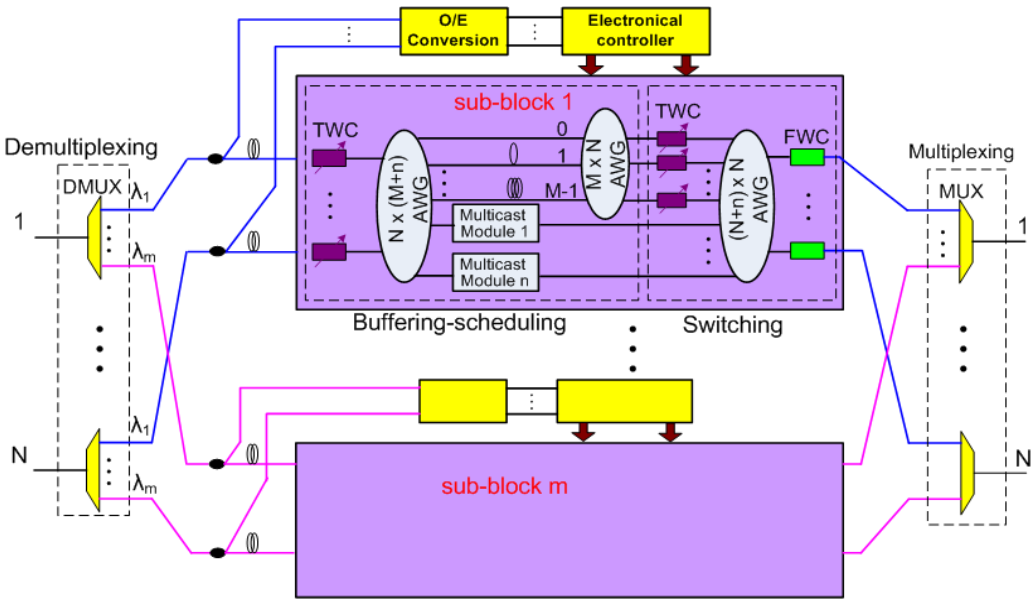

Figure 3-1: Architecture of wavelength-routed multicast packet switch utilizing multicast modules

The incoming packets are first demultiplexed in wavelength and fed into respective sub-blocks according to their wavelengths. Unicast and multicast packets are distinguished by the identifiers in their packet headers. As shown in **Figure 3-1**, a small portion of an incoming optical packet signal is tapped to an electronic controller in which the packet header is processed and used for scheduling before the entire optical packet enters the sub-block. Each sub-block consists of a buffering-scheduling section and a switching section. The buffering-scheduling section is composed of a set of N tunable wavelength converters (TWCs), an $N\times(M+n)$ AWG, an $M\times N$ AWG, a set of M fiber delay lines (FDLs) used for buffering unicast packets, and n identical multicast modules used for storing multicast packets. The TWCs are controlled by the electrical controller to route the packets in different manner according to their types. For unicast packets, the TWCs would change their wavelengths such that they can be routed to appropriate FDLs to avoid contention. For multicast packets, the TWCs would convert their wavelengths such that they would be routed to appropriate multicast modules where they are to be replicated into desired copies in one or more timeslots.

The function of a multicast module is to make desired copies of each multicast packet in appropriate timeslots such that there is no collision at each output fiber of the switch. Each multicast module, as shown in **Figure 3-2**, is constructed by a WDM loop buffer and a multi-wavelength converter. The loop buffer consists of a 2×2 optical coupler, a fiber delay line with one timeslot length, an EDFA, and two identical wavelength selectors, each of which is formed by a pair of wavelength demultiplexer and multiplexer and a set of SOA gates. A multicast packet is circulated in the WDM loop

until it is selected out of the buffer by properly setting the SOA gates in the two wavelength selectors. Once a multicast packet is selected out of the loop buffer, it will be fed to the multi-wavelength converter where it is converted into multiple copies with different wavelengths. The multi-wavelength converter is realized based on the cross phase modulation (XPM) in an SOA-based Mach-Zehnder interferometer. The details of this multi-wavelength converter will be given in the next section (Section 3.3). In order to avoid output contention, the copies of a multicast packet are allowed to be made by the multi-wavelength converter in multiple timeslots rather than in a single timeslot, which is referred as to multi-timeslot multi-wavelength conversion [191-193].

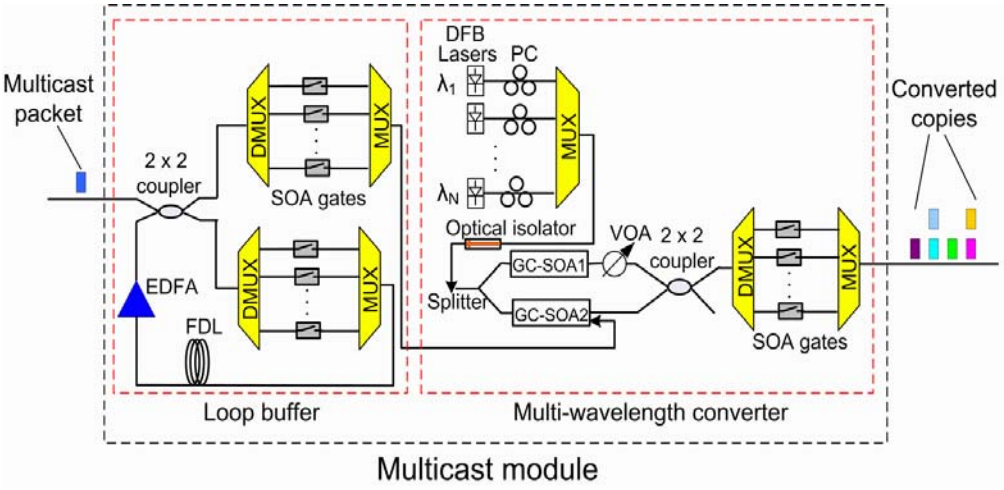

Figure 3-2: Configuration of multicast module

Unicast packets and copies of multicast packets are then forwarded to the subsequent switching section. The switching section consists of N TWCs, an $(N+n)\times N$ AWG and N fixed wavelength converters (FWCs). The unicast packets would be routed to respective outputs of the AWG by setting the corresponding TWCs, and the copies of multicast packets could be directly routed to desired outputs of the AWG without

requirement of any TWCs, since these copies have been converted into the required wavelength by the multi-wavelength converters in multicast modules. At last, a set of *N* FWCs will convert the unicast packets and copies of multicast packets back to their original wavelengths before they are transmitted to the output fibers of the switch.

3.3 Principle of Multi-wavelength Converter in Multicast module

For constructing a multi-wavelength converter as a built-in component, several requirements on physical performance should be met for the optical packet multicasting. Firstly, a good extinction ratio (ER) and bit error rate (BER) performance of the output signals are necessary to allow long distance propagation. However, XGM-based and XAM-based multi-wavelength converters suffer from poor extinction ratio [157]. Secondly, optical multicast operation requires uniform power levels among all multicast wavelengths. In this regards, optical parametric amplifier (OPA)-based multi-wavelength converter suffers from unbalanced power penalty for the converted wavelengths [195]. Thirdly, a wide wavelength range with flat conversion efficiency is important for multi-wavelength conversion. Four-wave mixing (FWM) multi-wavelength converter can only perform effective multi-wavelength conversion in very near field of the pump signal, or requires multiple pumps to improve conversion efficiency [145].

To meet these essential requirements, an SOA-MZI-based multi-wavelength converter is employed in a multicast module of the wavelength-routed multicast packet switch.

The operation principle is based on the cross phase modulation (XPM) in the SOA-MZI [191, 193]. As illustrated in **Figure 3-2**, an input optical data signal (pump light) is sent to one arm of the SOA-based MZI. At the same time, the combined lights (probe lights) formed by a group of polarization-controlled CW lasers are split by an optical splitter and launched into both arms of the SOA-MZI. In the lower arm of the SOA-MZI, the input data will induce a phase change over those CW wavelengths simultaneously due to the cross-phase modulation in SOA, and such change is weakly dependent on wavelengths. In the upper arm, due to the absence of input data, the phases of those CW lights are not affected. Afterward, the phase modulation of those CW lights is converted into intensity modulation through the interference between the CW lights from the lower arm and the upper arm of the converter. Since the input optical data signal and the CW lights enter the wavelength converter from opposite directions and propagate against each other inside the wavelength converter, the converted signals can be obtained without any optical filter to remove the original input data signal. And the multi-wavelength conversion based on XPM in an SOA-MZI can achieve a relatively high extinction ratio in comparison with the cross gain modulation in an SOA and provide both non-inverted and inverted data conversion [173, 189].

However, the course of XPM may be companied with other optical nonlinear effects such as XGM, self phase modulation (SPM), and four-wave mixing (FWM) that may introduce crosstalk and degrade the converted signal quality. In order to optimize the wavelength conversion, the gain-clamped SOAs (GC-SOAs) are employed in the multi-wavelength converter to suppress other optical nonlinear effects [196, 197]. Moreover, since the injected currents of the two GC-SOAs might be different, which

may result in different gains provided by the two GC-SOAs, a variable optical attenuator (VOA) is added in one of the arms to balance the power of the probe lights in both arms of the SOA-MZI.

More importantly, if all the copies of a multicast packet are not able to be made in the same time slot due to output contention, they are to be made in multiple time slots by allowing the original multicast packet to circulate in the buffer loop of the multicast module until all the copies have been processed. After multi-wavelength conversion, a multi-wavelength selector is used to select multiple copies of packets at desired wavelengths.

3.4 Packet Scheduling Technique

Although some algorithms have been proposed to support multicast in packet switches, such as the TATRA [97], WBA [98], and load-balanced algorithm [100], they might be quite complex to be applied in the proposed multicast switch. Those algorithms assume a large buffer size in packet switches. Such assumption would not be practically applicable in the optical packet switches, as it would require a large amount of long fiber delay lines or loop buffers, which would induce extra power loss and noise, thus severely degrade the signal quality of optical packets. Since the proposed multicast switch can be viewed as a multicast version of the wavelength-routed packet switches in [50, 51], to facilitate the scheduling in the proposed multicast switch, the packet scheduling technique that was originally designed for unicast packets in [50, 51] is modified to support both unicast and multicast packets.

Since all the sub-blocks in the proposed wavelength-routed multicast packet switch are identical, we only focus on the operation of one sub-block shown in **Figure 3-3**, and explain how both unicast and multicast packets are scheduled.

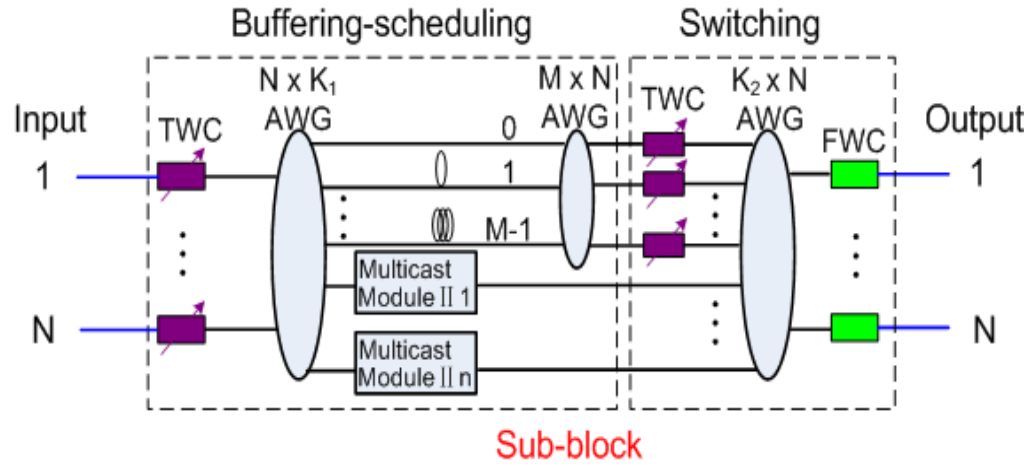

Figure 3-3: Sub-block of the proposed wavelength-routed multicast packet switch

Similar to the wavelength-routed unicast packet switch in [50, 51], the sub-block can be modeled as a time-space-time (TST) switch as shown in **Figure 3-4**. The TST switch is composed of $N+n$ input ports, N output ports and a switching section. The input ports are divided into two parts. The first part is composed of N identical timeslot interchanges (TSIs) used for handling the unicast packets coming from N different inputs, and each of these TSIs contains M timeslots corresponding to M fiber delay lines in a sub-block. The second part that consists of n identical TSIs, corresponding to n multicast modules in a sub-block, is used for handling multicast packets. Each of these n TSIs contains T_m timeslots, where T_m is the max number of timeslots for a multicast packet to be stored in the loop buffer of a multicast module. Due to the accumulation of the ASE noise induced by the EDFA and SOA gates in the

loop buffer of a multicast module, the OSNR of the multicast packet would deteriorate with the number of circulation in the loop buffer, which will further affect the signal quality of the converted copies by the subsequent multi-wavelength converter, hence it is not advisable to let a multicast packet be stored in the loop buffer for many timeslots. Each output port has a TSI which contains T_o timeslots, where T_o=max(M, T_m).

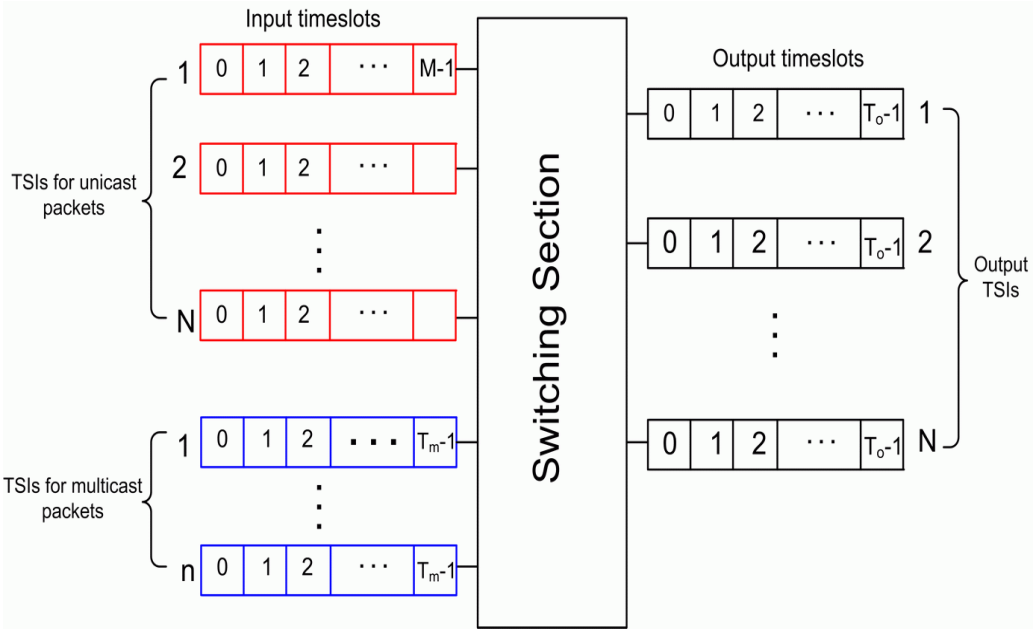

Figure 3-4: Schematic of the TST switch representing one sub-block of the wavelength-routed multicast packet switch

Assume that packets (unicast or multicast) arrive at the input of the switch synchronously by timeslot. For an arbitrary unicast packet at the *i*th input destined for the *j*th output, as illustrated in **Figure 3-5**, the scheduling is to find a matched idle timeslot at both of *i*th input TSI and *j*th output TSI. If there are multiple matched idle timeslots, the one with minimum delay will be selected. A unicast packet will be discarded if there is no any matched timeslot at both of input and output TSIs.

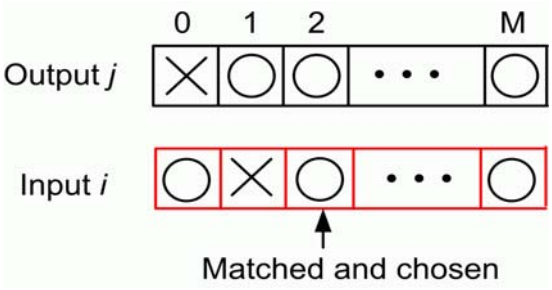

Figure 3-5: Assignment of matched idle timeslot for unicast packets

For an arbitrary multicast packet arriving at *i*th input destined for multiple outputs, the scheduling includes two processes. Firstly, find a multicast module through which the most number of the copies of this multicast packet can be made by scanning the TSI of each multicast module and the TSIs of those desired output ports. If there are more than one choice of multicast modules, the one in which the multicast packet is stored with minimum delay will be selected. If none of the multicast modules can be selected, the multicast packet will be dropped. Secondly, find a matched idle timeslot in both of the TSIs of the selected multicast module and the desired output ports for each copy of the multicast packet. As illustrated in **Figure 3-6**, for a multicast packet with *j* copies, the scheduling will scan the TSIs of both the selected multicast module and desired output ports for each copy; if there are multiple matched idle timeslots for a copy, the one with minimum delay will be chosen. The copies that cannot be assigned to any idle timeslots will be discarded. Furthermore, once a copy has been successfully delivered to its output port, the corresponding timeslots in the TSIs of both selected multicast module and the output port will become idle for the next scheduling of new multicast packets. Note that for the packets arriving at the same timeslot, the multicast packets are given higher priority than unicast packets to be scheduled. This priority setting is for two reasons: 1) the multicast traffic is expected to be much less than

unicast traffic, 2) the number of multicast modules can be reduced since a multicast module is much more expensive than a travelling fiber delay line. Although such a priority setting may lead to imbalance of performance between unicast and multicast traffic, the overall packet loss performance would not be affected significantly as it reduces the multicast packet loss probability at the expense of increasing the unicast packet loss probability. The Round-Robin scheme is used to provide fair priority allocation among the *N* input ports [91]. The flow chart of the packet scheduling technique is illustrated in **Figure 3-7**.

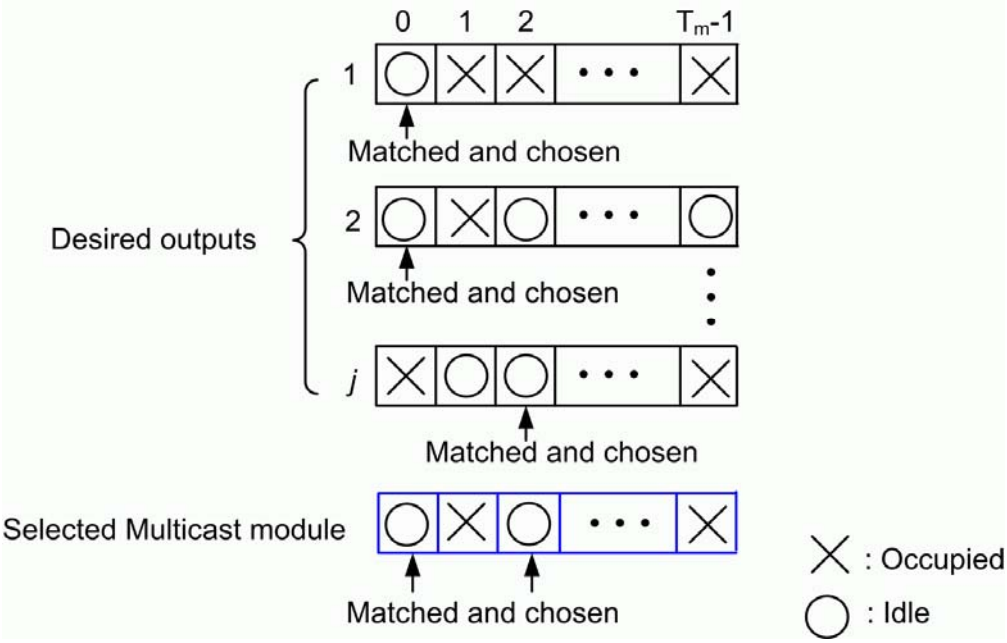

Figure 3-6: Assignment of matched idle timeslot for multicast packets

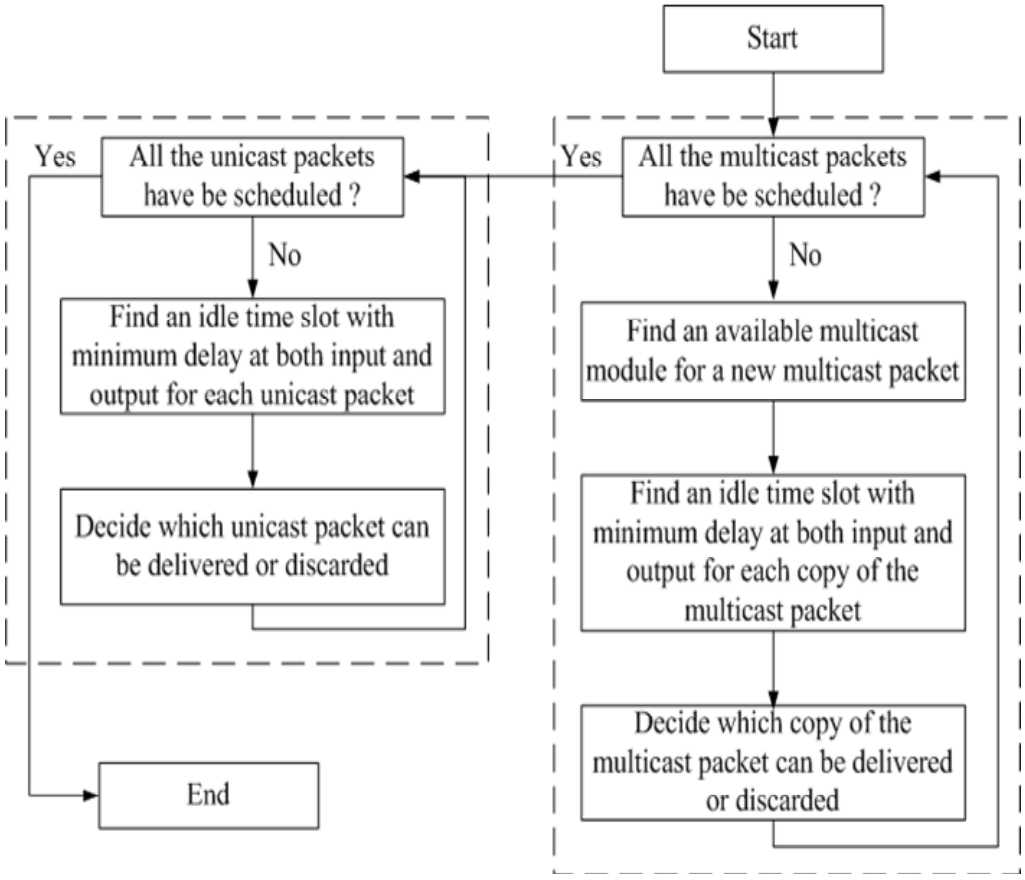

Figure 3-7: Flow chart of the packet scheduling technique

3.5 Physical Performance Evaluation

The physical performance of the multicast module is examined through simulation using OptiSystem 6.0 [198]. The simulation setup is illustrated in **Figure 3-8**. **Table 3-1** gives keys parameters used in the simulation. A distributed feed-back (DFB) laser source (λ = 1545.72 nm) is modulated at 10 Gbit/s by a MZ intensity modulator with 2^{23}-1 return-to-zero (RZ) pseudorandom binary sequence to generate input multicast packets.

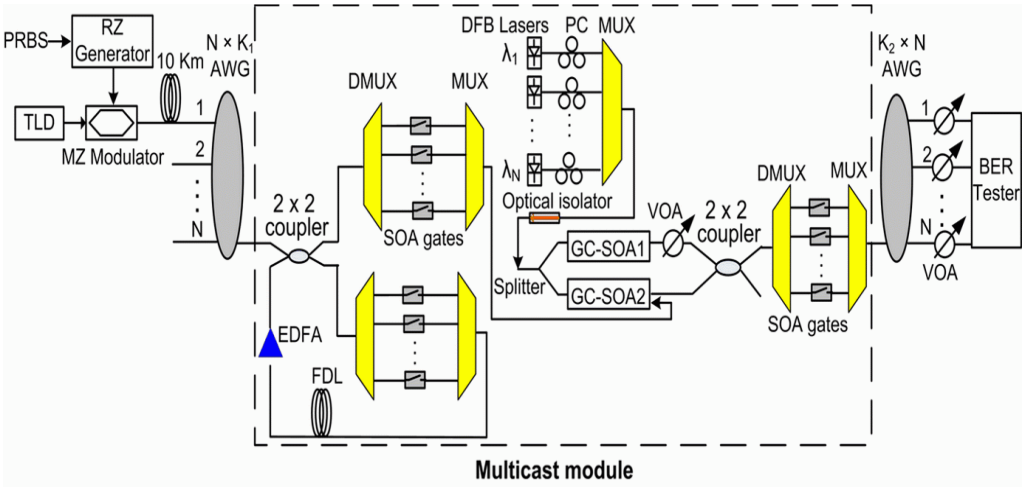

Figure 3-8: Simulation setup of the multicast module

For simplicity, the header information of each packet is not included within the packet. Each packet has a length of 880 nanoseconds (ns), including 800 ns packet duration and 80 ns guard time. The probe lights are formed by a group of DFB continuous-wave (CW) lasers with 100 GHz spacing from 1547.72 nm to 1559.79 nm, each of which is polarization-controlled for optimizing the conversion efficiency. The fiber delay line (FDL) in the loop buffer provides one timeslot delay (880 ns). In order to compensate the power loss of the loop buffer, the gain of the EDFA is set to 8.3 dB with 5.0 dB noise figure (NF). The noise figures of SOA gates are set to 6.0 dB. The average power of the input optical signal is set to 0.5 dBm, and the total power of the probe lights is about 0 dBm. **Table 3-2** gives parameters of the GC-SOAs used for the multi-wavelength conversion.

Table 3-1: Parameters in the simulation setup

Wavelength of input signal	1545.72 nm
Input signal (pump) power	0.5 dBm
Bit rate	10 Gbit/s
Modulation format	RZ
Wavelength of CW (probe) Lasers	1547.72 nm ~ 1559.79 nm (100 GHz spacing)
Total CW lasers power	0 dBm
NF of EDFA	5.0 dB
Gain of EDFA	8.3 dB

Table 3-2: Parameters of GC-SOA used in the SOA-based MZI

Symbol	Value	Explanation
L	2×10^{-5} m	Active region length
w	4×10^{-7} m	Active region width
d	4×10^{-7} m	Active region thickness
N_0	1.2×10^{24} m^{-3}	Carrier density at transparency
Γ	0.35	Confinement factor
a_0	2.78×10^{-20} m^2	Differential gain
γ_1	2.78×10^{-20} m^2	Material gain constant 1
γ_2	2.9×10^{-32} m^4	Material gain constant 2
k_0	6200 m^{-1}	Nonradiative recombination coefficient
A	360000000 1/s	Bimolecular recombination coefficient
B	5.6×10^{-16} m^3/s	Auger recombination coefficient
C	3×10^{-41} m^6/s	Differential refractive index
dn/dN	-1.54×10^{-26} m^{-3}	VCL reflectivity
β	10^{-4}	Spontaneous emission coupling coefficient
v_g	75000000 m/s	Group velocity
T	300 K	Temperature

In order to evaluate the characteristics of the multicast module, the BER performance is first examined. **Figure 3-9** shows the BER results of the wavelength-converted packets when 4 probe wavelengths (1547.72 nm, 1548.51 nm, 1549.32 nm, and 1550.12 nm) are applied without storing the input packet (pump wavelength: 1545.72 nm) in the loop buffer of the multicast module. The injection currents for GC-SOA1 and GC-SOA2 are about 200 mA and 210 mA, respectively. It is observed that the converted signals have better BER performance than the input signal. This is due to the regeneration characteristics of the SOA-MZI structure used in the multi-wavelength converter. The receiver power discrepancy among these 4 converted wavelength channels at 10^{-9} BER is just about 0.2 dB.

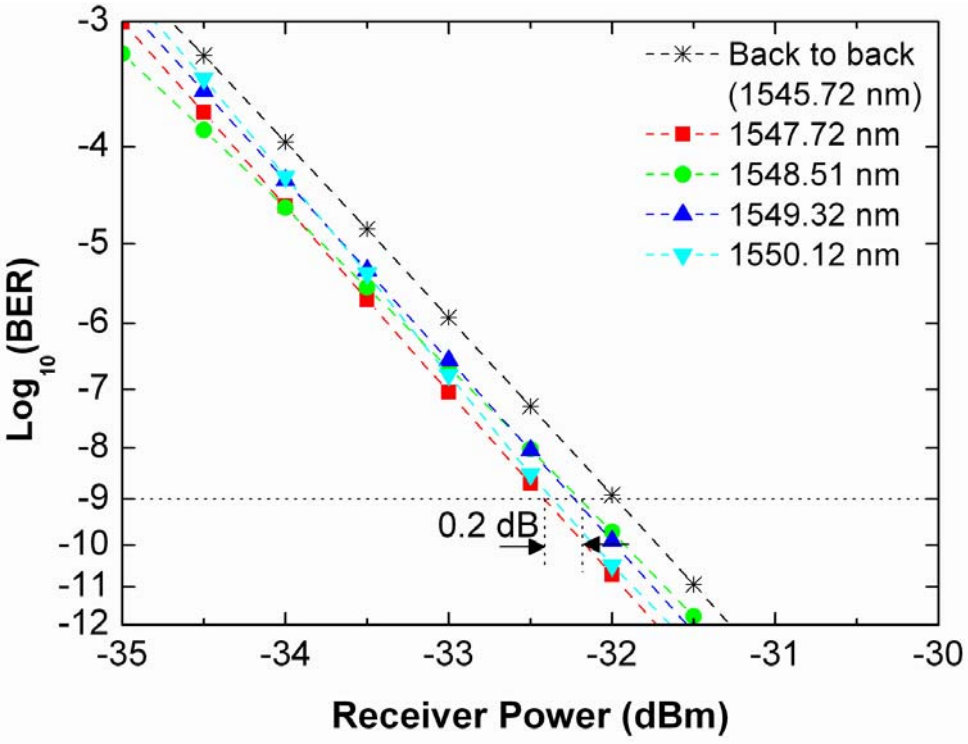

Figure 3-9: BER performance of 4 converted packets (probe wavelengths) in the case that the input packet (pump wavelength) is not stored in the loop buffer

After storing the input packet for 16 timeslots in the loop buffer, as shown in **Figure 3-10**, the BER performance of these converted channels would deteriorate with different power penalties. The receive power discrepancy among these wavelengths at 10^{-9} BER increases to 0.6 dB.

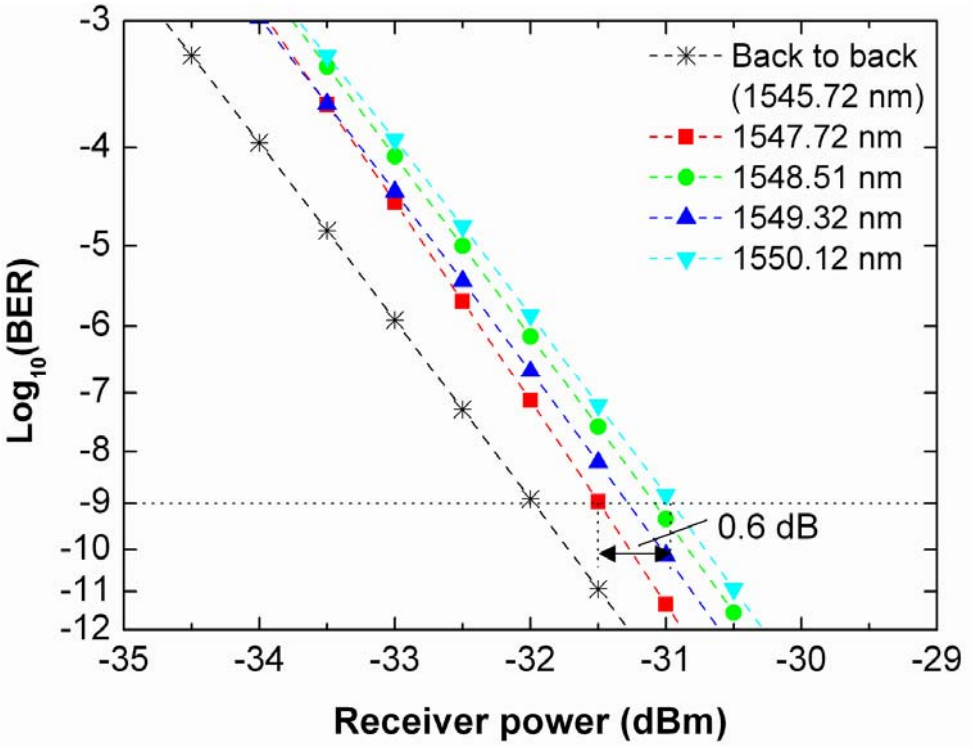

Figure 3-10: BER performance of 4 converted packets (probe wavelengths) in the case that the input packet (pump wavelength) is stored for 16 timeslots in the loop buffer.

Figure 3-11 shows the receiver power for each converted wavelength at the BER of 10^{-9} when there are 16 probe wavelengths (ITU-T standard wavelengths from 1547.72 nm to 1559.78 nm with 100 GHz spacing) in the multicast module. The injection currents for GC-SOA1 and GC-SOA2 are adjusted to 250 mA and 280 mA,

respectively, for optimizing the wavelength conversion. It is shown that in the case the input packet is not stored in the loop buffer, the average required received power of these 16 converted channels is about -32 dBm at the BER of 10^{-9}; while after storing the input packet for 16 timeslots in the loop buffer, this value is increased by 1.4 dB to maintain the same BER of 10^{-9}. This power penalty might be explained as follows. Since the phase modulation depth of the probe channels is affected by the extinction ratio (ER) of the pump signal in XPM, the degradation of ER of the pump signal would reduce the ER of the converted probe wavelengths, thus resulting in BER deterioration. The ER of the pump signal, as shown in **Figure 3-12**, is gradually reduced with the times that the pump signal (packet) circulates in the loop buffer. Although the power loss in the loop buffer can be compensated by the EDFA, it would also deteriorate the optical signal-to-noise ratio (OSNR) due to the induced ASE noise [77].

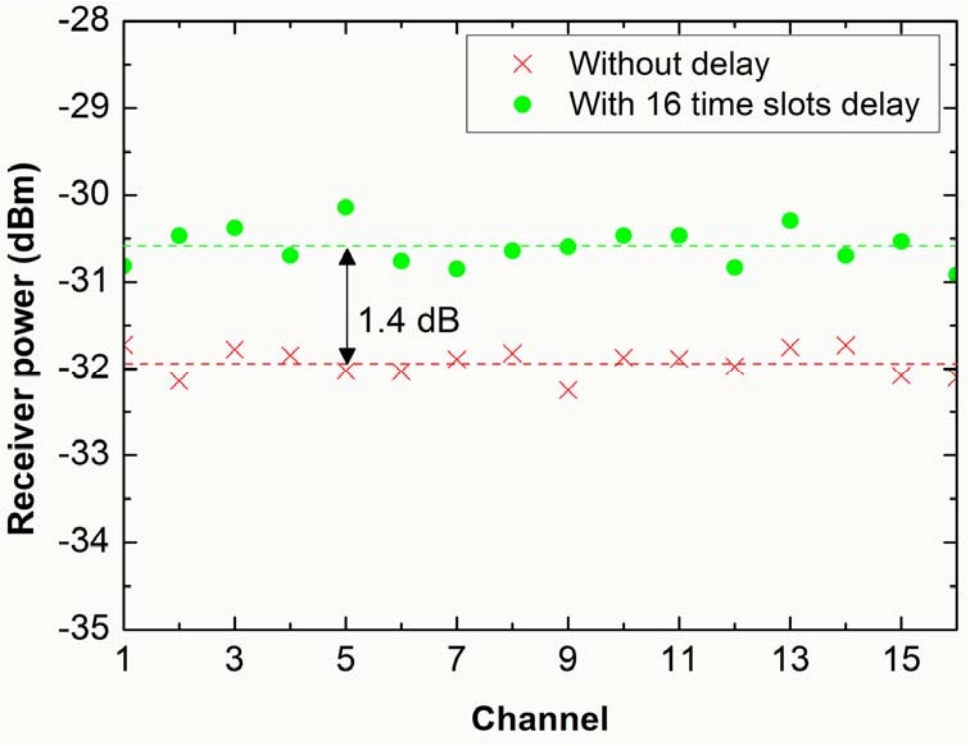

Figure 3-11: Receiver power of 16 converted channels at the BER of 10^{-9}

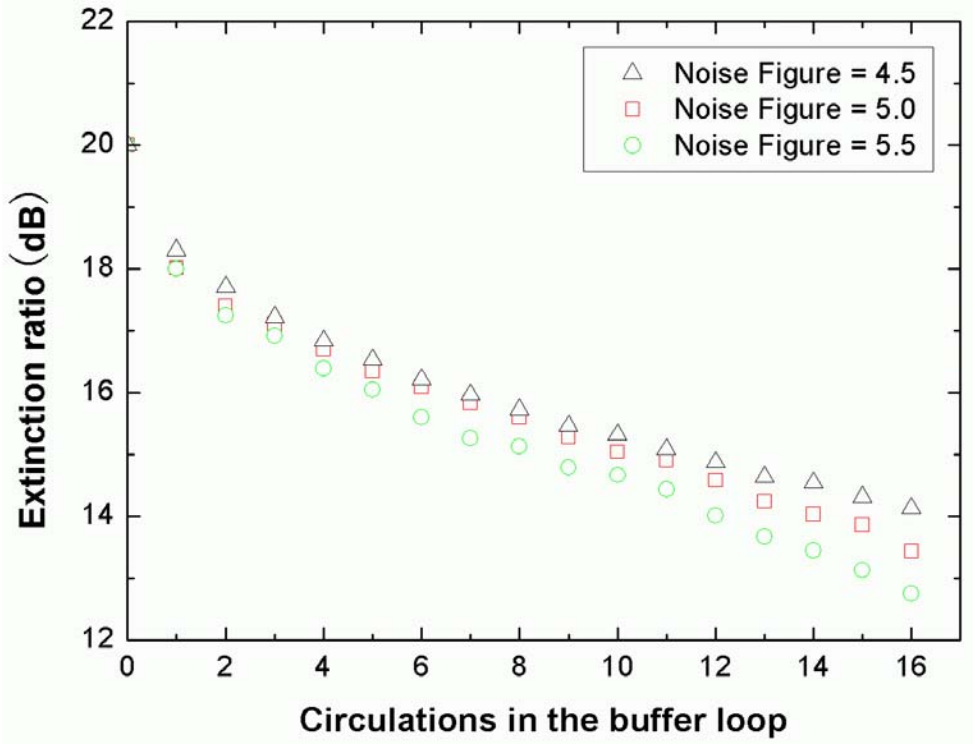

Figure 3-12: Extinction ratio of the pump signal circulating in the loop buffer

Meanwhile, it is found that the required receiver power of each channel at the BER of 10^{-9} for the case of 16 converted channels is larger than that for the case of 4 converted channels, which means that the BER performance would also deteriorate with the number of the converted channels increasing. This deterioration may be attributed to the crosstalk induced by other nonlinear effects such as XGM and FWM. **Figure 3-13** shows optical spectral characteristics of the 16 probe lights before and after the multi-wavelength converter. It is shown that the FWM effect in the multi-wavelength converter would become severer when the number of the converted channels is increasing.

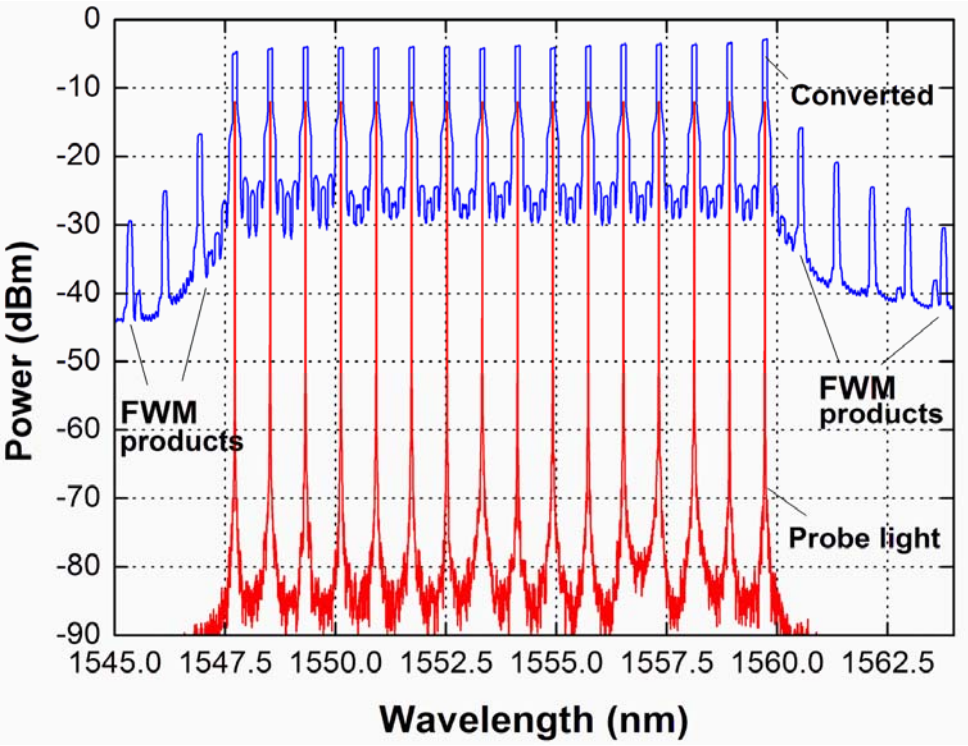

Figure 3-13: Spectral characteristic of the 16 probe lights before and after wavelength conversion by the multi-wavelength converter in the multicast module

3.6 Traffic Performance Evaluation

3.6.1 Traffic Model

Most of the traffic models adopted for the traffic performance study of packet switches assume that the arrivals and destinations of packets are independent [199, 200]. However, those models are not suitable for the study of multicast packet switches. Because of the multiple copies of each multicast packet, the input offered traffic load could not be regarded as the output traffic load in a multicast packet switch [201]. In

this section, a new traffic model is introduced for the traffic performance study of the multi-wavelength multicast packet switch forementioned.

We consider the input traffic to be a combination of unicast and multicast packets, and the packet arrivals from every wavelength channel of any input fiber are of independent and identical Bernoulli processes. Next, the notations used in this study are introduced:

Traffic parameters

λ Probability of a packet arriving from every wavelength channel of any input fiber in a timeslot.

R Probability that an arrival packet is a multicast packet.

X Random integer representing the number of copies of a multicast packet.

$E(X)$ Mean value of X.

ρ_{eff} Effective total traffic load at every wavelength channel of any output fiber of the switch.

ρ_u Effective unicast traffic load at every wavelength channel of any output fiber of the switch.

ρ_m Effective multicast traffic load at every wavelength channel of any output fiber of the switch.

r Multicast traffic ratio, which is defined as the ratio of the effective multicast traffic load to the effective total traffic load at each output wavelength, i.e., $r=\rho_m/\rho_{eff}$.

Each packet (unicast and multicast) is assumed to be of fixed length and no more than one packet arrives at any input wavelength channel in a timeslot, hence λ can be considered as the average input offered traffic load. It is also assumed that a unicast packet is equally likely to be destined for any output fiber of the switch; a multicast packet has multiple copies, each of which is also uniformly distributed over the N output fibers of the switch, but no two or more copies are destined for the same output fiber. Since the geometric distribution is often adopted for the study of multicast traffic [201-203], in this study, the number of copies of an incoming multicast packet (i.e., the random variable X) is assumed to follow a truncated geometric distribution with parameter q ($0 < q < 1$), and the probability of a multicast packet having k copies is given:

$$P(X=k)=\frac{(1-q)q^{k-1}}{q-q^{N}},\quad 2\le k\le N \tag{3.1}$$

The average number of copies of a multicast packet can be calculated.

$$E(X)=\sum_{k=2}^{N}k\cdot P(x=k)=\frac{2q-q^{2}-(N+1)q^{N}+Nq^{N+1}}{(1-q)(q-q^{N})} \tag{3.2}$$

Figure 3-14 shows the value of $E(X)$ versus value of q for different values of N. It is found that when $q \le 0.7$, the value of $E(X)$ ($E(X)<4$) is almost independent of N.

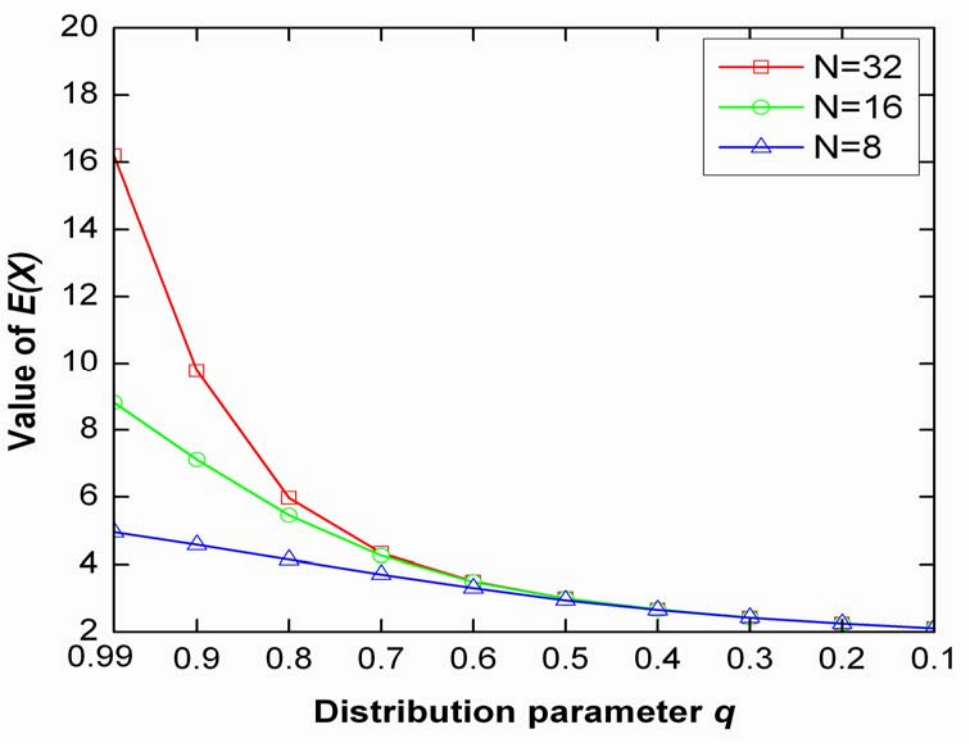

Figure 3-14: Value of $E(X)$ versus parameter q for different values of N

In each input wavelength channel, the probability that an arrival packet is a unicast packet or multicast packet is 1-R or R. For an arrival unicast packet, the probability that this unicast packet is destined for an output fiber is given by $1/N$; for an arrival multicast packet with X copies, the probability that one copy is destined for a particular output fiber is given by X/N, and no two or more copies are destined for the same output fiber. Hence, considering the packet arrival rate λ, and the values of R and $E(X)$, the probability that an arrival packet will result in one packet (a unicast packet or copy of a multicast packet) being addressed to each output fiber is given.

$$P_e = \lambda\left(\frac{1}{N}(1-R)+\frac{1}{N}RE(X)\right) \tag{3.3}$$

Considering the contribution of different traffic (unicast and multicast) to each wavelength channel of any output fiber, the effective unicast, multicast and total traffic loads at each output wavelength can be calculated, respectively.

$$\rho_u = \lambda(1-R) \tag{3.4}$$

$$\rho_m = \lambda R E(X) \tag{3.5}$$

$$\rho_{eff} = \rho_u + \rho_m = \lambda\left((1-R)+RE(X)\right) \tag{3.6}$$

Here, only admissible traffic load is considered, i.e., $0 < \lambda < 1$, and $0 < \rho_{eff} < 1$. The relation between the multicast traffic ratio r and the probability R is plotted in **Figure 3-15**.

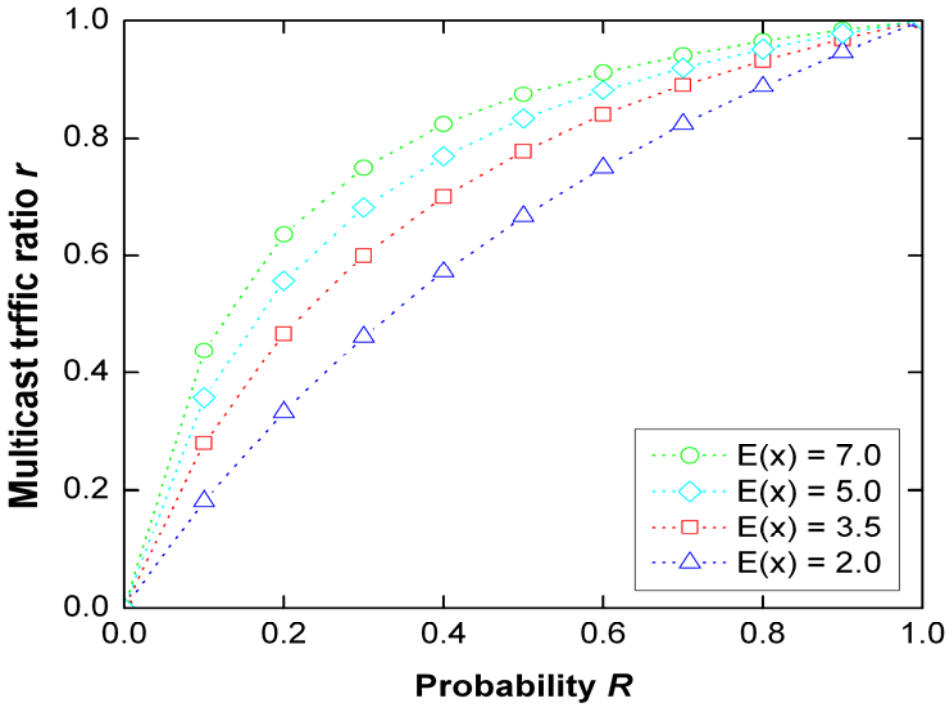

Figure 3-15: Multicast traffic ratio versus probability *R* for different values of *E*(*X*)

3.6.2 Simulation Results and Discussions

In this section, the traffic performance in terms of packet loss probability, mean delay and normalized throughput of the wavelength-routed multicast packet switch is evaluated through simulation. Since all the sub-blocks of the switch are identical, the traffic performance of the wavelength-routed multicast packet switch can be equivalently characterized by a single sub-block shown in **Figure 3-3**.

The simulation platform is also developed using the Network Simulator Version 2 (NS-2) [204]. The timeslot length T is set to 880 ns including 800 ns packet duration and 80 ns guard time. Let D_U, D_M, G_U, and G_M be the numbers of dropped unicast, dropped multicast, generated unicast and generated multicast packets, respectively. Then the unicast, multicast and total packet loss probabilities can be calculated by D_U/G_U, D_M/G_M, and $(D_U+D_M)/(G_U+G_M)$, respectively.

Firstly, the effect of T_m (maximum number of timeslots for a multicast packet to be stored in a multicast module) on traffic performance of the switch is examined. **Figure 3-16** shows the multicast packet loss probability versus the value of T_m for the switch with different values of n (number of multicast modules per sub-block), where the switch size N=8, the number of FDLs is fixed at M=8, the effective total traffic load is fixed at ρ_{eff}=0.8, and the multicast traffic ratio is r=0.2 with $E(X)$=4.

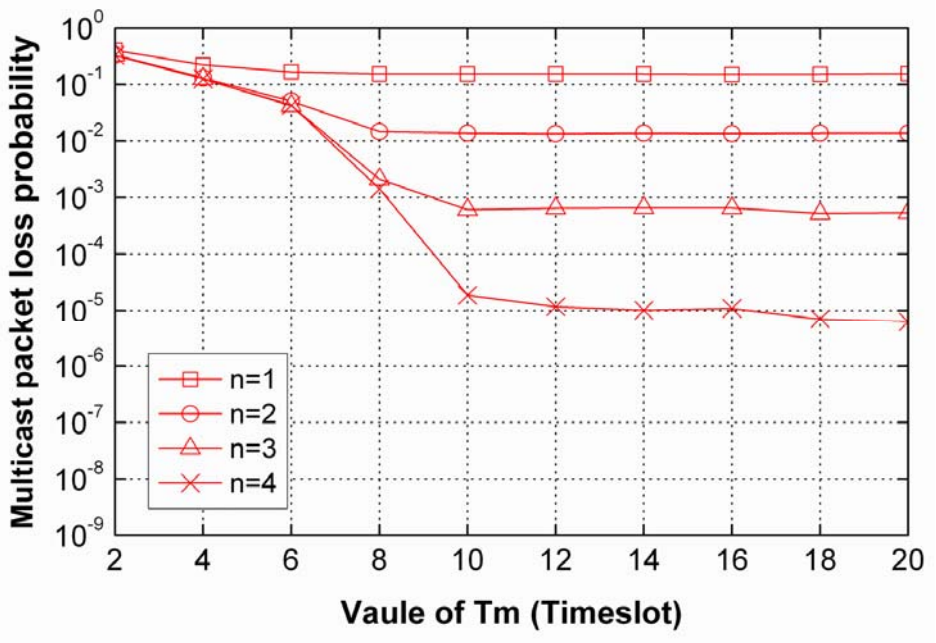

Figure 3-16: Multicast packet loss probability versus the value of T_m for an 8×8 wavelength-routed multicast packet switch with different values of n per sub-block

It is observed that (i) when n=1, the multicast packet loss is quite high and increasing the value of T_m can hardly reduce the multicast packet loss probability, it will reach a constant level after $T_m \geq 6$; (ii) although the multicast packet loss probability can be further improved by increasing the value of n, it will reach a new constant level after T_m is greater than a certain value. It is shown that when $T_m \geq 12$, the switch can achieve a constant multicast packet loss probability of 10^{-5} with n=4. This is because that although an increase in the value of T_m can allow multicast packets to be stored in a multicast module for more timeslots, each multicast packet in a multicast module would occupy a wavelength. When all the wavelengths in the loop buffer have been occupied, a further increase in the value of T_m cannot help the new coming multicast

packet be stored in the loop buffer, which would result in a constant level of packet loss probability.

Similar results can also been seen for a 16×16 (N=16) switch in **Figure 3-17**. Since the multicast packet loss probability would reach to a constant level after T_m is increased to a certain value, further increase in T_m would not improve the packet loss performance of the switch, but deteriorate the signal quality of copies of a multicast packet as the multicast packet may be stored in the loop buffer for many circulations, resulting in an accumulation of ASE noise. According to the results of **Figures 3-16** and **3-17**, we fix T_m =12 in the following investigations of traffic performance for the switch.

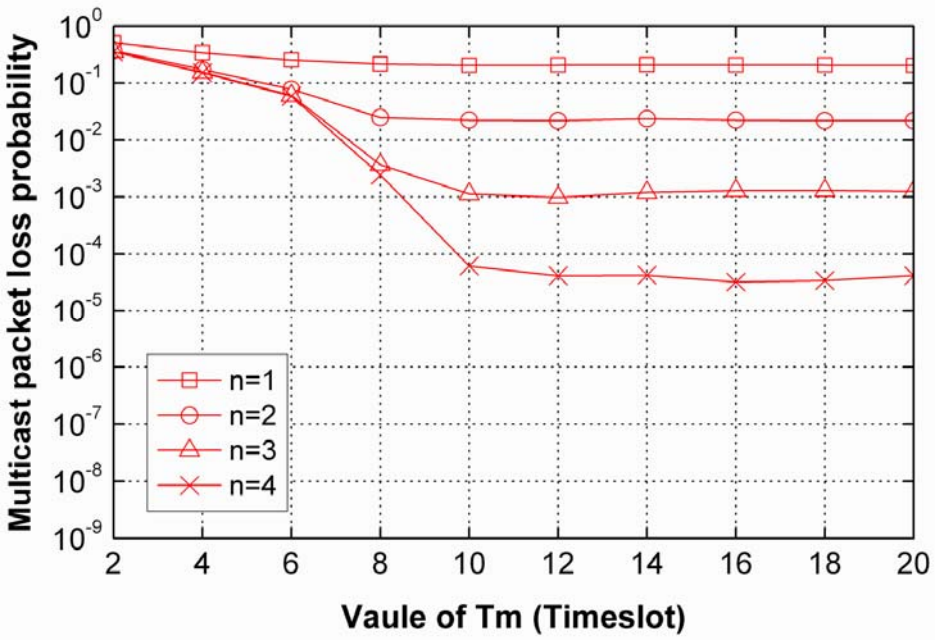

Figure 3-17: Multicast packet loss probability versus the value of T_m for a 16×16 wavelength-routed multicast packet switch with different values of *n* per sub-block

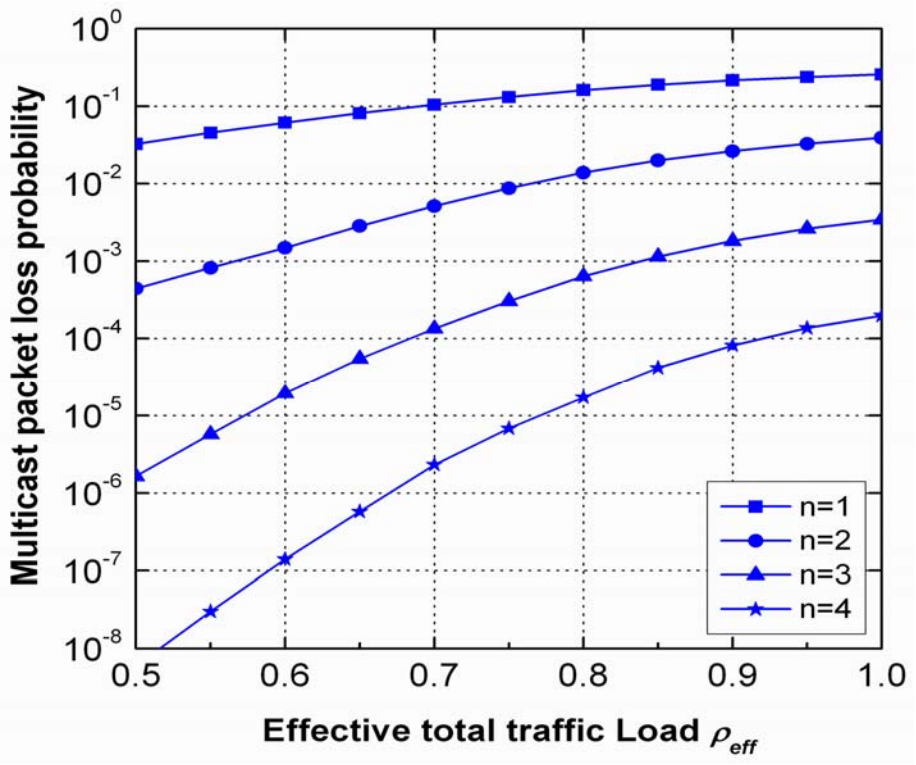

Figure 3-18: Multicast packet loss probability versus effective total traffic load for a 16×16 wavelength-routed multicast packet switch with different multicast modules per sub-block

Next, the multicast, unicast and total packet loss probabilities as a function of effective total traffic load for a 16×16 wavelength-routed multicast packet switch are evaluated, respectively. In this study, T_m is fixed at 12 timeslots (T_m =12) and the number of FDLs is 8 (M=8), the multicast traffic ratio is r=0.2 with $E(X)$=4. As shown in **Figure 3-18**, the multicast packet loss probability is significantly reduced by slightly increasing the number of multicast modules per sub-block (value of n). This can be explained by two reasons. Firstly the multicast packets are given higher priority for switching than the unicast packets arriving at the same timeslot. Secondly, in the switch, the copies of a multicast packet are allowed to be made in multiple timeslots,

instead of a single timeslot, to avoid output contention, leading to a small number of multicast modules to achieve a low multicast packet loss probability.

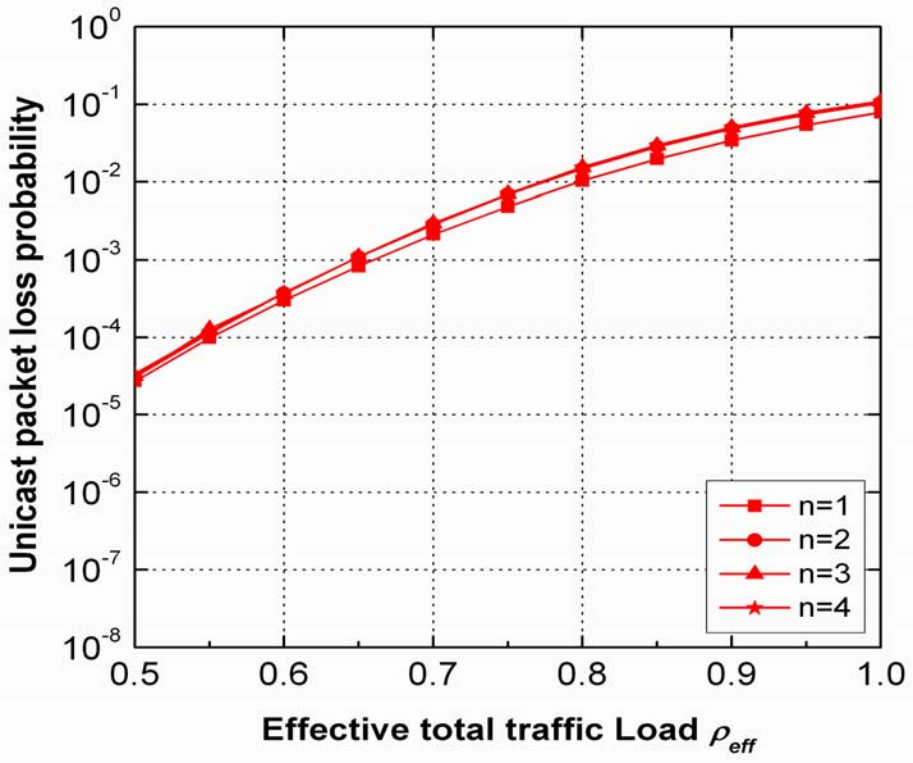

Figure 3-19: Unicast packet loss probability versus effective total traffic load for a 16×16 wavelength-routed multicast packet switch with different multicast modules per sub-block

On the other hand, an increase in the value of *n* hardly affects the unicast packet loss performance as observed in **Figure 3-19**. This is because the multicast modules are only used for handling the multicast packets.

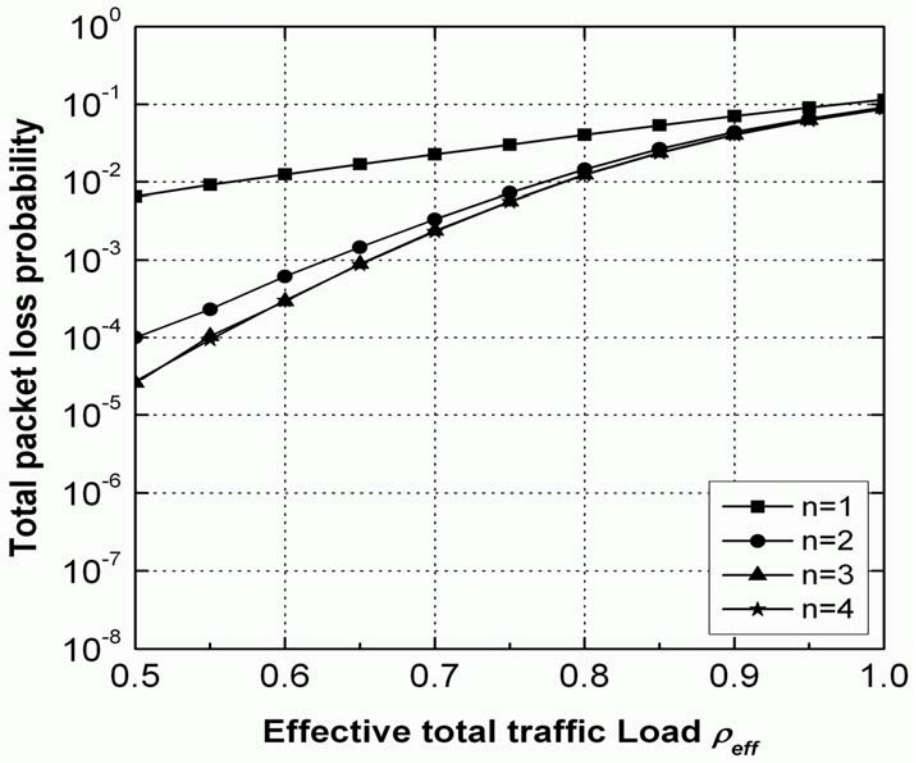

Figure 3-20: Total packet loss probability versus effective total traffic load for a 16×16 wavelength-routed multicast packet switch with different multicast modules per sub-block

The total packet loss probability, as shown in **Figure 3-20**, is determined by both of multicast and unicast packet loss probabilities. It is observed that slight increase in the value of n ($n \leq 3$) can help reduce the total packet loss probability due to the reduction in multicast packet loss probability; however, when $n>3$, the total packet loss performance cannot be further improved by increasing in the value of n. That is because when $n>3$, the multicast packet loss probability is much smaller than the unicast packet loss probability, which is the major contribution to the total packet loss probability. In this case, an increase in the number of FDLs can reduce the unicast packet loss probability, leading to further reduction in the total packet loss probability.

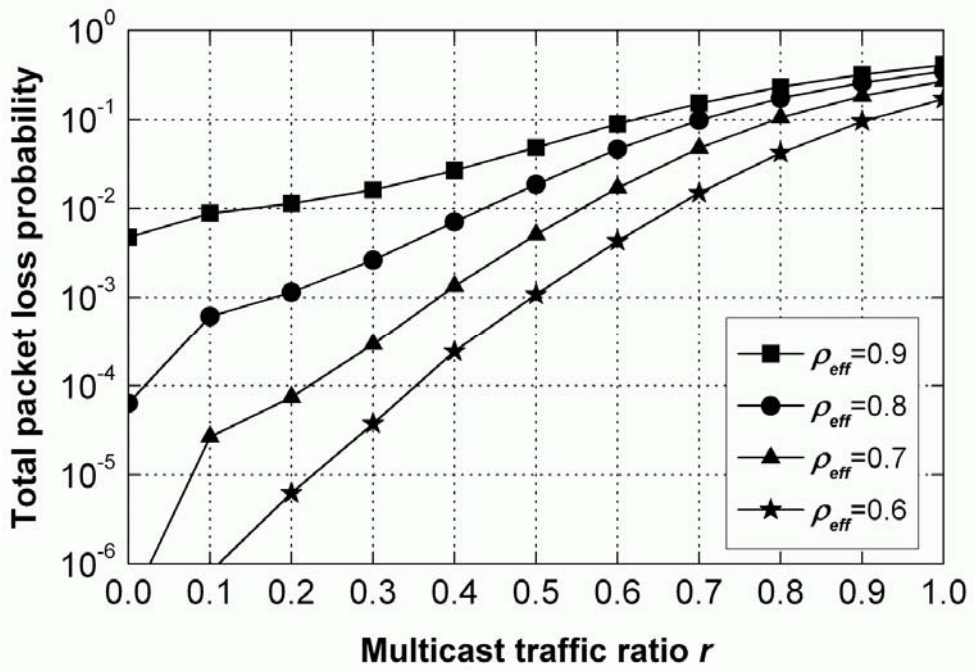

Figure 3-21: Total packet loss probability versus multicast traffic ratio for a 16×16 wavelength-routed multicast packet switch under different effective total traffic loads

Next, the effect of multicast traffic ratio on the packet loss performance is investigated. **Figure 3-21** shows total packet loss probability as a function of multicast traffic ratio r for a 16×16 wavelength-routed multicast packet switch under different effective total traffic loads with $E(X)$=4. In **Figure 3-21**, the number of FDLs is M=20, and the number of multicast modules per sub-block is n=3 with T_m=12. It is observed that for a given effective total traffic load and buffering capacity, the total packet loss probability of the switch would increase as the multicast traffic ratio increases. And such influence would become more obvious for the switch under smaller ρ_{eff}. As an example, when ρ_{eff}=0.6, the switch could achieve a total packet loss probability below 10^{-5} when $r \leq 0.2$; while this value is rapidly increased to above 10^{-1} when r is increased

to 0.9. This can be explained as follows. Given fixed values of M and n, an increase in multicast traffic ratio r results in an increase in the multicast packet loss probability; though the increase in r also means a reduction in the unicast traffic proportion, due to the lower priority of unicast packets in switching, some of the FDLs may not be able to be utilized for buffering unicast packets, leading to an increase in the total packet loss probability.

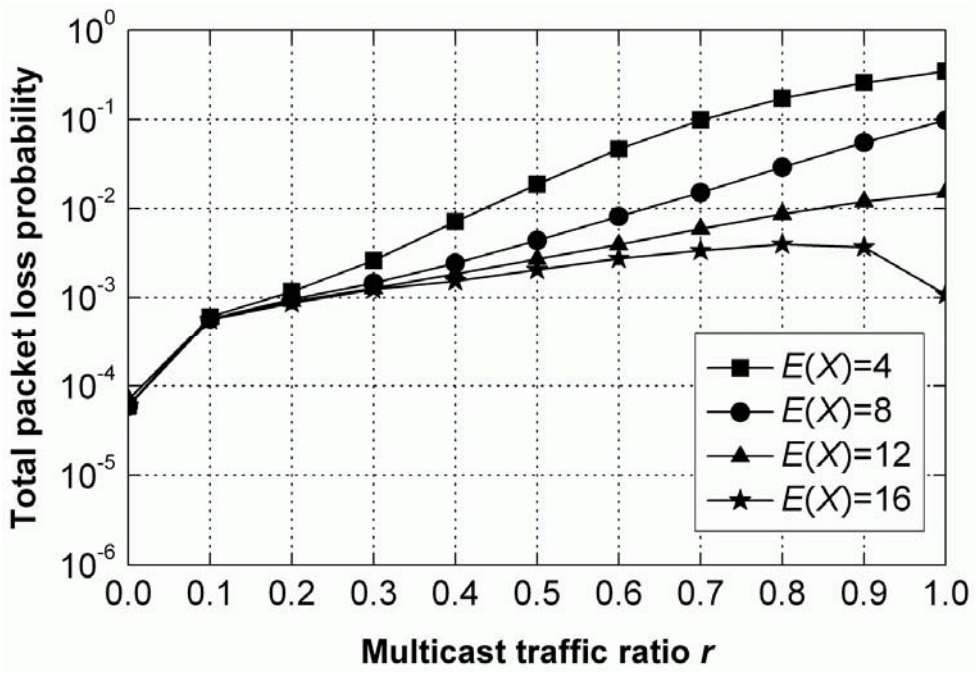

Figure 3-22: Total packet loss probability versus multicast traffic ratio for a 16×16 wavelength-routed multicast packet switch under different values of $E(X)$

Figure 3-22 shows the effect of $E(X)$ on the total packet loss probability of the switch, where the effective total traffic load is fixed at ρ_{eff}=0.8. The number of multicast modules per sub-block is n=5, and the number of FDLs is M=25. It is observed that for a given effective total traffic load with a fixed multicast traffic ratio, the total packet loss probability is reduced as the value of $E(X)$ increases. This is because the multicast

modules are used for storing the incoming multicast packets instead of their copies; with a fixed multicast traffic ratio, a larger value of $E(X)$ means a lower arrival rate of multicast packets, which results in a lower multicast packet loss probability if the effective total traffic load is fixed, thereby leading to a lower total packet loss probability. Note that when $E(X)$=16, the switch is in the broadcast operation.

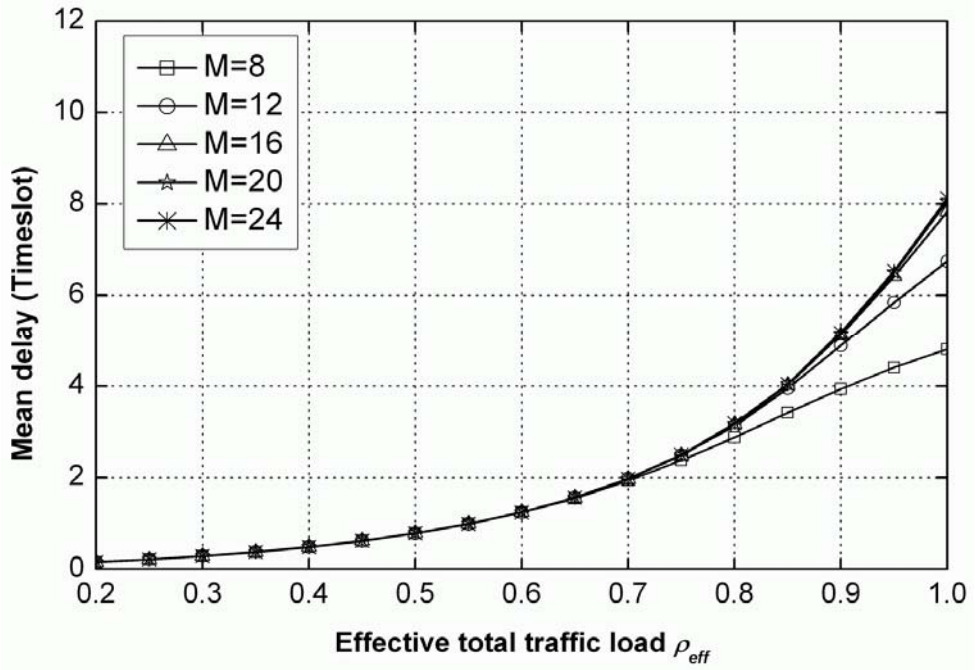

Figure 3-23: Mean packet delay versus effective total traffic load for a 16×16 wavelength-routed multicast packet switch with different values of *M*

Figure 3-23 shows the mean packet delay versus the effective total traffic load for a 16×16 wavelength-routed multicast packet switch with different values of M. The multicast traffic ratio is r=0.2 and the value of $E(X)$ is set to be 4. As shown in **Figure 3-23**, where the value of n is fixed at n=1, when the effective total traffic load ρ_{eff}>0.8, increasing the value of M would result in an increase in the mean delay, but when $M \geq 16$, the mean delay performance would not be affected by further increasing the value of M. This is because: 1) the mean delay is the average of multicast packet delay

and unicast packet delay; 2) as in the case shown in **Figure 3-23**, the multicast traffic ratio (20%) is much smaller than unicast traffic ratio (80%), the mean delay mostly depends on the unicast packet delay. Although increasing the value of *M* (number of FDLs) may provide more timeslots for unicast packets, it does not have significant effect on the unicast packet delay, as the effective unicast traffic load only accounts for 80% of the effective total traffic load .

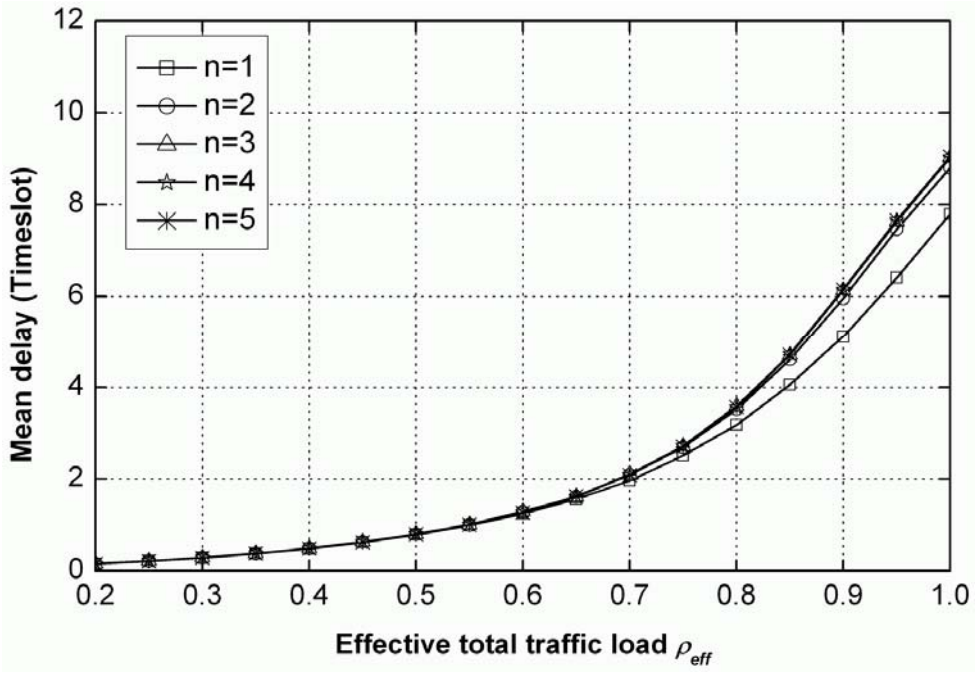

Figure 3-24: Mean packet delay versus effective total traffic load for a 16×16 wavelength-routed multicast packet switch with different values of *n*

Similarly, in **Figure 3-24**, where the number of FDLs per sub-block is *M*=16, increasing the number of multicast modules per sub-block would not greatly deteriorate the delay performance of the switch. It is observed that the switch would achieve a constant mean delay at a particular effective total traffic load ρ_{eff} after the value of *n* reaches to 2.

3.7 Improved Design

From the above discussions, it is found that there are two main limitations associated with the multicast modules: 1) a loop buffer cannot store two or more multicast packets from the same input of the switch concurrently due to wavelength collision. If a multicast packet from a certain input is stored in the loop buffer of a multicast module, a new multicast packet from the same input must be routed into other multicast modules; 2) due to the accumulated ASE noise induced by the EDFA and SOA gates in the loop buffer, the OSNR of the converted packets would be deteriorated gradually [77], it is not advisable to store an optical multicast packet for many circulations in the loop buffer. To address the limitations, in this section, an improved design is proposed to modify the multicast modules.

Figure 3-25 shows the modified multicast module that is derived from the previous multicast module shown in **Figure 3-2** by replacing the 2×2 optical coupler in the loop buffer with a $k\times2$ optical coupler, where $k\geq2$. The remaining parts of the modified multicast module are the same as those of the previous multicast module. Accordingly, the output size of the first AWG in the buffering-scheduling section of a sub-block needs to be increased after the multicast module is modified.

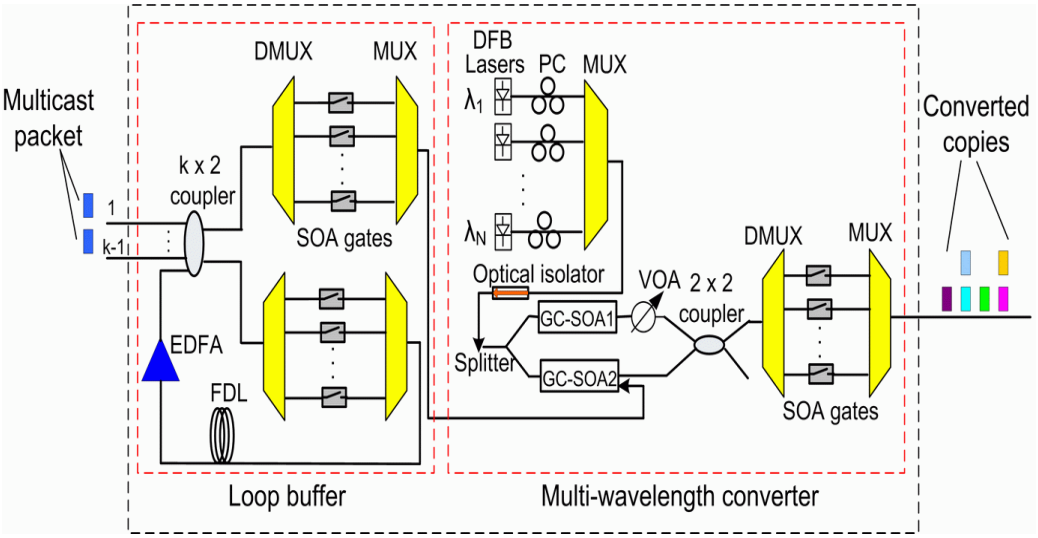

Figure 3-25: Configuration of the modified multicast module

In the previous multicast module, only one multicast packet coming from an input can be stored at a time. Using the modified multicast module, up to *k*-1 wavelengths could be used to route the multicast packets from the same input into the same multicast module, i.e., up to *k*-1 multicast packets coming from the same input can be stored in the loop buffer of the same modified multicast module concurrently without wavelength collision. Therefore, the utilization of the modified multicast module can be considerably enhanced, and the use of the modified multicast modules is expected to improve the traffic performance of the wavelength-routed multicast packet switch without adding more multicast modules.

Although increasing the value of *k* might lead to more multicast packets to be stored in a modified multicast module, the power loss of optical signal incurred by the $k \times 2$ optical coupler in the loop buffer of the modified multicast module is also increased with the value of *k*. Hence, the signal power of an incoming multicast packet before

entering the loop buffer should be increased accordingly so that when it is selected out of the loop buffer, its power can be maintained at the same level as the pump for the subsequent multi-wavelength converter. Furthermore, the gain provided by the EDFA in the loop buffer has to be adjusted to compensate the power loss of a multicast packet of each circulation in the modified multicast module.

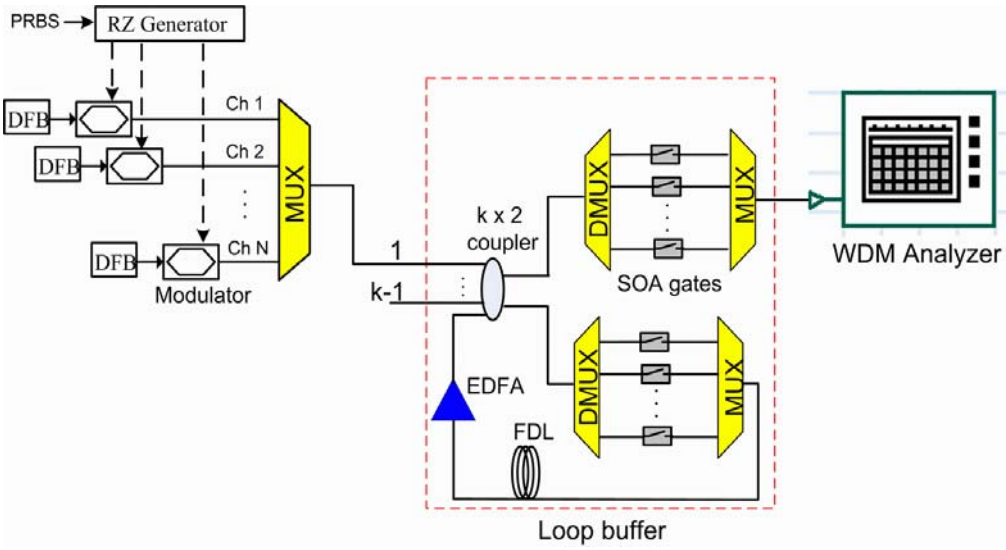

Figure 3-26: Measurement of OSNR of the multicast packets circulating in loop buffer of the modified multicast module

In order to examine the characteristics of the modified multicast module, the OSNR of multicast packet signals circulating in the loop buffer of the modified multicast module is evaluated through simulation. The simulation software used is the OptiSystem 7.0 [198]. The simulation setup is illustrated in **Figure 3-26**. The input multicast signals are generated by a group of *N* DFB lasers with 100 GHz channel spacing, each of which is modulated with 2^{23}-1 return-to-zero (RZ) pseudorandom binary sequence (PRBS) at a rate of 10 Gbit/s by an external Mach-Zehnder intensity

modulator. The noise figures of the EDFA and SOA gates in the loop buffer are set to 5 dB and 7 dB, respectively. The fiber delay line in the loop buffer provides one timeslot delay (880 ns) of one circulation.

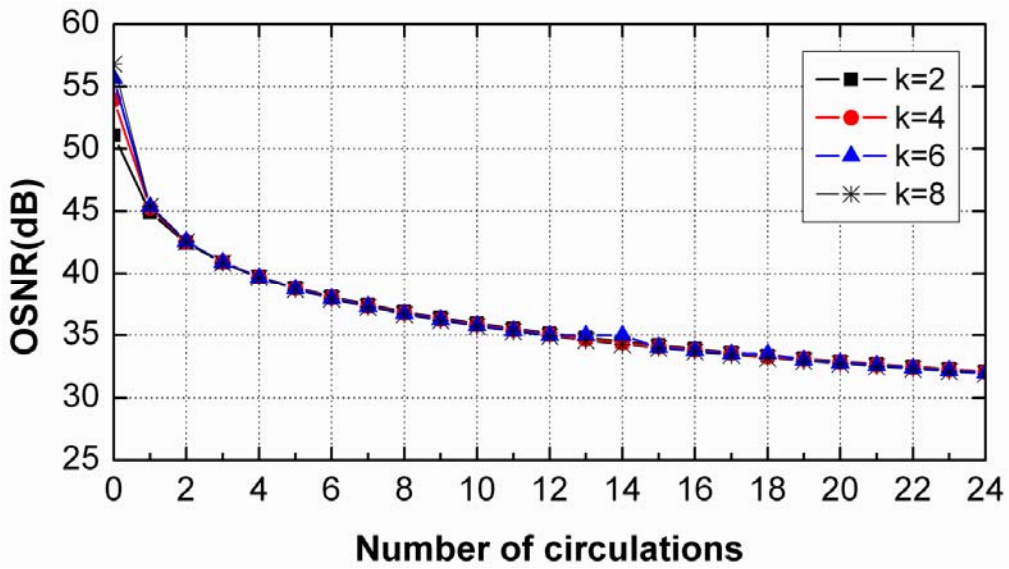

Figure 3-27: The worst OSNR among 8 channels in the loop buffer of a modified multicast module with various values of *k*

Figure 3-27 shows the worst OSNRs among 8 multicast signals at different wavelengths (from 1547.72 nm to 1553.52 nm) versus the number of circulations in the loop buffer of the modified multicast module with different values of *k*. The input power of each multicast signal is set to 3.2, 6.2, 7.8 and 9.2 dBm for *k*=2, 4, 6, and 8, respectively. This is to ensure that the power of the multicast signal entering the subsequent multi-wavelength converter (not shown in **Figure 3-26**) could be maintained at about 0.2 dBm. The gain of the EDFA in the loop buffer is adjusted according to the value of *k* for compensating the power loss in the loop buffer. It is

observed that the OSNRs of the multicast signal are rapidly decreased with the number of circulations increasing and then such deterioration slows down after a few circulations. Similar results can also be observed for the case of 16 wavelengths as shown in **Figure 3-28.**

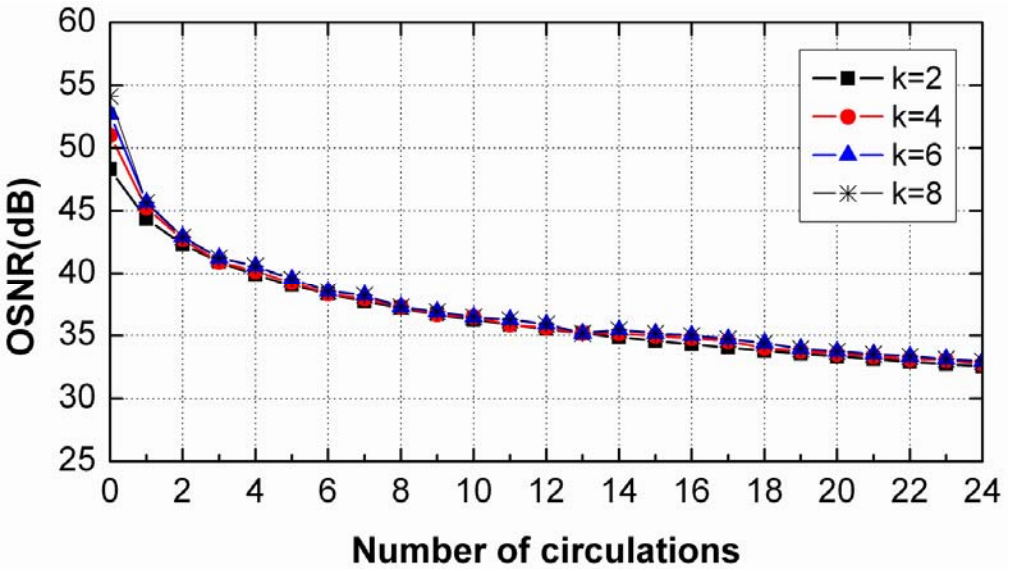

Figure 3-28: The worst OSNR among 16 channels in the loop buffer of a modified multicast module with various values of *k*

It is interesting to find in both of **Figures 3-27** and **3-28** that the deterioration of the SONR is almost independent of the value of *k*, which means that the value of *k* does not affect the signal quality of multicast packets. This can be explained as follows. On one hand, an increase in the value of *k* would result in an increase in the power loss induced by the $k\times 2$ optical coupler in the modified multicast module, although such loss can be compensated by accordingly increasing the gain of EDFA, it would also increase the ASE noise power in the loop buffer. On the other hand, the power of input optical signal entering the loop buffer would be increased accordingly with the value of *k* increasing. Therefore, the resultant OSNR is maintained at almost the same level.

In this case, the extra increased power of the input optical signal might be regarded as a power penalty associated with the value of *k*.

However, since the ASE noise would be accumulated gradually with the increasing number of circulations, which would result in a deterioration of OSNR, and such deterioration would in turn degrade the signal quality of the converted packets in the subsequent multi-wavelength converter, the number of circulations for a multicast packet in the loop buffer must be controlled. In light of the study in [193], an acceptable BER performance can be achieved if the number of circulations is no greater than 16.

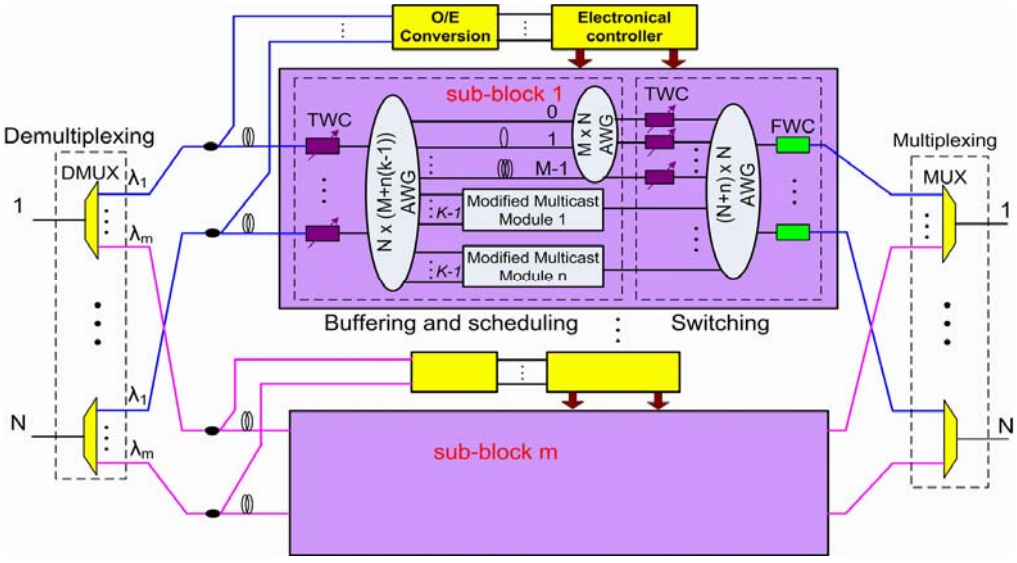

Figure 3-29: Architecture of the modified wavelength-routed multicast packet switch

Figure 3-29 shows the architecture of the newly modified wavelength-routed multicast packet switching using the modified multicast modules. The size of the first AWG in the buffering-scheduling section of a sub-block is changed to $N\times(M+n(k-1))$. The operation principle of the modified switch is also similar to that of the previous switch as introduced in Section 3.2. In order to examine the enhancement on the packet loss performance of the multicast switch by the improved design, the packet loss probabilities of the previous and modified multicast packet switches are compared through simulations. The previous multicast packet switch can be treated as a particular case of the modified switch with k=2.

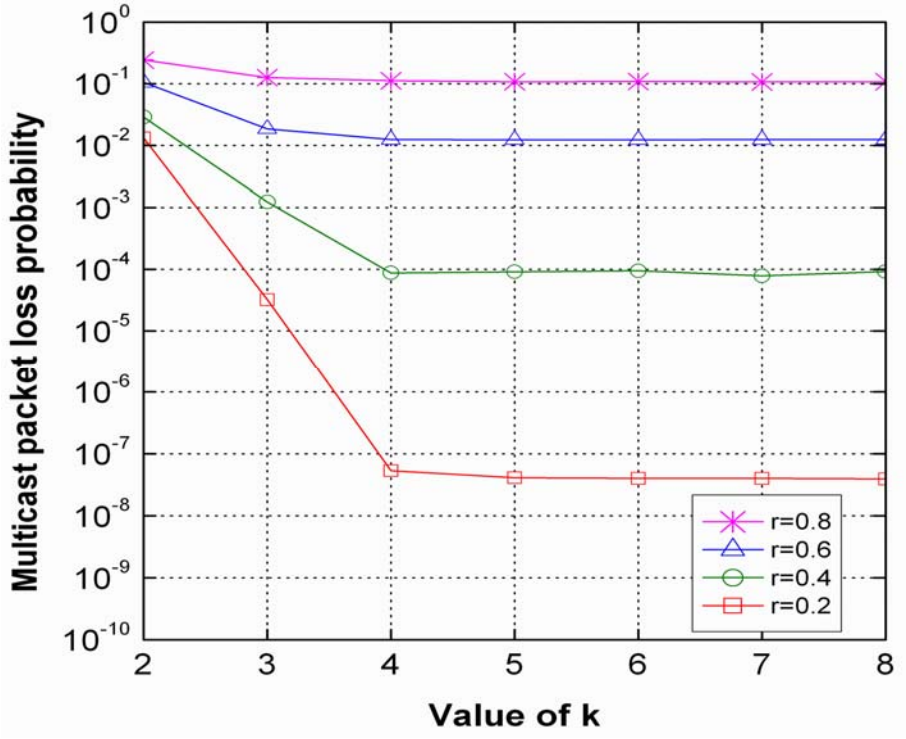

Figure 3-30: Multicast packet loss probability versus the value of k of an 8×8 modified multicast switch with different values of r when T_m=12, n=2, M=8 and ρ_{eff}=0.8

The effect of the value of k on the packet loss probability is firstly examined. **Figure 3-30** shows the multicast packet loss probability versus the value of k for an 8×8 (N=8) modified multicast switch with two modified multicast modules (n=2) per sub-block, where the effective total traffic load is ρ_{eff}=0.8 with multicast traffic ratio r=0.2. The number of FDLs is M=8, and the T_m is set to 12 timeslots. It is found that with a fixed multicast traffic ratio r, the multicast packet loss probability is reduced by a slight increase in the value of k and then becomes constant when k≥4.

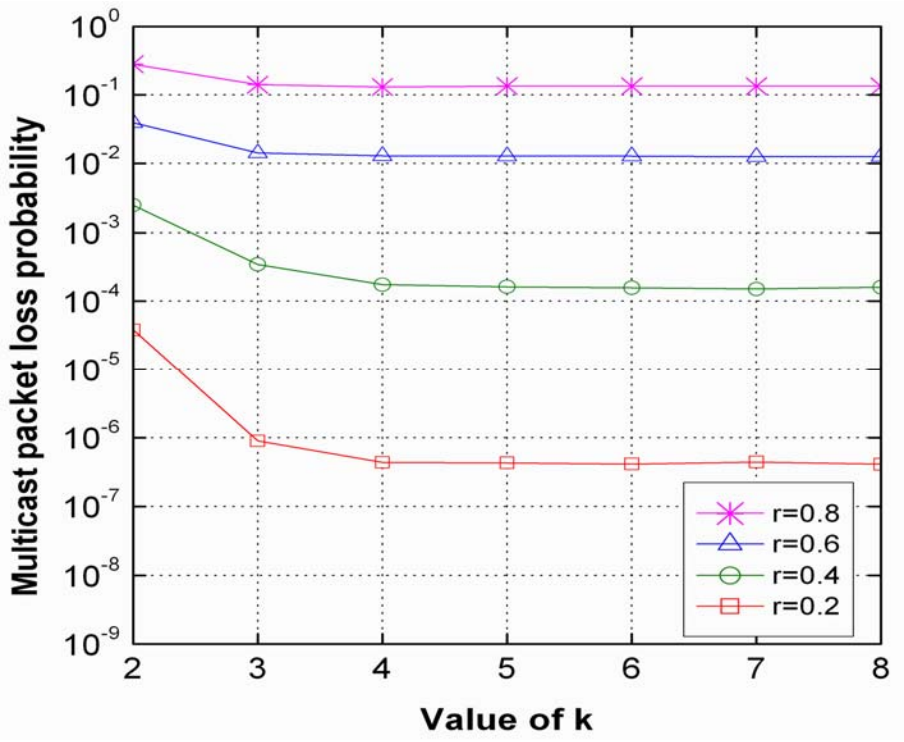

Figure 3-31: Multicast packet loss probability versus the value of k of a 16×16 modified multicast switch with different values of r when T_m=12, n=4, M=8 and ρ_{eff}=0.8

Similar results can also be observed for a 16×16 (N=16) modified multicast switch with n=4 in **Figure 3-31**. This effect is due to the reason that though increasing the value of k can help store more multicast packets coming from the same input in a

modified multicast module concurrently, there should be a maximum number of multicast packets that can be stored in the loop buffer due to the restriction of T_m and available wavelength resources; once this maximum number is reached by increasing k to a certain value, the multicast packet loss probability will also reach a fixed level. In such case, further increasing k cannot reduce the multicast packet loss probability but will incur a greater input power penalty as discussed in the previous section. On the other hand, this feature suggests an optimum k for the modified multicast switch to achieve a multicast packet loss probability as low as possible without considerably increasing the complexity. It is also found that the improvement of multicast packet loss probability by increasing the value of k is more apparent when the multicast traffic ratio r is smaller.

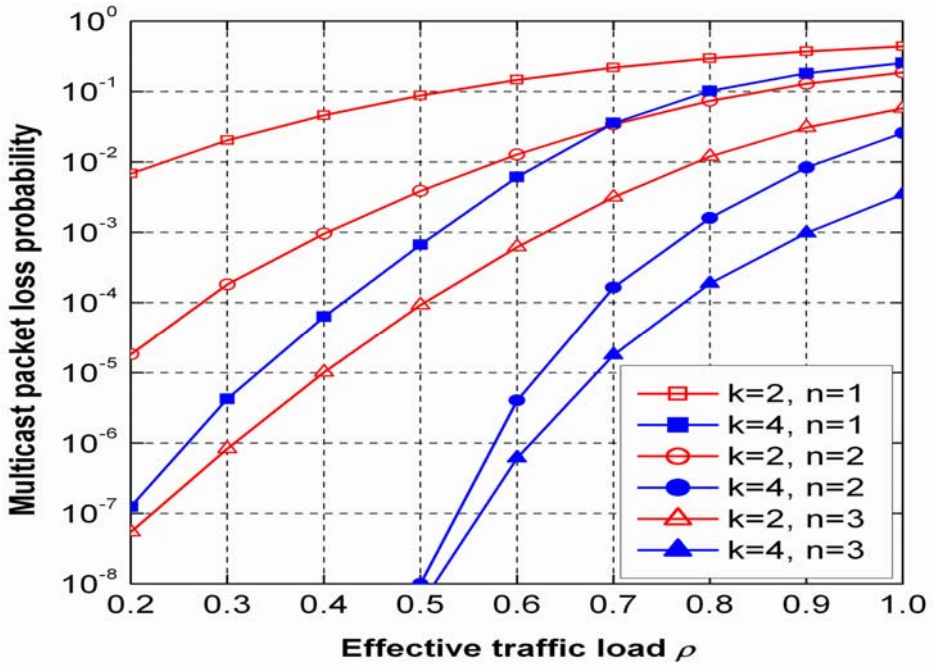

Figure 3-32: Multicast packet loss probability versus the effective total traffic load for an 8×8 modified wavelength-routed multicast packet switch with various values of k and n when T_m=12, M=8, $E(X)$=3 and r=0.5

Next, we evaluate the multicast, unicast and total packet loss probability versus the effective traffic for an 8×8 modified multicast switch, respectively. The multicast traffic ratio is fixed at r=0.5 with $E(X)$=3, and the number of FDLs is 8 (M=8) and T_m= 12. As shown in **Figure 3-32**, the multicast packet loss probability of the modified switch is reduced as the value of n increases; and the multicast packet loss probability for the case of k=4 and n=2 is even lower than that of the switch for the case of k=2 and n=3 under the same effective traffic load. This means, to improve the multicast packet loss probability for the switch, it is more effective to use a multicast module with an optical coupler with a larger number of inputs instead of adding more multicast modules.

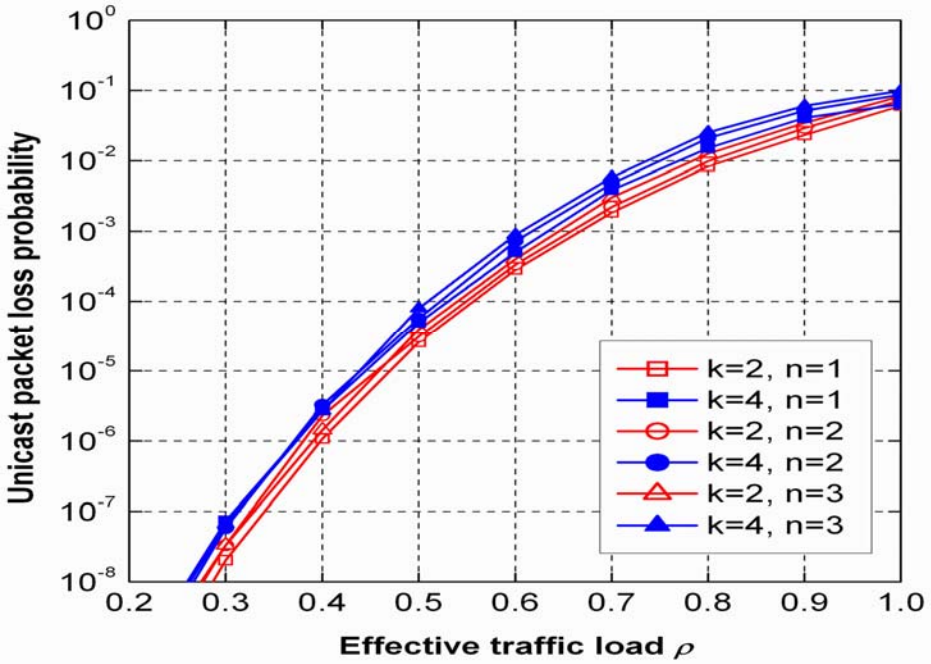

Figure 3-33: Unicast packet loss probability versus the effective total traffic load for an 8×8 modified wavelength-routed multicast packet switch with various values of k and n when T_m=12, M=8, $E(X)$=3 and r=0.5

In **Figure 3-33**, the unicast packet loss probability of the modified switch is almost independent of the values of *n* and *k*, though there is a slight degradation when *n* and *k* are increased. This is because the incoming unicast packets are handled only by the FDLs, an increase in the value of *k* cannot reduce the unicast packet loss probability for the switch.

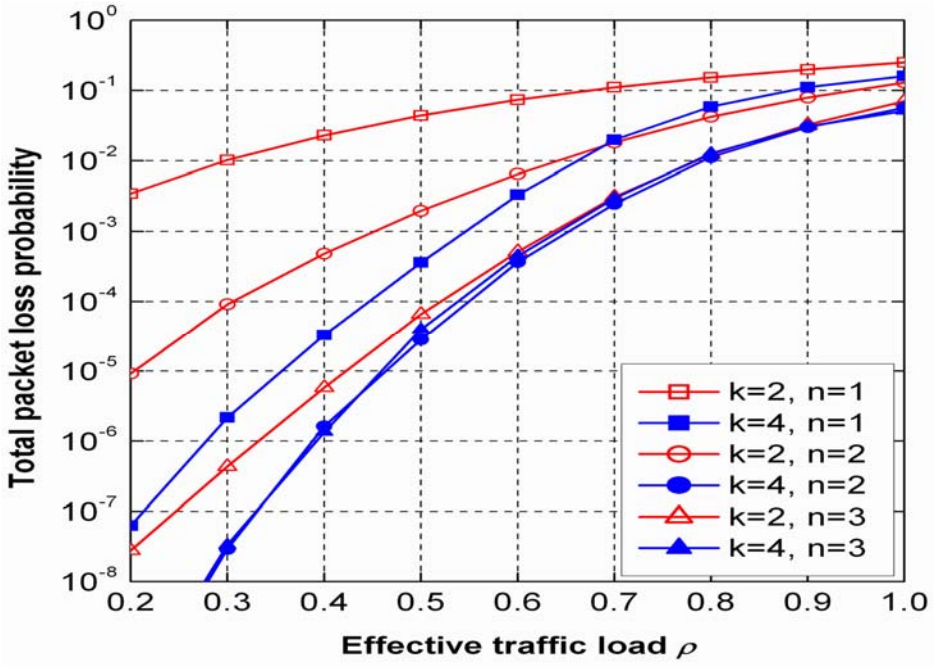

Figure 3-34: Total packet loss probability versus the effective total traffic load for an 8×8 modified wavelength-routed multicast packet switch with various values of *k* and *n* when T_m=12, *M*=8, *E(X)*=3 and *r*=0.5

On the other hand, the total packet loss probability of the switch, as shown in **Figure 3-34**, is determined by both of multicast and unicast packet loss probabilities. It is found that without increasing the value of *n*, the total packet loss probability of the switch can still be reduced by a slight increase in the value of *k* as the multicast packet loss probability is significantly reduced. It is also found that the total packet loss probability for the case of *k*=4 and *n*=2 is quite close to that for the case of *k*=4 and *n*=3. This is because the multicast packet loss probability is much lower than the

unicast packet loss probability, which means that the unicast packet loss probability is dominant in the total packet loss probability.

The switch scalability before and after the improved design is also discussed. Figure 3-35 compares the number of multicast modules and number of SOA gates used in the multicast switch before (k=2) and after the improvement (k=4) to achieve 10^{-6} multicast packet loss probability when ρ_{eff}=0.8. The multicast traffic ratio is fixed at 0.2, and the number of FDLs is 8. Note that since a multicast module contains $3N$ SOA gates, the total number of SOA gates in the switch is $3nN$, where n is the number of multicast modules. It can be seen that although the switch with larger size may need more multicast modules to achieve a targeted packet loss probability, the use of the improved design can cut down the required number of multicast modules, leading to a reduction in the number of SOA gates.

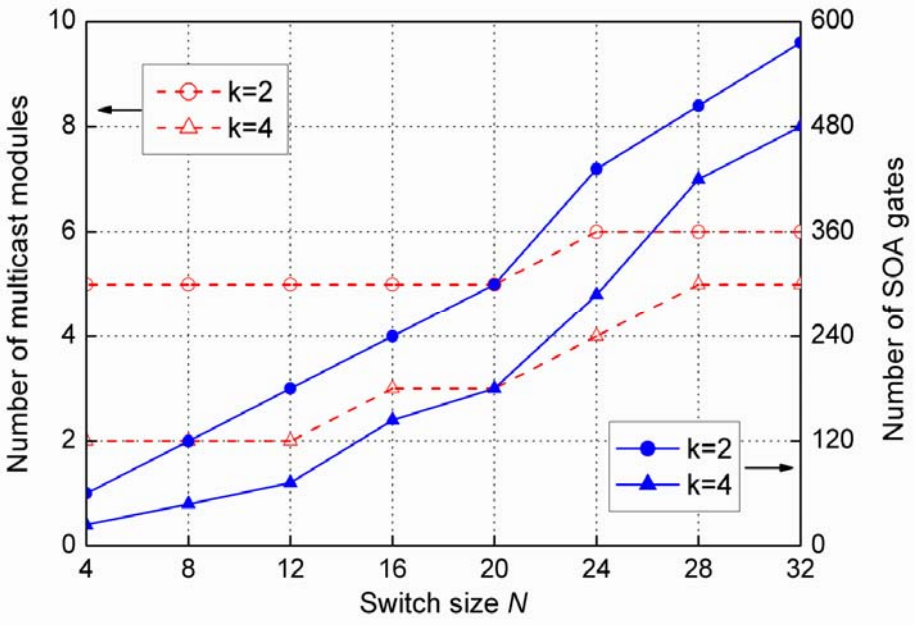

Figure 3-35: Number of multicast modules (left axis) and number of SOA gates (right axis) used in the multicast switch to achieve 10^{-6} multicast packet loss probability when ρ_{eff}=0.8

3.8 Summary

In this chapter, a wavelength-routed multicast packet switch utilizing multicast modules was proposed and investigated. The novelty of the multicast module is that it allows a multicast packet to be duplicated in multicast timeslots to reduce packet contention, and the copies of a multicast packet can be routed to their desired outputs without going through tunable wavelength converters like unicast packets. A packet scheduling technique was presented to resolve packet contention for the switch. The physical performance metrics such as bit-error-rate, extinction ratio, and spectral characteristic of the multicast module were examined by simulation. It was found that the signal quality could be maintained within an acceptable level if a multicast packet was stored for no more than 16 timeslots in a multicast module. Various traffic performance of the wavelength-routed multicast packet switch was investigated by simulation. The results showed that the multicast packet loss probability could be significantly reduced by a slight increase in the number of multicast modules. However, due to wavelength collision, the multicast module cannot concurrently store two or more multicast packets coming from the same input of the switch, resulting in a low utilization of the multicast module. To eliminate this limitation, an improved design was proposed for the switch by modifying the multicast modules rather than adding more multicast modules. The modified multicast module allows more multicast packets arriving from the same input to be stored in the loop buffer of the multicast module. Traffic performance in terms of packet loss probability of the modified switch was also examined by simulations. The results showed that the use of the modified multicast modules could significantly reduce the multicast packet loss probability without increasing the number of multicast modules, which could lead to a great reduction in the implementation cost for the switch.

Chapter 4
Wavelength-Routed Multicast Packet Switch with Shared FDLs Buffer

4.1 Introduction

The wavelength-routed multicast packet switch studied in Chapter 3 utilizes the multicast modules to achieve packet multicasting and buffering, where the copies of a multicast packet are allowed to be made in multiple timeslots by storing the multicast packet in a loop buffer to avoid output contention, and to be directly switched to the desired output ports without going through any more tunable wavelength converters. It is shown that the multicast packet loss probability of the switch can be considerably reduced when the copies of a multicast packet are allowed to be made in multiple timeslots, rather than in a single timeslot. The switch, however, can handle only a small proportion of multicast traffic, since the packet loss performance would be deteriorated with the increase of multicast traffic. Furthermore, the unicast packets are handled by a set of fiber delay lines (FDLs) that act as a buffer (referred to as an FDL buffer), while the multicast packet are stored in multicast modules each consisting of a

loop buffer, thus these two types of buffers cannot be shared, resulting in a low utilization of the buffers.

In this chapter, to eliminate these restrictions, we propose a wavelength-routed multicast packet switch with a shared-FDL buffer, in which both unicast and multicast packet can share a set of FDLs for buffering, and the copies of a multicast packet are allowed to be made in multiple timeslots by means of multi-wavelength conversion in conjunction with the shared-FDL buffer [205-207]. The rest of this chapter is organized as follows. Section 4.2 presents the architecture and operation of the newly proposed wavelength-routed multicast packet switch. In Section 4.3, a packet scheduling technique is designed to assist contention resolution for the switch. In Section 4.4, the traffic performance of the switch is evaluated in comparison with other multicast switches through simulation. Section 4.5 investigates the complexity of the newly proposed switch. Finally, the conclusions are drawn in Section 4.6.

4.2 Architecture and Operation

The architecture of the wavelength-routed multicast packet switch with a shared-FDL buffer is shown in **Figure 4-1**, which is derived from the wavelength-routed unicast packet switch in [50, 51]. The switch having N input/output ports consists of a controller, a buffering section, and a switching section. The switch is assumed to be operated synchronously. That is, packets of fixed length T arrive at the inputs of the switch on a timeslot-by-timeslot basis. Here, we also assume that the incoming packet stream at each input port consists of unicast and multicast packets. The operation of the switch is described as follows.

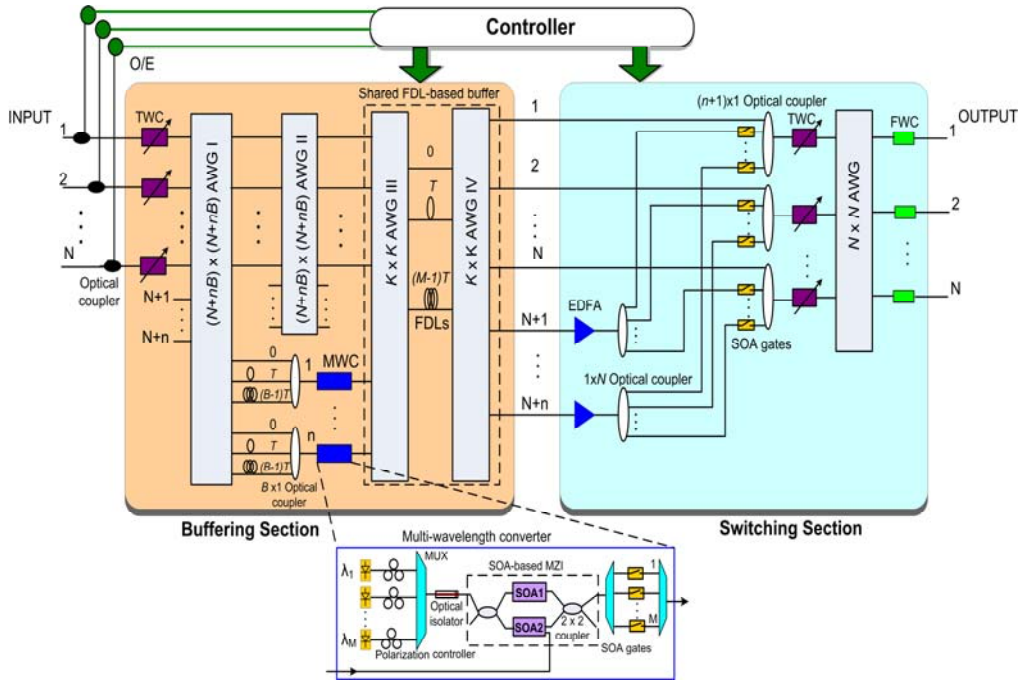

Figure 4-1: Architecture of the wavelength-routed multicast packet switch with a shared-FDL buffer

As shown in **Figure 4-1**, at each input port, a small portion of an incoming optical packet signal is tapped out by an optical coupler, and then converted into an electronic signal that is to be collected in the switch controller used for performing packet scheduling and configuring the TWCs and SOAs in both the buffering section and the switching section. The buffering section is composed of a set of N TWCs, two identical $(N+n)\times(N+n)$ AWGs (AWG I and AWG II), n MWCs, a set of FDLs and a $B\times1$ optical coupler placed in front of each MWC, and a shared-FDL buffer constructed by two identical $K\times K$ AWGs (AWG III and IV) and a set of M fiber delay lines which offer delay time varying from 0 to $(M\text{-}1)T$, where T is the duration of a timeslot, and $K=\max(N+n, M)$. Note that since AWG I and AWG II are identical, according to the operation of AWG [50, 51], a unicast packet entering from the ith ($1 \le i \le N$) input port of AWG I will always leave from the ith ($1 \le i \le N$) output port of

AWG II, regardless of its wavelength. Similarly, a unicast packet entering from the *i*th ($1 \le i \le N$) input port of AWG III will always leave the buffering section from the *i*th output port of AWG IV after receiving a certain delay determined by its wavelength, which is given by the corresponding TWC placed in front of AWG I. For an incoming multicast packet, it will be routed by the corresponding TWC placed in front of AWG I to receive a certain delay time before it is converted in an MWC. The MWC, as shown in **Figure 4-1**, is realized based on the cross-phase modulation in a semiconductor optical amplifier (SOA)-based Mach-Zehnder interferometer (MZI), which has been discussed in Chapter 3. The function of the MWC is to concurrently make multiple copes with different wavelengths of the original multicast packet, and the wavelengths of these copies are dedicated so that they can be routed to the subsequent fiber delay lines in the shared-FDL buffer to receive respective delay time, providing multiple delay time for the original multicast packet. Similar to a unicast packet, the copies of a multicast packet entering the shared-FDL buffer from the *j*th ($N+1 \le j \le N+n$) input port of AWG III will leave from the *j*th output of AWG IV after receiving respective delay times in the buffer.

As shown in **Figure 4-1**, the switching section has ($N+n$) inputs and N outputs. The first N inputs carry unicast packets, while the last n inputs carry multicast packets. It consists of n EDFAs, n $1 \times N$ optical couplers, a set of SOA gates, N $(n+1)\times 1$ optical couplers, N TWCs, a $N \times N$ AWG as well as N fixed FWCs. A unicast packet entering the switching section from the *i*th ($1 \le i \le N$) input will be directly routed to its desired output by a TWC and the $N \times N$ AWG; while a multicast packet entering the switching section from the *j*th ($N+1 \le j \le N+n$) input will be first pre-amplified by an EDFA, and then split into N copies by a $1 \times N$ optical coupler, only desired copies will be selected

by the subsequent SOA gates and routed to their respective outputs. At the output side of the switching section, both unicast packets and copies of multicast packets will be wavelength converted by the FWCs before they are transmitted to the output ports of the switch. Since the optical couplers in the switching section would induce power loss to multicast packets, the EDFA gain should be adjusted to compensate the power loss.

In comparison with the multicast packet switch utilizing multicast modules studied in Chapter 3, the present multicast packet switch provides a shared-FDL buffer for both incoming unicast and multicast packets, and also the copies of a multicast packet could be made in multiple timeslots to reduce packet contention by means of multi-wavelength converters and the shared-FDL buffer, which is more efficient in resolving packet contention.

4.3 Packet Scheduling Technique

To avoid packet contention in the present wavelength-routed multicast packet switch with a shared-FDL buffer, the packets arriving at the input ports of the switch need to be scheduled before they enter the switch. The present switch can also be modeled as a time-space-time (TST) switch as shown in **Figure 4-2**. It consists of $N+n$ input timeslot interchanges (TSIs), N output TSIs, and a switching section. Among the $N+n$ input TSIs, the first N identical TSIs are used for storing unicast packets, each of which contains M timeslots corresponding to the M FDLs in the shared FDL buffer; and the remaining n identical TSIs are used for handling multicast packets, corresponding to the n multi-wavelength converters in the switch, and each of these n TSIs contains $B+M$ timeslots, corresponding to the B FDLs placed in front of each

multi-wavelength converter and the *M* FDL in the shared FDL buffer. At the output ports of the switch, each output TSI contains *L* timeslots, where *L=B+M*-1.

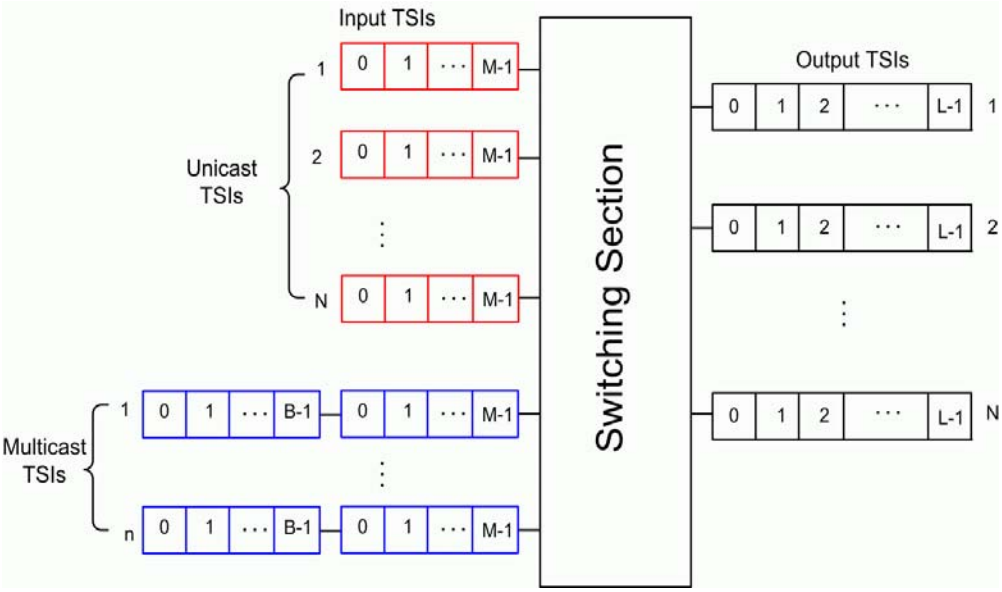

Figure 4-2: TST switch model representing the wavelength-routed multicast packet switch with a shared-FDL buffer

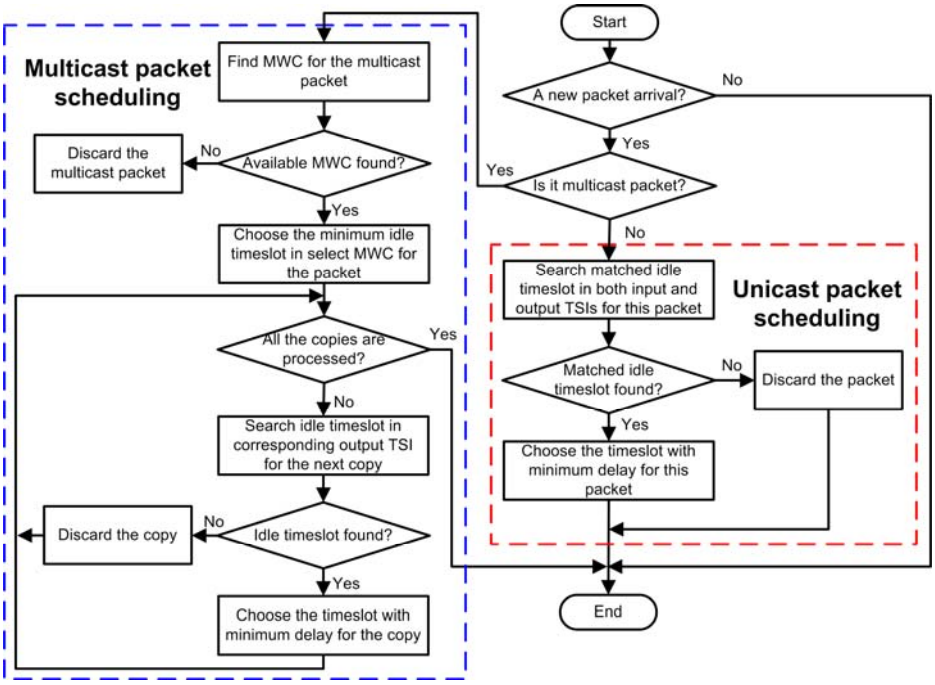

Figure 4-3: Flow chart of the packet scheduling technique of the present switch

Unlike the multicast switch in Chapter 3 where unicast and multicast packets are stored in two different types of buffers and hence are treated differently, the multicast switch proposed in this Chapter uses only FDLs to buffer both unicast and multicast packets, and there is no priority setting between these two types of packets. The scheduling would be easier to be performed. In each timeslot, packets arriving at the different input ports are scheduled in accordance with the Round-Robin scheme. The flow char of the packet scheduling technique for the switch is illustrated in **Figure 4-3**. At each input port, the switch will perform the corresponding scheduling technique (unicast packet scheduling or multicast packet scheduling) according to the type of the packet.

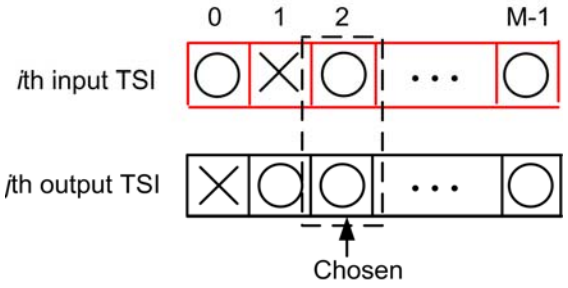

Figure 4-4: Assignment of idle timeslots for a unicast packet

For an arbitrary unicast packet at input *i* destined for output *j*, as shown in **Figure 4-4**, the switch performs the unicast packet scheduling by two steps. Firstly, search matched idle timeslots in both the *i*th input TSI and the *j*th output TSI for this packet. Secondly, if there is no such timeslot, the packet will be discarded; if there are multiple matched idle timeslots, the one with minimum delay will be chosen for this packet.

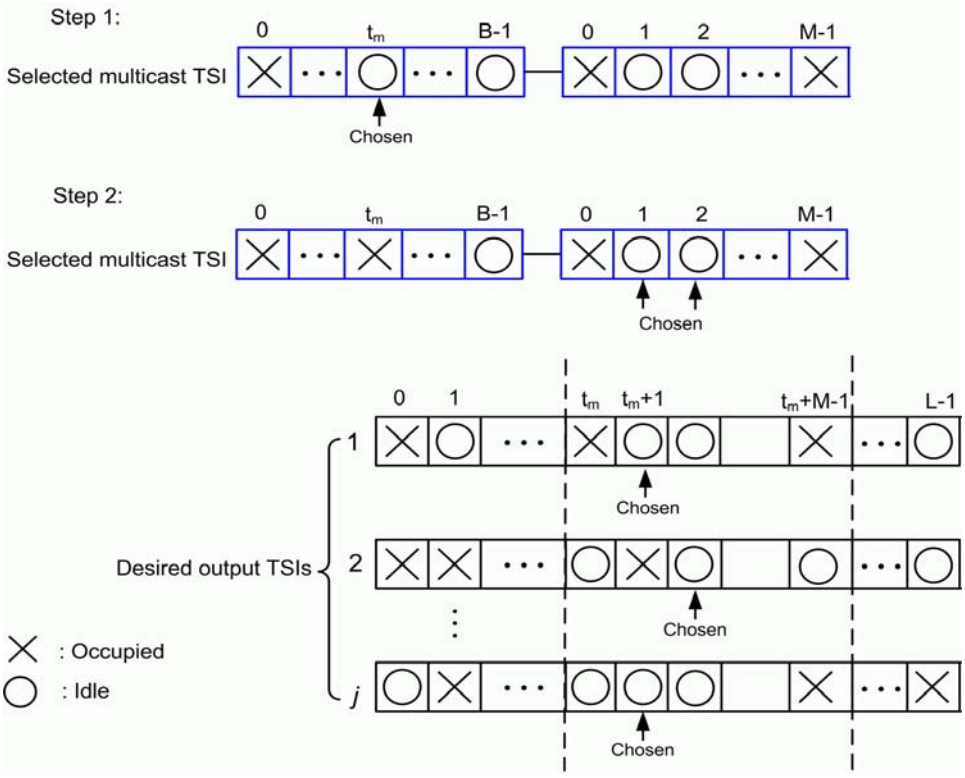

Figure 4-5: Assignment of idle timeslots for a multicast packet

For an arbitrary multicast packet at input *i* destined for multiple outputs, as shown in **Figure 4-5**, the switch performs the multicast packet scheduling by two steps:

Step 1**:** Find an available multicast TSI and choose the minimum timeslot t_m ($0 \le t_m \le B$-1) in the first part of the input multicast TSI to store the multicast packet. If there is no such multicast TSI, the multicast packet will be directly discarded.

Step 2**:** Search matched idle timeslots in the second part of the selected input multicast TSI and desired output TSIs for all the copies of the multicast packet. A copy that cannot be given any matched idle timeslot will be discarded. If there are multiple idle timeslots for a copy, the one with minimum delay will be chosen.

4.4 Traffic Performance Evaluation

To evaluate the traffic performance, the proposed multicast switch (referred to as the present switch) is compared with the broadcast-and-select switch (referred to as the BS switch) in [31] and the wavelength-routed multicast packet switch utilizing multicast modules studied in Chapter 3 (referred to previously studied switch). Note that the BS switch is a pure output-queued switch with a shared buffer and hence achieves the best traffic performance. As such the BS switch is selected for the comparison in this study.

In the simulation, all the three switches have N input ports and N output ports. The number of wavelengths per input/output port is 1 (m=1). For the previously studied switch shown in **Figure 3-3**, M is the number of FDLs used for buffering unicast packets, while for the present switch and the BS switch, there are M FDLs shared by both unicast and multicast packets. More specifically, the number of FDLs placed in front of each MWC in the present switch is set to 3 (B=3), as a greater value of B would induce more extra power loss to multicast packets before they are fed to MWCs. n is the number of the MWCs used in the present switch and the previously studied switch in Chapter 3. Note that for the previously studied switch, since the multicast packets are stored in loop buffers, the max number of timeslots for a multicast to store in a loop buffer is set to be 12 timeslots to maintain a tolerable signal quality [193].

The traffic model studied in Section 3.6 is employed in the simulation for the three switches. It is assumed that the packet arrivals at all the inputs are of independent and identical Bernoulli processes. A unicast packet is equally likely to be destined for any

output of the switch; and the copies of a multicast packet are uniformly distributed over all the outputs of the switch, but no two or more copies are destined for the same output. The number of copies of a multicast packet follows a truncated geometric distribution, and the average number of copies for a multicast packet is set to $E(X) = 4$ for all simulation scenarios.

The packet loss probability versus the effective total traffic load for the three switches is shown in **Figures 4-6, 7 and 8**, where the switch size N=8, 16, and 32, respectively. The multicast traffic ratio is r=0.5 (50%), the number of FDLs is M=12, and the number of MWCs is n=4. When the switch size N=8 as shown in **Figure 4-6**, given an effective total traffic load and the same values of M and n, the packet loss probability of the present switch is consistently lower than that of the switch utilizing multicast modules, and it is almost the same as that of the broadcast-and-select switch. Similar results can also be observed in **Figure 4-7** when N=16.

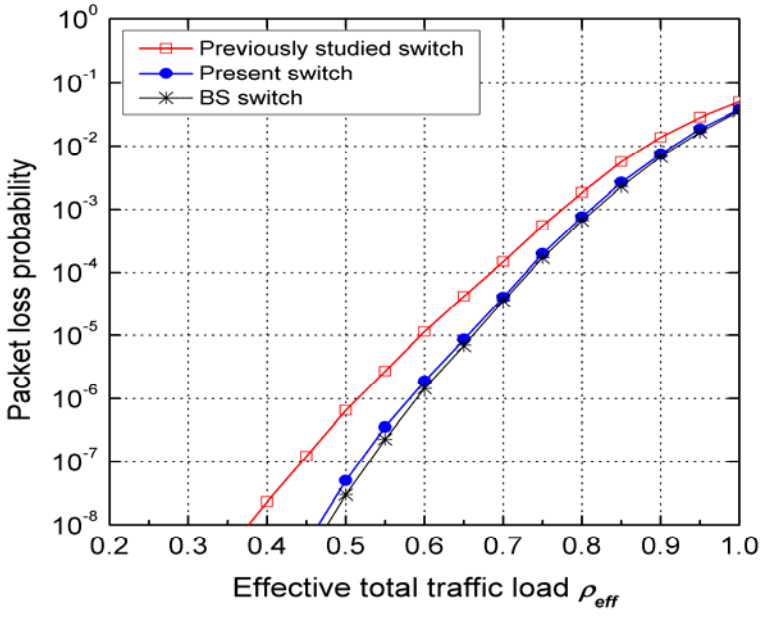

Figure 4-6: Packet loss probability versus the effective total traffic load for three switches with N=8

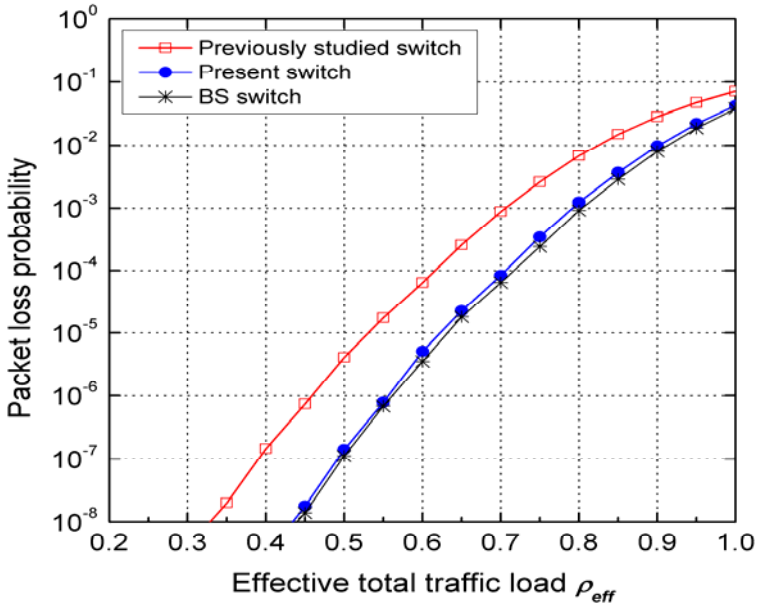

Figure 4-7: Packet loss probability versus the effective total traffic load for three switches with *N*=16

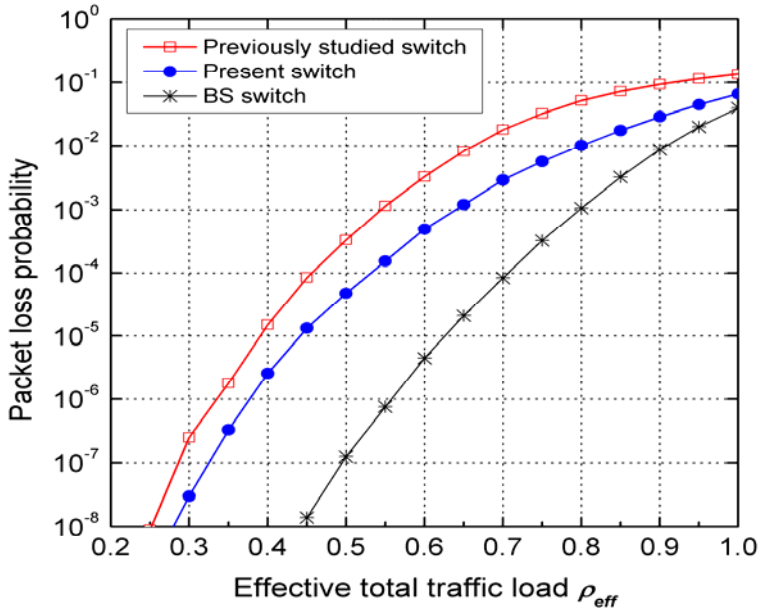

Figure 4-8: Packet loss probability versus the effective total traffic load for three switches with *N*=32

However, when the switch size increases to 32 (N=32) as shown in **Figure 4-8**, the packet loss probabilities of the present switch and the previously studied switch both become worse, but the packet loss probability of the BS switch is lower than both of them.

For both of the present switch and the previously studied switch, since the MWCs are shared by all the input multicast packets for storing, and each MWC can only handle one multicast packet in a timeslot, once all the MWCs are occupied, the subsequent multicast packets will be dropped. Hence, an increase in the switch size N with a fixed effective total traffic load will lead to more multicast packets arriving at the inputs of the switch concurrently, resulting in an increase of the packet loss probability. On the other hand, with the same values of N, M and n, the present switch achieves lower packet loss probability than the previously studied switch under the same effective total traffic load. This is because in the previously studied switch, a multicast packet is being stored in a loop buffer until all of its copies have been made by a MWC, which means that this MWC might be occupied by a multicast packet in multiple times so that its copies could be made in multiple timeslots to reduce output contention. Differently, in the present switch, a multicast packet can be replicated in multiple timeslots by only once multi-wavelength conversion in conjunction with the subsequent shared-FDL buffer, i.e., the MWCs in the present switch can accept more multicast packets than the previously studied switch, leading to a significant reduction in the packet loss probability.

Next, the effect of the multicast traffic ratio on packet loss performance is inspected. We compare the packet loss probability as a function of the multicast traffic ratio for

the three switches when the effective total traffic load is 0.8 (ρ_{eff} = 0.8), where the switch size N=16, and the number of FDLs is M=27. For the previously studied switch as shown in **Figure 4-9**, the packet loss probability increases rapidly as the multicast traffic ratio grows. This is because that an increase of the multicast traffic ratio will result in more multicast packets concurrently arriving at the inputs of the switch. It is also shown that increasing the value of n (number of MWCs) can help store more input multicast packets for avoiding output contention, leading to a reduction in packet loss probability; however, once the packet loss probability at a given multicast traffic ratio is reduced to a certain level, it cannot be further reduced by increasing the value of n. This is due to the limited timeslots for a multicast packet to be stored in the loop buffer; the previously studied switch can only handle a small proportion of multicast traffic.

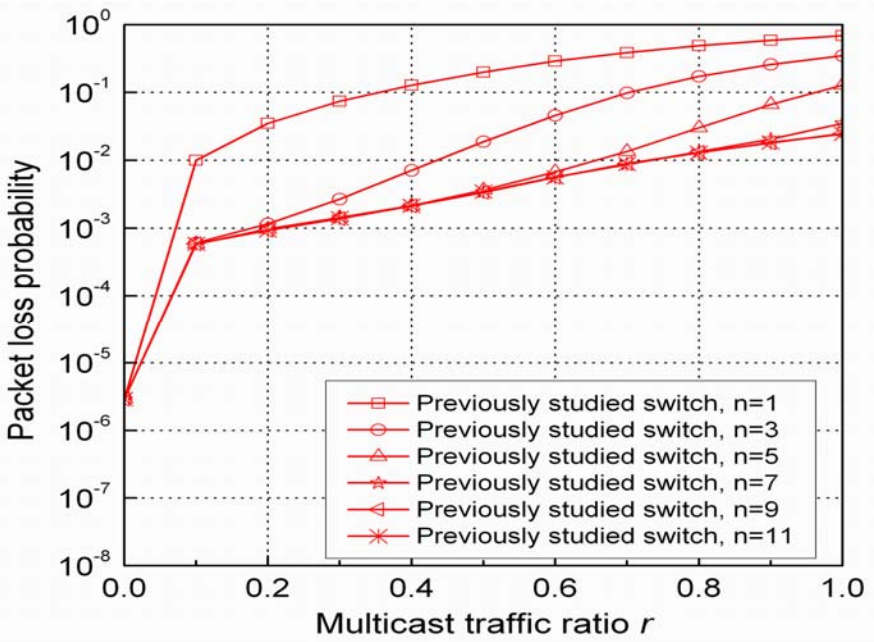

Figure 4-9: Packet loss probability as a function of multicast traffic ratio for the previously studied switch when the effective total traffic load ρ_{eff} = 0.8

As shown in **Figure 4-10**, the packet loss probability of the present switch also increases with the multicast traffic ratio increasing when the value of n is small (e.g., n=1), but a slight increase in the value of n can lead to a significant reduction in the deterioration of packet loss probability. It is shown that when n=7, the packet loss probability will be very close to the level of the BS switch. It is noted that since the BS switch is a pure output-queued switch, its packet loss probability can be calculated by using the analytical model introduced in Chapter 5. It is found that the packet loss probability of the BS switch depends on the effective total traffic load rather than the multicast traffic ratio.

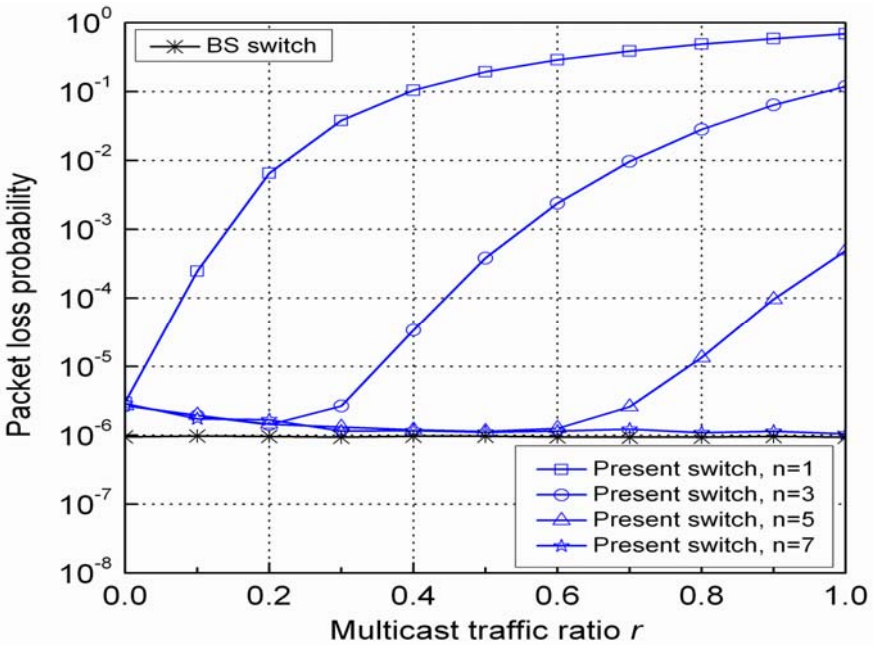

Figure 4-10: Packet loss probability as a function of multicast traffic ratio for the present switch and broadcast-and-select switch when the effective total traffic load ρ_{eff} = 0.8

Figures 4-11 (a)-(d) show the average packet delay versus the effective total traffic load for the three switches when the multicast traffic ratio r=0.2, 0.5, 0.8, and 1.0, respectively. Here the switch size is N=16, the number of FDLs is M=12, and the number of MWCs is n=4. It is observed that when r=0.2, as shown in **Figure 4-11 (a)**, the average delay for the previously studied switch is close to that of the present switch; when the multicast traffic ratio r increases, the average delay for the previously studied switch would considerably increases, while the average delay for the present switch does not change significantly. This may be due to the following reasons. On one hand, in the previously studied switch, although the copies of a multicast are allowed to be made by a MWC in multiple timeslots to reduce output contention, the MWC might be occupied by a multicast packet in multiple timeslots, which would result in a multicast packet being stored for more timeslots in a loop buffer when the multicast traffic is increased. On the other hand, in the present switch, since an MWC is occupied by a multicast packet in only one timeslot, and only a few FDLs is placed in front of each MWC for storing the contending multicast packets, an increase of the multicast traffic would not have significant effect on the average delay for the present switch. Among the three switches, the BS switch achieves the smallest average delay at a given effective total traffic load, regardless of the multicast traffic ratio.

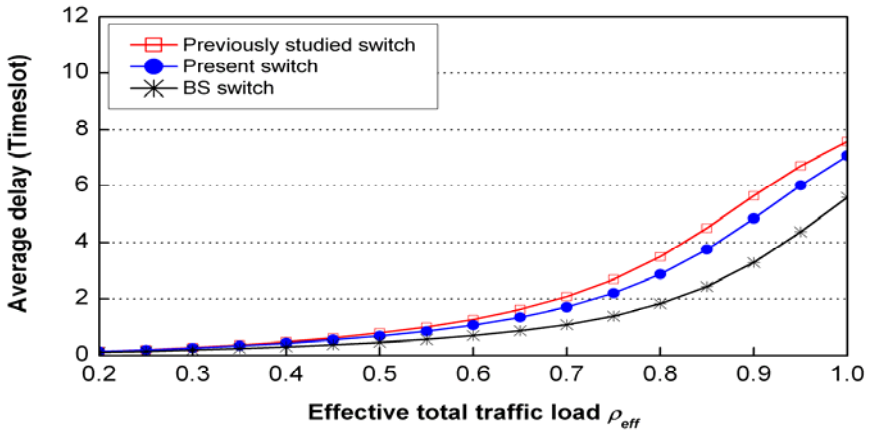

(a)

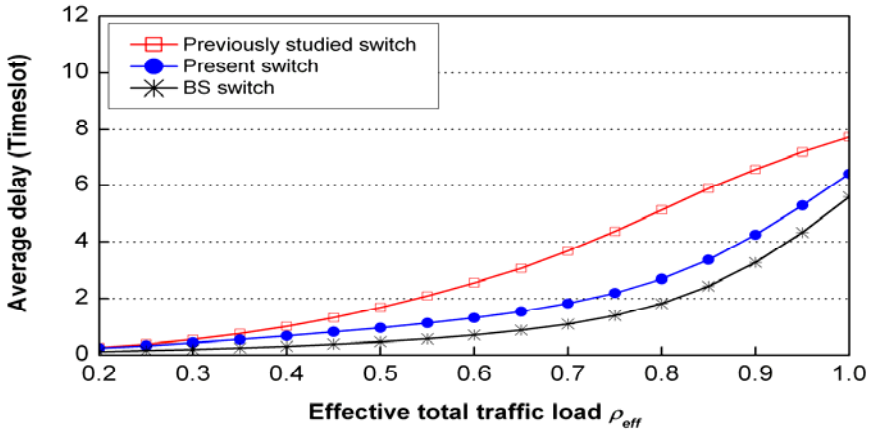

(b)

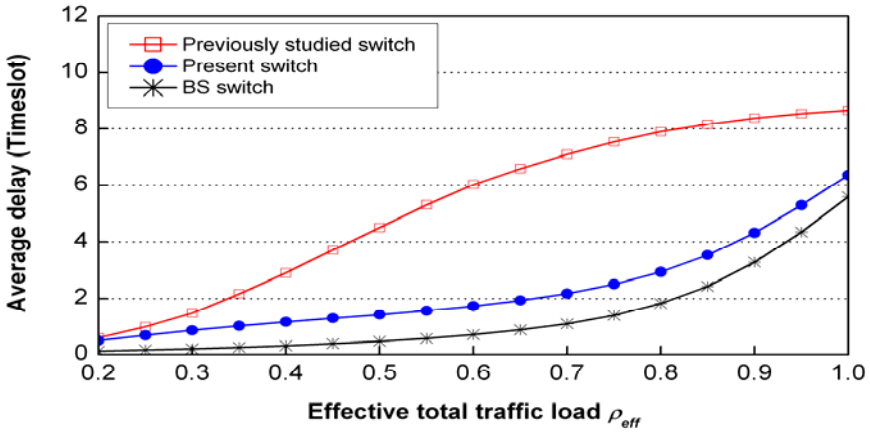

(c)

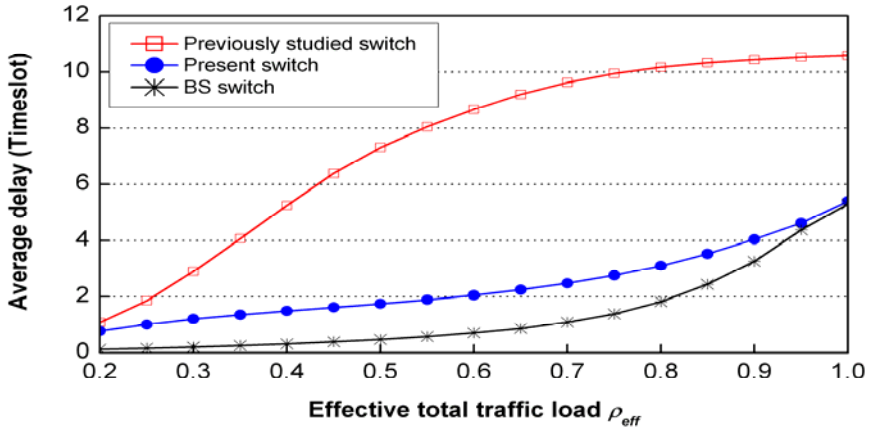

(d)

Figure 4-11: Performance of average packet delay versus the effective total traffic load for the three switches under different multicast traffic ratios (a) *r*=0.2, (b) *r*=0.5, (c) *r*=0.8, and (d) *r*=1.0

4.5 Complexity Discussion

Based on the discussion on traffic performance of the three switches, it can been seen that the previously studied switch can be applied to packet multicasting only when the multicast traffic is small, since its traffic performance would be considerably deteriorated with increase of multicast traffic; while the present switch can achieve almost the same packet loss performance and average packet delay as the broadcast-and-select switch regardless of the multicast traffic ratio, provided that it is given a certain number of required components, such as the MWCs and SOA gates. Here, we compare the complexity in terms of components counts for the present switch and the broadcast-and-select switch.

Let N be the switch size, and M be the number of FDLs used in the packet buffer. **Table 4-1** gives the formulae to calculate the counts of SOA gates, TWCs, FWCs, and MWCs for the two switch architectures. Note that the SOA gates in the present switch include the ones used in the MWCs and the ones used in the switching section. It can be seen that the numbers of FWCs for both switches are determined by the switch size N, while the broadcast-and-select switch does not need any TWC or MWC as the present switch does.

Table 4-1: Component counts of two switch architectures with multicast capability

	SOA Gate	TWC	FWC	MWC
Broadcast-and-select switch	$NM+N^2$	*0*	*2N*	*0*
Present switch	*n(M+N)*	*2N*	*N*	*n*

With reference to **Figure 4-10**, we note that the packet loss probability of the broadcast-and-select switch is independent of the multicast traffic ratio, which means that the component counts of the broadcast-and-select switch is also independent of the multicast traffic ratio. For the present switch, since the packet loss probability would be affected by the multicast traffic ratio, its component counts might depend on the multicast traffic ratio.

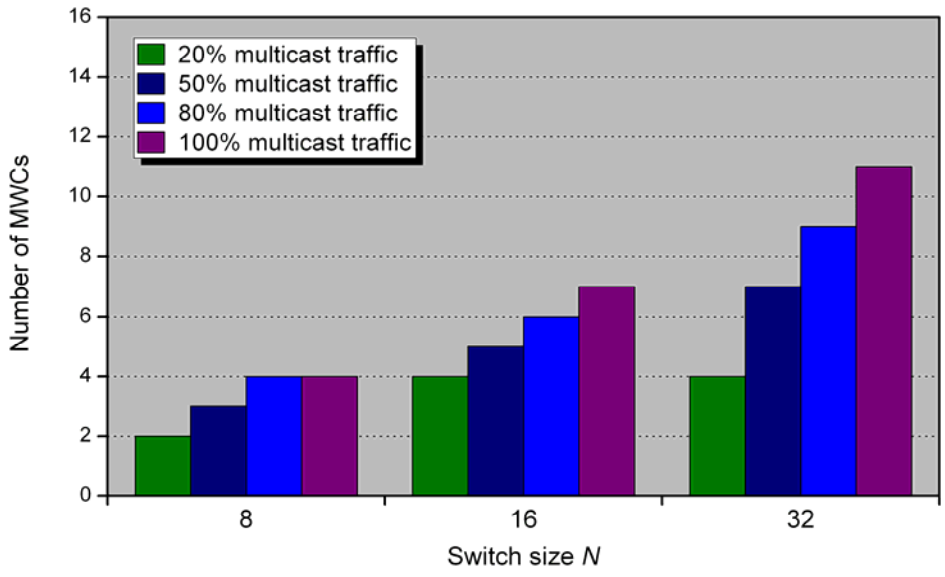

Figure 4-12: Number of MWCs used in the present switch to achieve a packet loss probability of 10^{-6} for different switch sizes when ρ_{eff} = 0.8

Figure 4-12 indicates the number of MWCs required in the present switch with different switch size to achieve a packet loss probability of 10^{-6} when ρ_{eff} = 0.8. The number of FDLs used in the present switch is M=26, 27, and 30 for N=8, 16, and 32, respectively. It is shown that to achieve a fixed packet loss probability at a given effective total traffic load, the present switch requires a certain number of MWCs, depending on the multicast traffic ratio r and the switch size N.

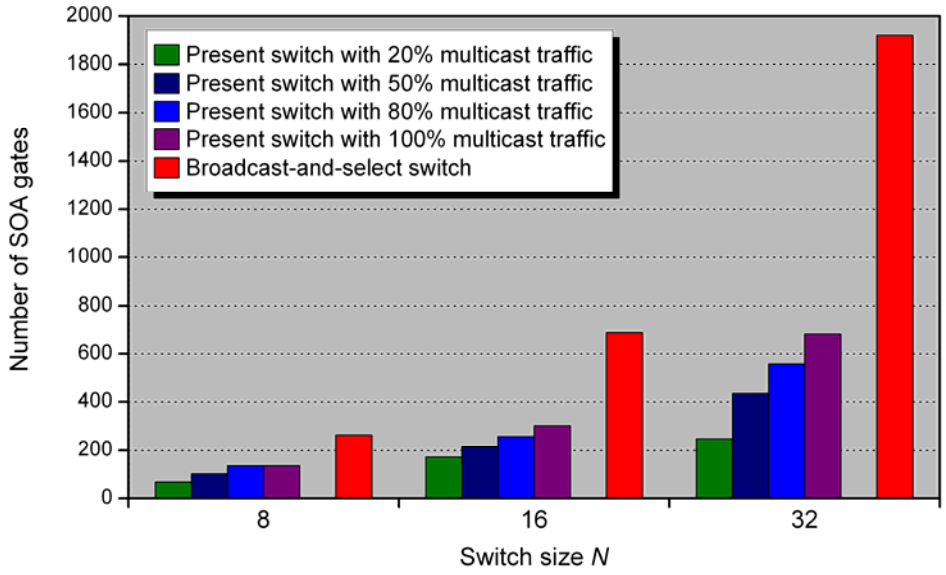

Figure 4-13: Number of SOA gates used in the present switch and broadcast-and-select switch to achieve a packet loss probability of 10^{-6} in different switch sizes when ρ_{eff} = 0.8

Figure 4-13 compares the number of SOA gates between the broadcast-and-select switch and the present switch to achieve the same packet loss probability of 10^{-6} in different switch sizes when ρ_{eff} = 0.8. The number of FDLs used in the

broadcast-and-select switch is M=25, 27, and 28 for N=8, 16, and 32, respectively. It is found that the number of SOA gates used in the broadcast-and-select switch will considerably increase with the switch size. In contrast, the number of SOA gates used in the present switch increases slowly with the multicast traffic ratio and switch size, and it is much smaller than that used in the broadcast-and-select with the same switch size. Therefore, when the switch size is large (N>8), the present switch is shown to outperform the broadcast-and-select switch in component counts, though it may require a few multi-wavelength converters depending on the multicast traffic ratio; when the switch size is small (N<8), the broadcast-and-select switch is preferred thanks to its advantages in easy implementation and outstanding traffic performance as well as acceptable component counts.

4.6 Summary

In this chapter, a novel wavelength-routed multicast packet switch with a shared fiber delay lines buffer was proposed to deal with traffic performance deterioration caused a large volume of multicast traffic. The novelty of the present switch lies in that both unicast and multicast packets can share a set of fiber delay lines whenever they need to be buffered in the switch. More importantly, a multicast packet could be replicated in multiple timeslots by multi-wavelength conversion in conjunction with the shared buffer, which is more efficient than storing multicast packet in a loop buffer to reduce packet contention. A packet scheduling technique was designed to assist packet contention resolution for the switch. The traffic performance of the present switch was evaluated by comparison with other switch architectures. The results showed that the present switch could effectively avoid traffic performance deterioration caused by a large volume of multicast traffic, thus achieve much better traffic performance than the wavelength-routed multicast packet switch utilizing multicast modules. The study on the complexity in terms of optical component counts showed that the present switch would require much fewer SOA gates to achieve the same packet loss probability than the broadcast-and-select switch does, but it may need a few multi-wavelength converters depending on the multicast traffic ratio.

Chapter 5
Multi-wavelength Broadcast-and-select Packet Switch for Multicasting

5.1 Introduction

The broadcast-and-select architecture is one of the popular schemes to realize optical packet multicast due to its easy implementation and good traffic performance [18]. Most of the existing optical packet switches utilizing the broadcast-and-select architecture were only focused on unicast packet switching with a single wavelength per input/output fiber [29, 31, 32, 44, 133], which could not fully utilize the huge bandwidth of optical fibers in WDM networks. Hence, multi-wavelength/WDM-based optical packet switches were subsequently proposed to exploit the wavelength dimension for packet switching and buffering [43, 167, 199]. In Chapter 3 and Chapter 4, we have studied two kinds of wavelength-routed multicast packet switches based on an efficient multicast scheme, in which the copies of a multicast packet are allowed to be made in multiple timeslots rather than in a single timeslot. This scheme can lead to a substantial reduction in output contention and hence a significant improvement in multicast packet loss performance. However, the multicast switches studied in Chapter

3 and Chapter 4 require the inclusion of multi-wavelength converts to perform replication of multicast packets for each wavelength channel, and a set of FDLs for buffering unicast packets. As a result, the traffic performance of these multicast switches will be affected by the multicast traffic ratio and the wavelength channels on each output fiber cannot be shared.

This chapter presents a multi-wavelength multicast packet switch based on the broadcast-and-select architecture with special focus on its multicast traffic performance [134, 208]. The distinct features of the switch are that: (i) a set of feed-forward FDLs are shared by all the wavelength channels of the input fibers for buffering both unicast and multicast packets, (ii) the wavelength channels of each output fiber are shared so that packet loss probability and packet delay can be significantly reduced. This chapter is organized as follows. Section 5.1 gives the background and motivation. Section 5.2 presents operation principle of the multicast-wavelength multicast packet switch in conjunction with a packet contention resolution, which is referred to as the multi-timeslot replication scheme in this thesis. Section 5.3 describes an analytical model for traffic performance investigation of the switch. In Section 5.4, the analytical model is verified through computer simulations. Section 5.5 compares the traffic performance of the switch with and without the multi-timeslot replication scheme in two different traffic types. Section 5.6 discusses the scalability of the multi-wavelength multicast packet switch. Finally, Section 5.7 concludes this chapter.

5.2 Operational Principle

In comparison with single-wavelength optical packet switches, multi-wavelength optical packet switches can fully take the advantage of wavelength dimension for packet switching and buffering [46, 188, 209]. In this study, a multi-wavelength multicast packet switch utilizing broadcast-and-select architecture is presented.

Figure 5-1 shows the architecture of the multi-wavelength multicast packet switch with N input and N output fibers, each of which is carrying m wavelengths from λ_1 to λ_m. The switch is assumed to be operated synchronously. That is, all the incoming optical packets are of fixed length and they arrive at the input fibers of the switch on a timeslot-by-timeslot basis. The duration of a timeslot equals to one packet length plus a guard time between two adjacent packets. The incoming packets are considered to be a combination of unicast and multicast packets.

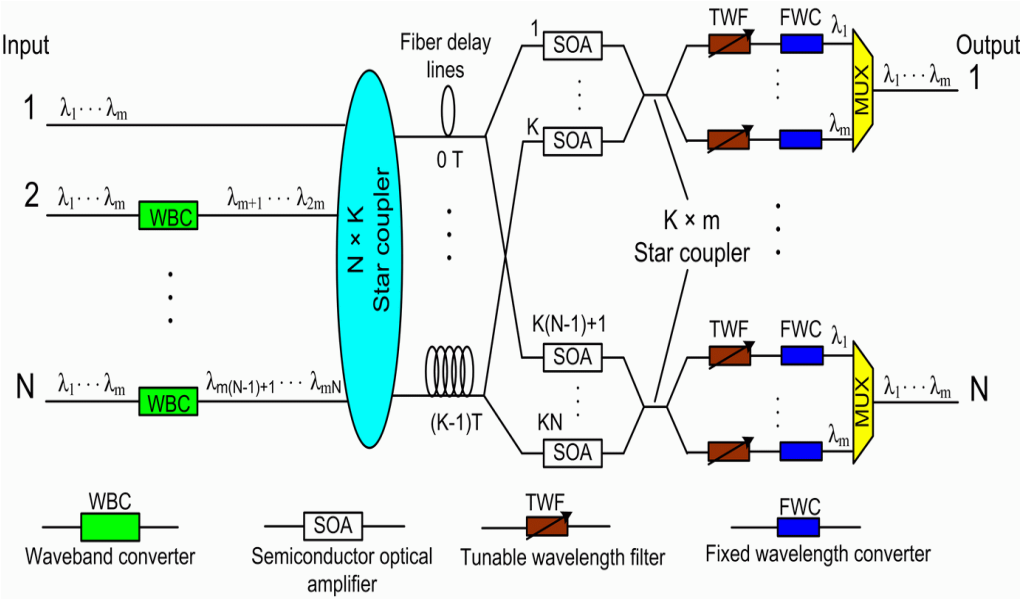

Figure 5-1: Architecture of multi-wavelength multicast packet switch

The incoming optical packets carried by different wavelengths from the second input fiber to the last input fiber are shifted into new wavelengths by corresponding waveband converters (WBCs), each of which is a wavelength converter that shifts the whole band of input wavelengths into a new band of converted wavelengths. A waveband conversion of 10 Gbit/s×103 channels based on the difference frequency generation (DFG) has been demonstrated in [210, 211]. As illustrated in **Figure 5-2**, the packets coming from the *i*th input fiber ($2 \le i \le N$) will be shifted to wavelengths $\lambda_{(i-1)m+1}$ to λ_{im}. Due to the use of the WBCs at the inputs of the switch, no two optical packets arriving in the same timeslot have the same wavelength when they are combined at the subsequent star coupler. The $Nm \times K$ star coupler is used to combine all the packets and broadcast them to each of the K fiber delay lines (FDLs) whose lengths vary from 0 to $(K\text{-}1)T$, where T is the duration of a timeslot. These FDLs in conjunction with the star coupler function as a shared buffer for all the incoming packets.

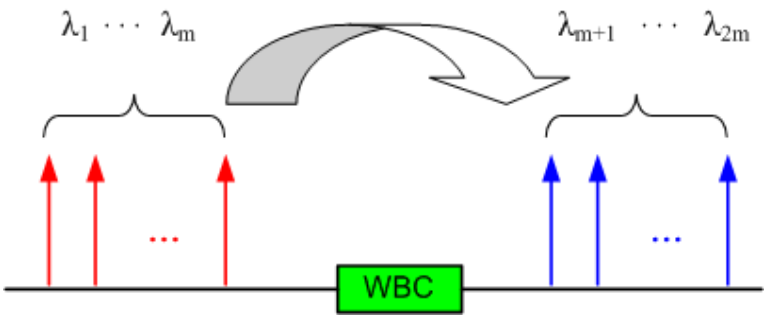

Figure 5-2: Principle of a waveband converter

Each multiplexed optical packet signal, after passing through a fiber delay line, is subsequently split into N equal copies, corresponding to N output fiber of the switch,

and then fed into respective SOA gates. In order to avoid contention, the SOA gates associated with a particular output fiber will only choose one multiplexed optical packet signal out of the K multiplexed optical packet signals in one timeslot. The chosen optical packet signal is further split into m parts (copies) by an $K \times m$ optical coupler, each of which is fed to a tunable wavelength filter (TWF). The TWF will select a packet destined for that output fiber at a certain wavelength from the chosen optical packet signal. For this purpose, Some TWFs in [51, 212] with the configuration time in nanoseconds might be utilized.

Since there are m tunable filters associated with a particular output fiber, up to m packets can be selected in each timeslot for each output fiber. The selection of the packets destined for a particular output fiber is on the basis of the round-robin scheduling scheme. After that, the selected packets are subsequently converted to respective fixed wavelengths ranging from λ_1 to λ_m before being multiplexed and transmitted to the output fiber. Since there are m tunable filters and m fixed wavelength converters associated with one output fiber, up to m packets with different wavelengths can be transmitted to one output fiber simultaneously, which is an advantage of the multi-wavelength packet switch compared with the single wavelength packet switch.

According to the principle of the switch above, it can been seen that a unicast packet can be buffered by the FDLs for up to (K-1) timeslots, depending on from which FDL the packet is selected and delivered to its desired output fiber, and after being buffered by one of the K FDLs, only one copy of that unicast packet will be selected by an SOA gate. For a multicast packet, it can be also buffered for up to (K-1) timeslots, and more

importantly all the copies of a multicast packet can be independently scheduled to be delivered to their desired output fibers within *K* timeslots, depending on which FDLs are selected for the multicast packet. This scheme is referred as to the multi-timeslot replication scheme and has been used in the single wavelength multicast switch in Chapters 3 and 4. The traffic performance of the multi-wavelength broadcast-and-select switch employing the multi-timeslot replication scheme will be analyzed and examined in the next section.

5.3 Traffic Performance Analysis

5.3.1 Analytical Formulation

In this section, the traffic model studied in Chapter 3 is used for traffic performance analysis of the multi-wavelength broadcast-and-select switch shown in **Figure 5-1**. Let *N*, *m*, and *K* be the number of input/output fibers, number of wavelengths per fiber, and number of FDLs in the switch, respectively. The queuing model at each output fiber of the switch, as illustrated in **Figure 5-3**, includes *mN* input wavelength channels and *m* parallel queues. Each queue can store packets for up to (*K*-1) timeslots, corresponding to the *K* FDLs.

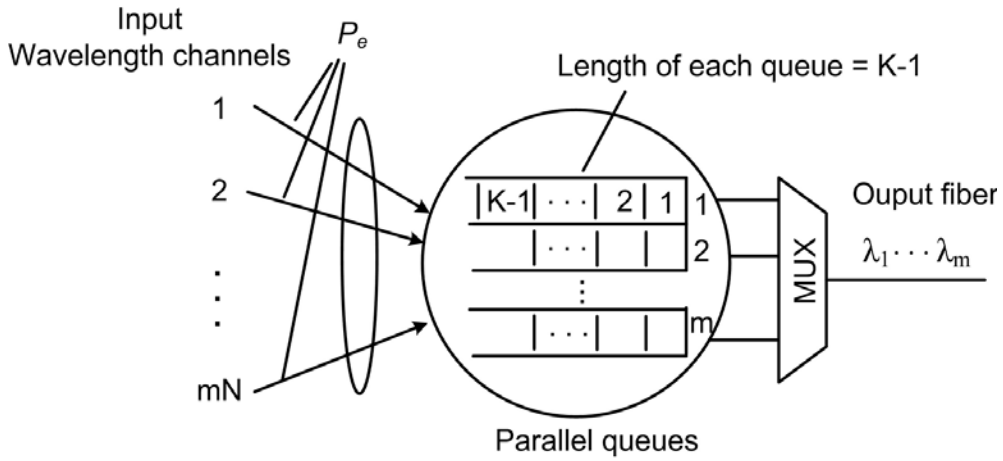

Figure 5-3: Queuing model at each output fiber of the multi-wavelength broadcast-and-select packet switch

The packet (unicast or multicast) arrivals at all the input wavelength channels are of independent and identical Bernoulli processes with a probability of λ in any timeslot. Since the packets are of fixed length and no more than one packet arrives at any input wavelength channel in one timeslot, λ can be considered as the average offered traffic load. The probability that an arrival packet is multicast packet is denoted by R. The number of copies of a multicast packet is assumed to follow a truncated geometric distribution with a mean of $E(X)$. The destinations of unicast packets and copies of multicast packets are uniformly distributed over N output fibers. According to **(3.3)**, an arrival packet will result in a probability of P_e for one packet (a unicast packet or a copy of a multicast packet) being addressed to a particular output fiber. In each timeslot, up to mN packets may arrive at the input fibers of the switch. Hence, the probability of k packets (unicast packets or copies of multicast packets) from different input wavelength channels destined from a particular output fiber at a timeslot can be calculated by:

$$a_k = \binom{mN}{k} (P_e)^k (1-P_e)^{mN-k} \quad . \tag{5.1}$$

Using the multi-timeslot replication scheme, the copies of a multicast packet are allowed to be made in different timeslots and transmitted to their respective output fibers, which means that the copies of a multicast packet can be buffered and switched independently. Although there are *m* wavelength channels associated with an output fiber, there is no guarantee that *m* packets would be simultaneously transmitted to an output fiber. For instance, many packets may be buffered in one particular queue while no packet is buffered in other queues, which will bring down the traffic performance of the switch. Hence, to optimize the traffic performance, the round-robin scheme is used to equally distribute incoming packets to the queues, ensuring equal traffic load at each wavelength channel of an output fiber. In this case, up to *m* packets can be transmitted to an output fiber concurrently.

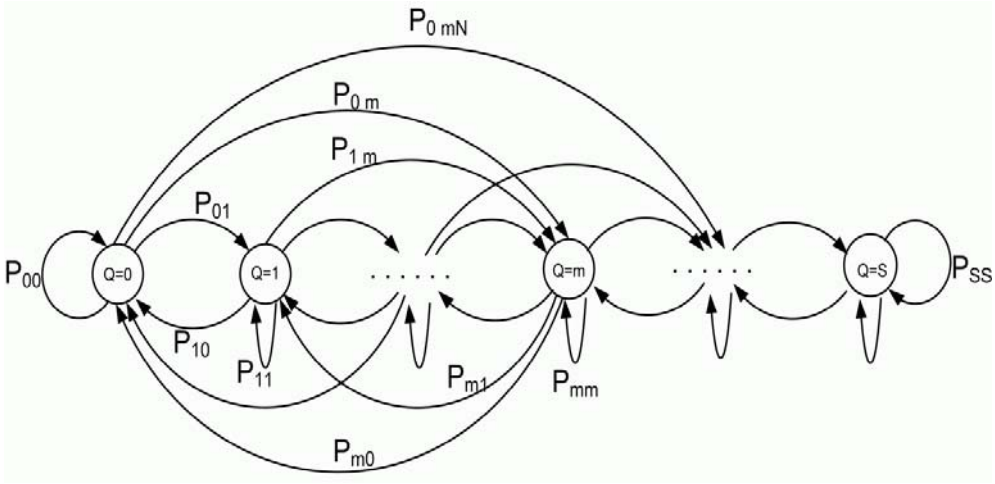

Figure 5-4: State transition diagram of the number of packets in the queues

Let Q be a random variable representing the number of packets in the queue at timeslot t, $0 \le Q \le S$, where $S = m(K-1)$. Then the state transition diagram of Q is depicted in **Figure 5-4**, where P_{ij} is the probability that there are i packets at timeslot t and j packets at timeslot t+1 in the queues, i.e, P_{ij} is the state transition probability from Q_i to Q_j., which can be calculated by

$$P_{ij} = \begin{cases} \sum_{k=0}^{m-i} a_k, & 0 \le i \le m, j = 0 \\ a_{j-i+m}, & 1 \le i \le m, 1 \le j \le S-1 \\ a_{j-i+m}, & m+1 \le i \le S-1, i-m \le j \le S-1 \\ \sum_{t=S-i+m}^{mN} a_t, & 0 \le i \le S, j = S \\ 0 & else \end{cases} . \qquad \textbf{(5.2)}$$

In order to obtain the probability distribution of the number of packets in the queues, let q_j be the probability that there are j packets in the queues at timeslot t+1. With reference to **Figure 5-4**, an equation is obtained when the queuing system reaches statistical equilibrium:

$$q_j = \Pr(Q = j) = \sum_{i=0}^{S} \Pr(Q = i) \cdot P_{ij} = \sum_{i=0}^{S} q_i \cdot P_{ij} . \qquad \textbf{(5.3)}$$

According to **(5.3)**, the probability matrix equation of q_j can be obtained:

$$\begin{bmatrix} q_0 \\ q_1 \\ \vdots \\ q_S \end{bmatrix} = \begin{bmatrix} P_{00} & P_{10} & \cdots & p_{S0} \\ P_{01} & p_{11} & \cdots & P_{S1} \\ \vdots & \vdots & \ddots & \vdots \\ P_{0S} & P_{1S} & \cdots & P_{SS} \end{bmatrix} \begin{bmatrix} q_0 \\ q_1 \\ \vdots \\ q_S \end{bmatrix}. \quad \textbf{(5.4)}$$

Considering the boundary condition $\sum_{j=0}^{S} q_j = 1$, the distribution of q_j can be found by solving **(5.5)**, which allows us to obtain the throughput, packet loss probability and mean delay of the switch with the multi-timeslot replication scheme.

$$\begin{bmatrix} P_{00}-1 & P_{10} & \cdots & P_{S0} \\ P_{01} & P_{11}-1 & \cdots & P_{S1} \\ \vdots & \vdots & \ddots & \vdots \\ P_{0S} & P_{1S} & \cdots & P_{SS}-1 \\ 1 & 1 & \cdots & 1 \end{bmatrix} \begin{bmatrix} q_0 \\ q_1 \\ \vdots \\ q_S \end{bmatrix} = \begin{bmatrix} 0 \\ 0 \\ \vdots \\ 0 \\ 1 \end{bmatrix} \quad \textbf{(5.5)}$$

5.3.2 Performance Statistics

In general, the packet loss probability, mean delay and throughput are three most important statistics to evaluate the traffic performance of a packet switch [56]. In this section, these statistics of the multi-wavelength multicast packet switch are given based on the analytical formulation obtained above.

Firstly, let U be the number of wavelengths that are not used in a timeslot at a given output fiber, and $0 \le U \le m$. Since each successfully transmitted packet is given a particular wavelength at a given output fiber, i unused wavelengths means m-i packets are successfully transmitted. Assuming that there are j packets in the queues, the probability distribution of U can be obtained by

$$u_i = \Pr(U = i) = \sum_{j=0}^{m-i} q_j \cdot a_{m-i-j} \quad . \tag{5.6}$$

Then, the average number of unused wavelengths in a timeslot is calculated by

$$E(U) = \sum_{i=0}^{m} u_i \cdot i = \sum_{i=0}^{m} \sum_{j=0}^{m-i} q_j \cdot a_{m-i-j} \cdot i \quad . \tag{5.7}$$

The normalized throughput, μ, of the switch can be presented by the wavelength utilization, which is given by

$$\mu = 1 - \frac{E(U)}{m} \quad . \tag{5.8}$$

Therefore, the packet loss probability (PLP) can be calculated by

$$PLP = 1 - \frac{\mu}{\rho} \quad . \tag{5.9}$$

5.4 Analytical Model Verification

In this study, the analytical model of the multi-wavelength broadcast-and-select packet switch with the multi-timeslot replication scheme introduced in Section 5.3 is verified through simulation. The traffic performance in terms of packet loss probability, mean delay and throughput of the switch obtained from the analysis in Section 5.3 are compared with those obtained from computer simulation. The simulation tools are developed in the Network Simulator Version 2 (NS-2) [204]. Each input wavelength channel generates a total of 10^9 packets in each simulation scenario. And each simulation result is the average of 20 runs performed for each scenario.

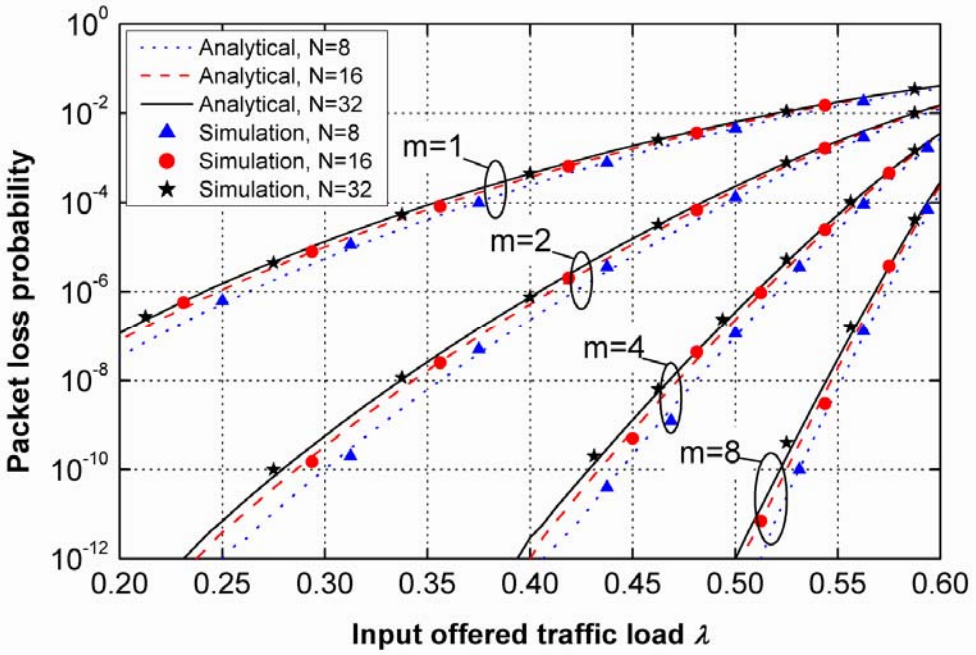

Figure 5-5: Packet loss probability as a function of the input offered traffic load for the broadcast-and-select switch with different values of *N* and *m*

Figure 5-5 shows both analytical and simulation results of the packet loss probability versus the input offered traffic load for the broadcast-and-select switch with different values of N (switch size) and m (number of wavelengths per fiber). The multicast traffic ratio is r=0.5 with an average number of copies of a multicast packet $E(X)$=4, and the number of fiber delay lines in the switch is K=8. As shown in the **Figure 5-5**, the analytical results match very well with the simulation results for different values of m. It is found that the switch size (N) has little effect on the packet loss probability; whereas, for a given N and input offered traffic load, the packet loss probability could be significantly reduced by increasing the value of m. This is because the wavelengths on each output fiber are shared by all the optical packets and more wavelengths per fiber would allow more optical packets to be transmitted at each output fiber concurrently, leading to a reduction in packet loss probability.

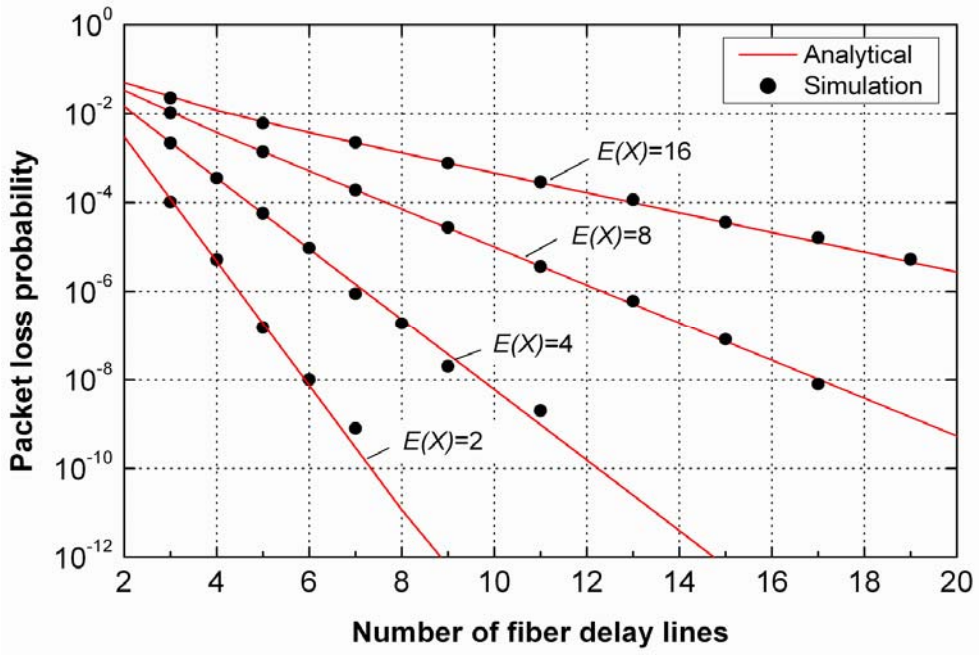

Figure 5-6: Packet loss probability as a function of the number of fiber delay lines for a 16×16 broadcast-and-select switch with different values of $E(X)$

The packet loss probability obtained from both analytical calculation and simulation versus the number of fiber delay lines, as shown in **Figure 5-6**, also match well for a 16×16 broadcast-and-select packet switch under different values of $E(X)$. The number of wavelengths per fiber is m=4, and the input offered traffic load is λ=0.5 with a multicast traffic ratio of r=0.5. It is observed that with a fixed $E(X)$, the packet loss probability is substantially reduced by increasing the number of fiber delay lines K. On the other hand, the switch requires more fiber delay lines to achieve a given packet loss probability under a larger value of $E(X)$. For instance, to guarantee a packet loss probability of 10^{-6} in the scenario shown in **Figure 5-6**, the switch requires the number of fiber delay lines K=5, 8, 12 and 22 for $E(X)$=2, 4, 8, and 16, respectively. This is because for a given input offered traffic load λ and a given multicast traffic ratio r, as discussed in Section 3.3, an increase in the value of $E(X)$ would lead to a corresponding increase in the effective total output traffic load ρ_{eff}, thus an increase in the packet loss probability. Increase in the number of FDLs could help store more contending packets to reduce packet loss probability.

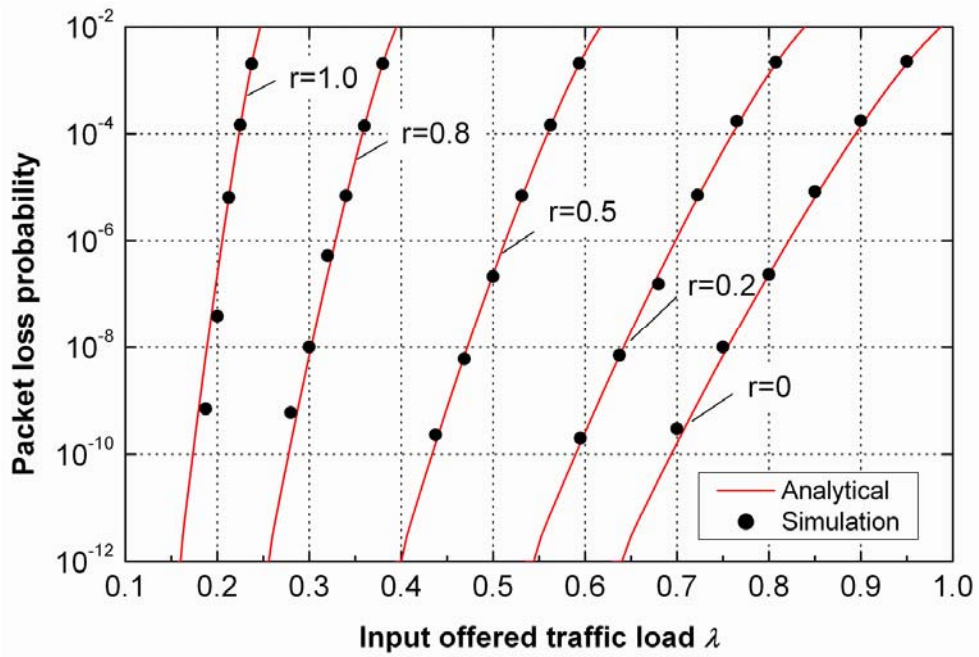

Figure 5-7: Packet loss probability as a function of the input offered traffic load for a 16×16 broadcast-and-select switch under different multicast traffic ratios

Figure 5-7 shows the packet loss probability as a function of the input offered traffic load for a 16×16 broadcast-and-select switch under different multicast traffic ratio r, where the number of wavelengths per fiber is m=4, the number of fiber delay lines is K=8, and $E(X)$=4. Note that there are only multicast packets in the case of r=1.0, and only unicast packets in case of r=0. As expected, the packet loss probability of the switch increases with the input offered traffic load for different multicast traffic ratios. With a larger multicast traffic ratio r, the packet loss probability would increase more rapidly, which results in a smaller acceptable input offered traffic load for the switch to guarantee a fixed packet loss probability. As observed in **Figure 5-7**, to guarantee a packet loss probability of 10^{-6}, the acceptable input offered traffic loads are about 0.82, 0.70, 0.51, 0.33, and 0.20 for r=0, 0.2, 0.5, 0.8 and 1.0, respectively.

The packet delay performance of the multi-wavelength broadcast-and-select packet switch is also studied by analytical calculation and simulation. The mean delay versus the input offered traffic load for a 16×16 broadcast-and-select switch with different values of *m* is shown in **Figure 5-8**, where the number of fiber delay lines in the switch is K=20, and the multicast traffic ratio is r=0.5 with $E(X)$=8. It is shown that the analytical results agree with the simulation results quite well for a different number of wavelengths per fiber, and it is also observed that the switch with more wavelengths per fiber can achieve lower mean delay at a given input offered traffic load. This can be explained as follows. The multicast packet switch with more wavelengths per fiber enables more optical packets (unicast packets and copies of multicast packets) to be transmitted at each output fiber simultaneously, which leads to fewer contending packets to be buffered by the fiber delay lines, thus a lower mean delay.

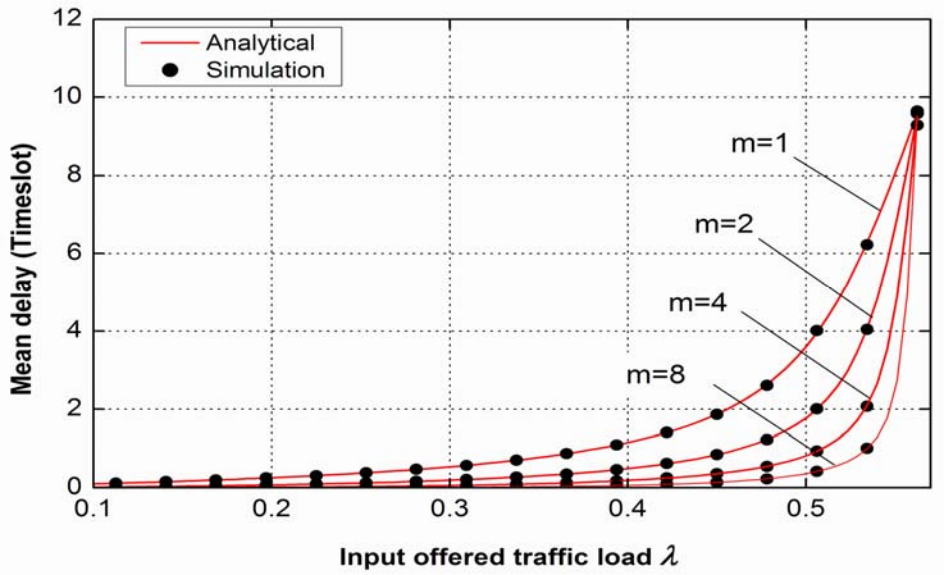

Figure 5-8: Mean delay as a function of the input offered traffic load for a 16× 16 broadcast-and-select switch under different values of *m*

Figure 5-9 compares the mean delay performance for a 16×16 broadcast-and-select switch with different values of $E(X)$, where the number of wavelengths per fiber is m=4, the number of fiber delay lines is K=20, and the multicast traffic ratio is r=0.5. It is observed that the mean delay performance is quite small and almost independent of $E(X)$ when the input offered traffic load $\lambda \leq 0.4$. However, when $\lambda > 0.4$, it will increase with the input offered traffic load more rapidly with greater $E(X)$. It can be seen that when r=0.53, the mean delay for the case of $E(X)$ =2 is almost 0, while it becomes nearly 10 timeslots for the case of $E(X)$ =16. The effect of $E(X)$ on the delay performance of the switch can be explained by the effective total traffic load. Given a greater $E(X)$ and a fixed multicast traffic ratio r, as discussed in Section 3.3, the effective total traffic load would increase more sharply as the input offered traffic load λ grows, which would lead to more packets addressed to a particular output fiber in one timeslot, and more packets to be buffered by the FDLs.

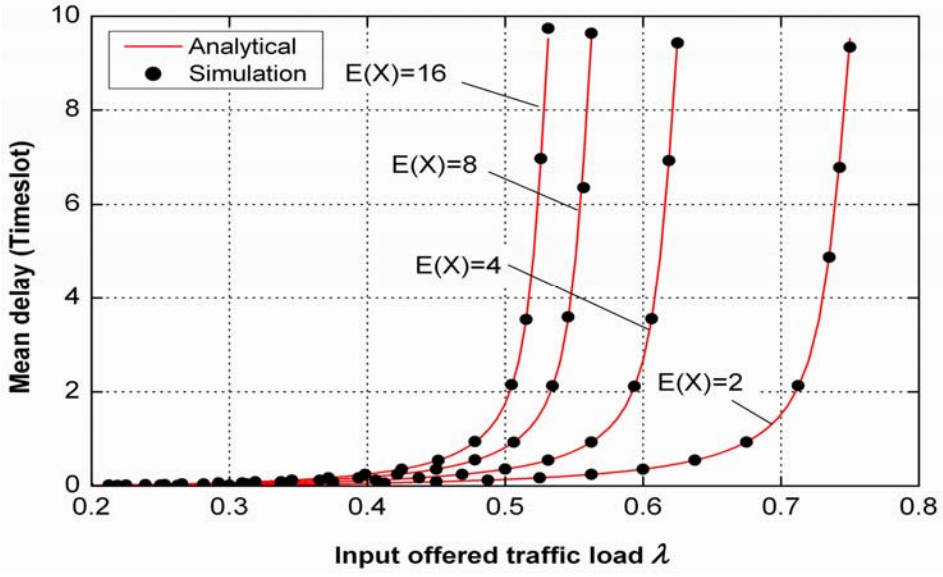

Figure 5-9: Mean delay as a function of the input offered traffic load for a 16×16 broadcast-and-select switch under different values of $E(X)$ when the multicast traffic ratio r=0.5

5.5 Performance Comparison

In the case that the multi-timeslot replication scheme is not used in the multi-wavelength broadcast-and-select packet switch, all of the copies of a multicast packet are needed to be made and transmitted in the same timeslot. If any of these copies loses contention for its output fiber, the multicast packet must be buffered until a timeslot in which all of its copies can be successfully transmitted, which is referred to as the one-timeslot replication scheme in this thesis. It is obvious that in the one-timeslot replication scheme, the switch may encounter severe output contention, especially when the multicast traffic load is large. With the multi-timeslot replication scheme, all the copies of a multicast packet are allowed to be made and transmitted in multiple timeslots, which means each copy of a multicast packet can be buffered and switched independently, expecting a better traffic performance. In this section, to assess the benefit of the multi-timeslot replication scheme, the multicast traffic performance of the multi-wavelength multicast packet switch with the multi-timeslot replication scheme and one-timeslot replication scheme are compared under both uncorrelated (traffic type in Section 3.6) and correlated traffic by simulations.

Here, the packet arrival processes at all the input wavelength channels are assumed to be independent with each other. As in [213], the correlated traffic is modeled as a two-state Markov process alternating between ON and OFF periods, both of which are assumed to be geometrically distributed with means of E[ON] and E[OFF], respectively. In an ON period, unicast or multicast packets with the same destinations will continuously arrive at an input wavelength channel, which is referred to as unicast or multicast burst. Thus the input offered load $\lambda = E[\text{ON}]/(E[\text{ON}]+E[\text{OFF}])$. Similar to

the uncorrelated traffic type described in Section 3.6, an arrival packet (unicast or multicast) is uniformly distributed across all the output fibers. Let *R* be the probability that a burst is multicast burst and E(X) be the average number of copies of a multicast packet. Then, the effective unicast, multicast and total traffic load under the correlated traffic can also be calculated by **(3.4)** – **(3.6)**, respectively.

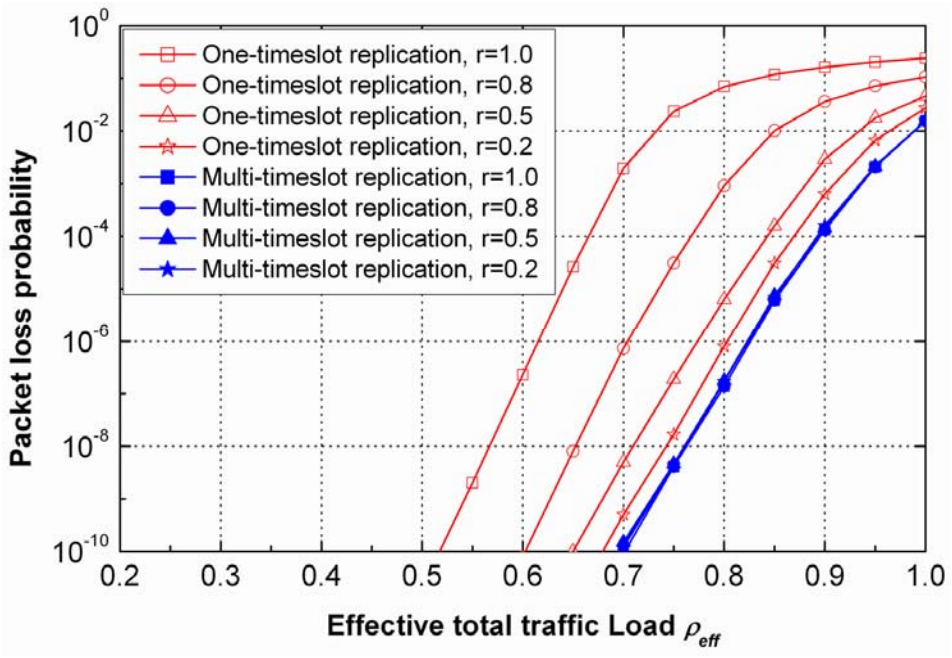

Figure 5-10: Packet loss probability for a 16×16 broadcast-and-select switch using one-timeslot and multi-timeslot replication schemes in uncorrelated traffic

Figure 5-10 compares the packet loss probability versus the effective total traffic load for a 16×16 broadcast-and-select switch with one-timeslot replication and multi-timeslot replication schemes in uncorrelated traffic (traffic type in Section 3.6) for different multicast traffic ratios with fixed $E(X)$=8. The number of wavelengths per fiber is m=4 and the number of FDLs is K=8. It is found that given an effective total traffic load, the packet loss probability of the switch with the one-timeslot replication

scheme would increase with the multicast traffic ratio growing; while using the multi-timeslot replication scheme, the switch can not only achieve a lower packet loss probability than that with one-timeslot replication scheme, but it is independent of the multicast traffic ratio *r*.

In the correlated traffic when *E*[ON]=4, as shown in **Figure 5-11**, though the packet loss probability would become worse compared with that under uncorrelated traffic, it is independent of the multicast traffic ratio when the multi-timeslot replication scheme is used.

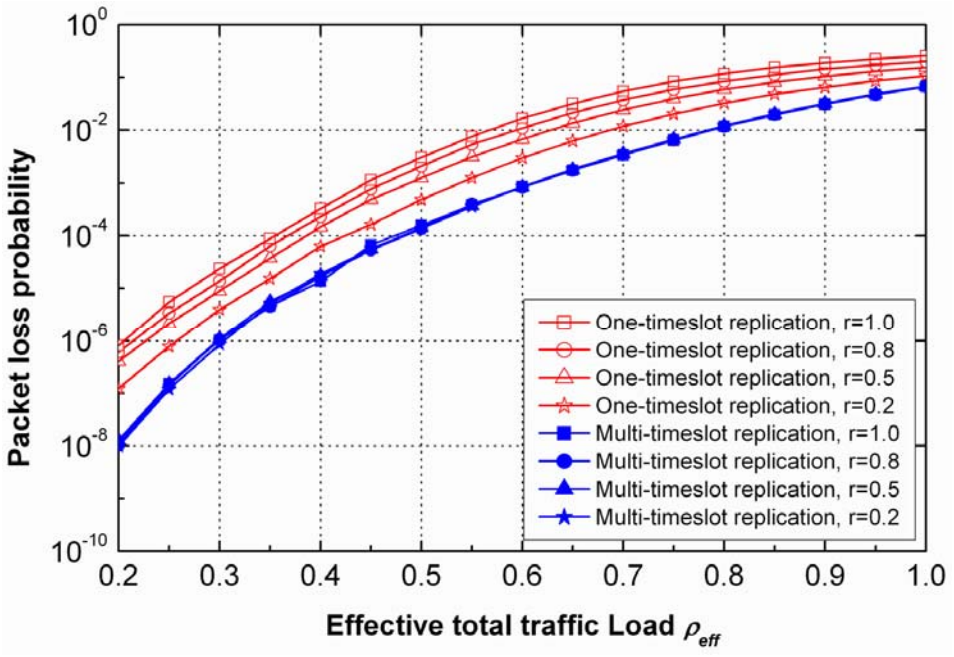

Figure 5-11: Packet loss probability for a 16×16 broadcast-and-select switch using one-timeslot and multi-timeslot replication schemes in correlated traffic

This is because: i) an increase in multicast traffic ratio *r* at a fixed effective total traffic load would result in more multicast packets concurrently arriving at the switch; ii) in the one-timeslot replication scheme, the multicast packet contending probability

is much higher than the unicast packet contending probability, which would lead to an increase in the packet loss probability; iii) in the multi-timeslot replication scheme, since all the copies of a multicast packet are allowed to be made in multiple timeslots independently, the packet contending probability is much lower than that in the one-timeslot replication scheme. Moreover, since each copy of a multicast packet is transmitted independently, the switch achieves a lower and constant packet loss probability in the multi-timeslot replication scheme.

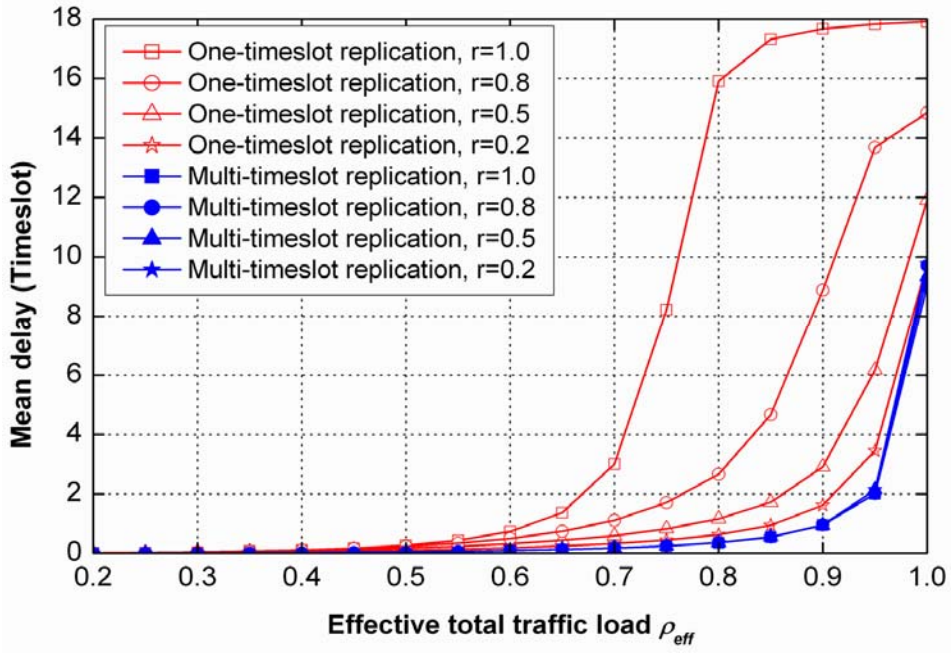

Figure 5-12: Mean delay for a 16×16 broadcast-and-select switch using one-timeslot and multi-timeslot replication schemes in uncorrelated traffic

Figure 5-12 shows the mean delay versus the effective total traffic load for a 16×16 broadcast-and-select switch using one-timeslot replication and multi-timeslot replication schemes for different multicast traffic ratios under the uncorrelated traffic.

Here the number of wavelengths per fiber is m=4; the number of FDLs is K=20; and the value of $E(X)$=8. It is observed that with the one-timeslot replication scheme, the mean delay increases as the value of r grows when the effective total traffic load $\rho_{eff} \geq 0.5$. In contrast, with the multi-timeslot replication scheme, the switch achieves a smaller and constant mean delay for a given ρ_{eff} regardless of the multicast traffic ratio r. Similar results can also be seen for the correlated traffic shown in **Figure 5-13**. This is because that in one-timeslot replication scheme, a multicast packet would be delayed by the FDLs if any of its copies loses contention for its output fiber, which makes more multicast packets to be stored by the FDLs; while in the multi-timeslot replication scheme, since the copies of a multicast packet are allowed to made in multiple timeslots independently, the packet contending probability is not affected by the multicast traffic ratio.

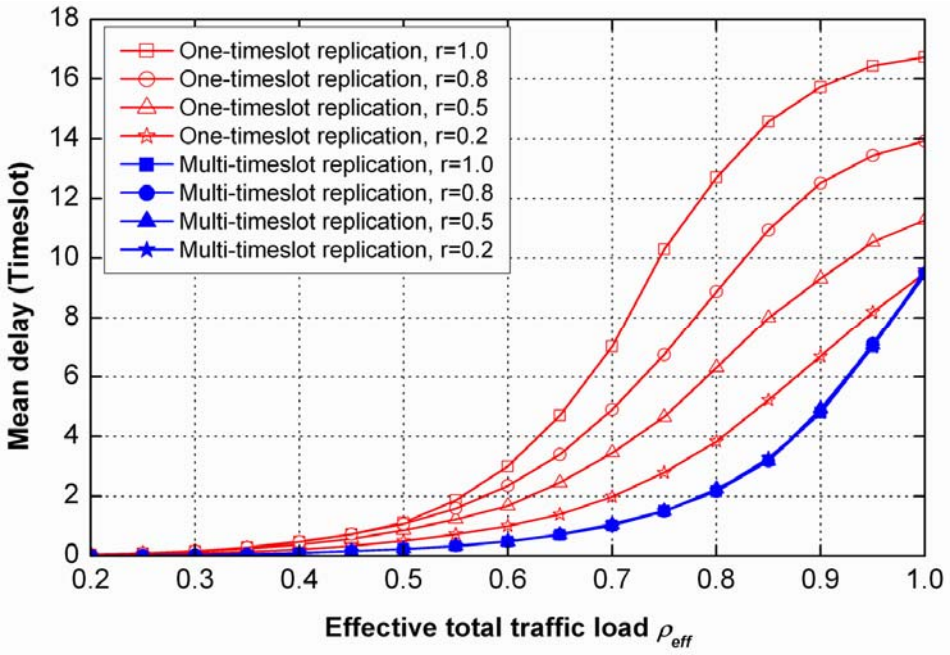

Figure 5-13: Mean delay for a 16×16 broadcast-and-select switch using one-timeslot and multi-timeslot replication schemes in correlated traffic

Figure 5-14 and **Figure 5-15** show the normalized throughput for a 16×16 broadcast-and-select switch using one-timeslot replication and multi-timeslot replication schemes with a different number of wavelengths per fiber in the uncorrelated and correlated traffic, respectively, where the multicast traffic ratio is r=1.0 with $E(X)$=8, and the number of fiber delay lines is K=4. It can be seen that the maximum throughput of the switch can be improved by increasing the number of wavelengths per fiber (value of m) in both of the one-timeslot and multi-timeslot replication schemes. However, the maximum throughput with the one-timeslot replication scheme is only about 0.80 for m=8 in both uncorrelated and correlated traffic; while in the multi-timeslot replication scheme, the maximum throughput can reach 0.90 for m=1 in the uncorrelated traffic, and 0.83 for m=2 in the correlated traffic, respectively.

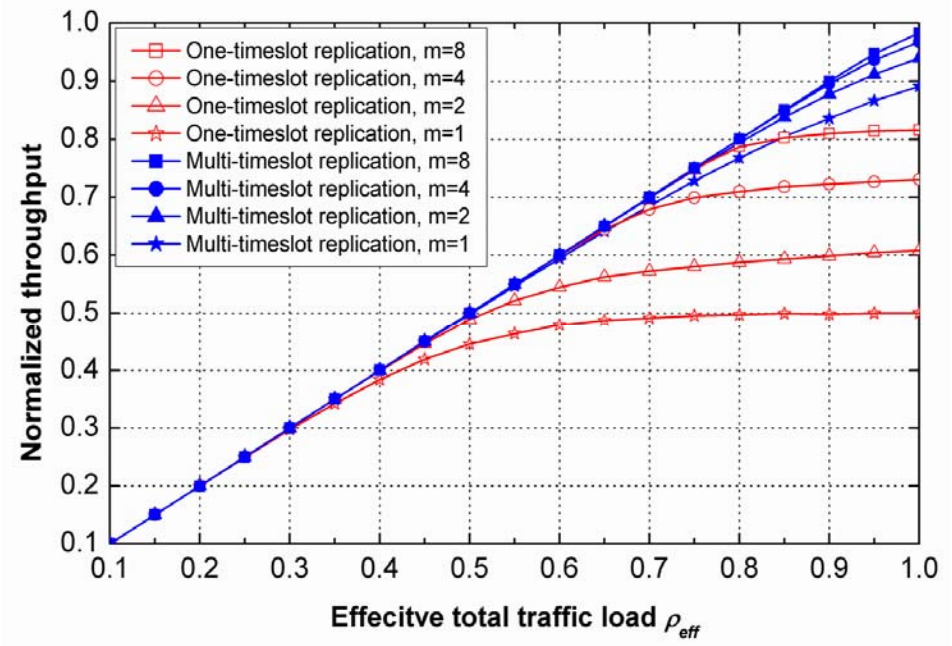

Figure 5-14: Normalized throughput of a 16×16 broadcast-and-select switch using one-timeslot and multi-timeslot replication schemes with a different number of wavelengths per fiber in uncorrelated traffic

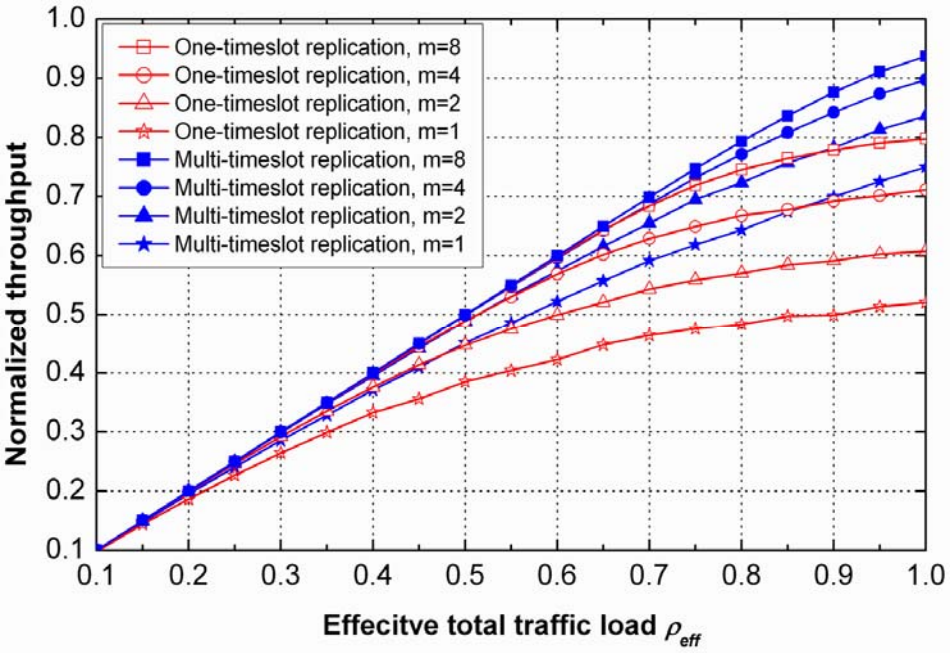

Figure 5-15: Normalized throughput of a 16×16 broadcast-and-select switch using one-timeslot and multi-timeslot replication schemes with a different number of wavelengths per fiber in correlated traffic

5.6 Scalability Discussion

In comparison with the other multicast switches such as the wavelength-routed multicast packet switches in [191-193], the multi-wavelength multicast packet switch based on the broadcast-and-select architecture using the multi-timeslot replication scheme can effectively avoid the problem of traffic performance deterioration caused by the increase in multicast traffic, thus it is desirable for optical packet multicasting even when the multicast traffic proportion is very large. Nevertheless, due to

employment of the star couplers and splitters, the power loss would be a critical issue limiting the scalability and actual implementation of the switch. In this section, we study the scalability of the multi-wavelength broadcast-and-select packet switch architecture in terms of switch size (N), number of wavelength per fiber (m), and number of FDLs (K), all of which would affect the power loss of the switch.

With reference to the switch architecture in **Figure 5-1**, let L_{SC1}, L_{FDL}, and L_{SC2} be the power losses induced by the $N\times K$ star coupler, optical splitters placed behind the FDLs, and the $K\times m$ star coupler, respectively, which can be calculated by:

$$L_{SC1} = \begin{cases} 10\log(N) & N \geq K \\ 10\log(K) & N < K \end{cases}, \quad \textbf{(5.10)}$$

$$L_{FDL} = 10\log(K), \quad \textbf{(5.11)}$$

$$L_{SC2} = \begin{cases} 10\log(m) & m \geq K \\ 10\log(K) & m < K \end{cases}. \quad \textbf{(5.12)}$$

Since the power loss induced by the star couplers and optical splitters are the dominant contributions to the power loss of the switch, for simplicity, the insertion losses introduced by the optical components such as MUXs, TWFs, and FWCs are not considered at this point. Thus the total power loss of the switch is given by

$$L_{input-output} = L_{SC1} + L_{FDL} + L_{SC2}. \quad \textbf{(5.13)}$$

Table 5-1: Number of FDLs in the present switch to achieve packet loss probability of 10^{-6} at ρ_{eff} = 0.8 in uncorrelated Traffic

N	m			
	1	2	4	8
4	22	11	7	4
6	24	13	7	4
8	25	13	7	4
10	26	14	7	4
12	26	14	7	4
14	27	14	7	4
16	27	14	7	4
18	27	14	7	4
20	27	14	7	4

With respect to the discussion in Section 5.5, the number of FDLs (K) in the switch with given N and m is determined by the expectation of traffic performance (like packet loss probability and mean delay). That is, the power loss of the switch would depend on the targeted traffic performance in this regard. **Table 5-1** gives the required number of FDLs (K) in the switch using the multi-timeslot replication scheme for different values of N and m to achieve 10^{-6} packet loss probability when the effective total traffic load ρ_{eff}=0.8 in uncorrelated traffic with $E(X)$=4. The corresponding power loss can be calculated by using **(5.10)** – **(5.13)**, which are shown in **Figure 5-16**. It is found that: (i) to achieve a fixed packet loss probability, the power loss of the switch increases with the switch size; (ii) with a fixed switch size, the switch with more wavelengths per fiber (value of m) has much less power loss. This is due to the fact

that the switch with more wavelengths per fiber needs fewer FDLs to achieve a fixed packet loss probability.

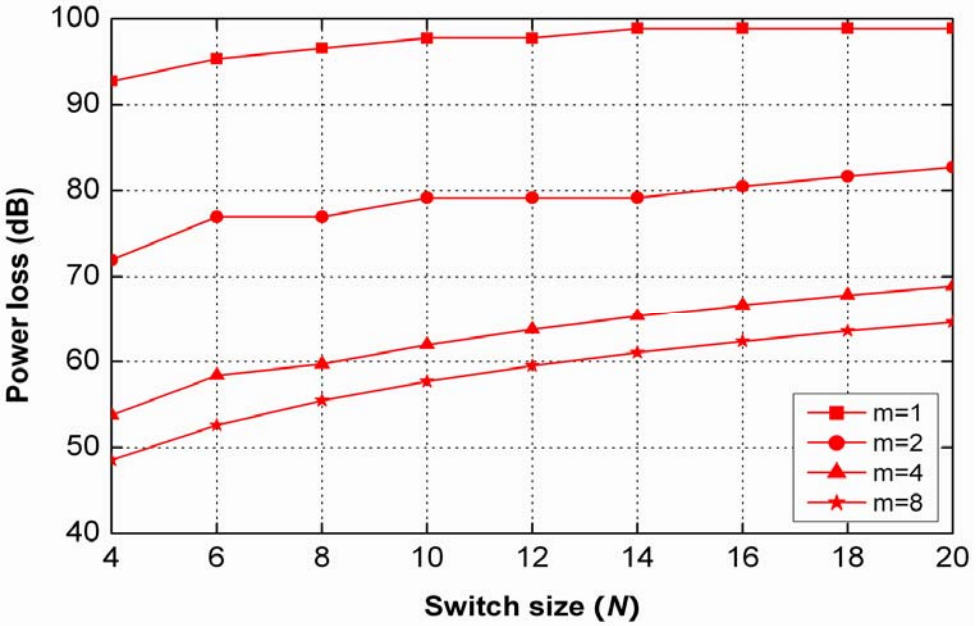

Figure 5-16: Power loss versus switch size (*N*) of the multicast switch using the multi-timeslot replication scheme with different values of *m* to achieve 10^{-6} packet loss probability at ρ_{eff} = 0.8 in uncorrelated traffic

For compensating power loss of the switch, it is not advisable to place an EDFA at each input or output fiber since the power loss is proportional to the switch size. To address this issue, **Figure 5-17** shows the improved switch architecture using the Couple-Amplify-Couple scheme in [214], where the $N\times K$ star coupler is replaced by an $N\times 1$ coupler, a few EDFAs and a $1\times K$ star coupler. In comparison with the switch architecture in **Figure 5-1**, the improved switch architecture needs much fewer EDFAs to compensate the power loss.

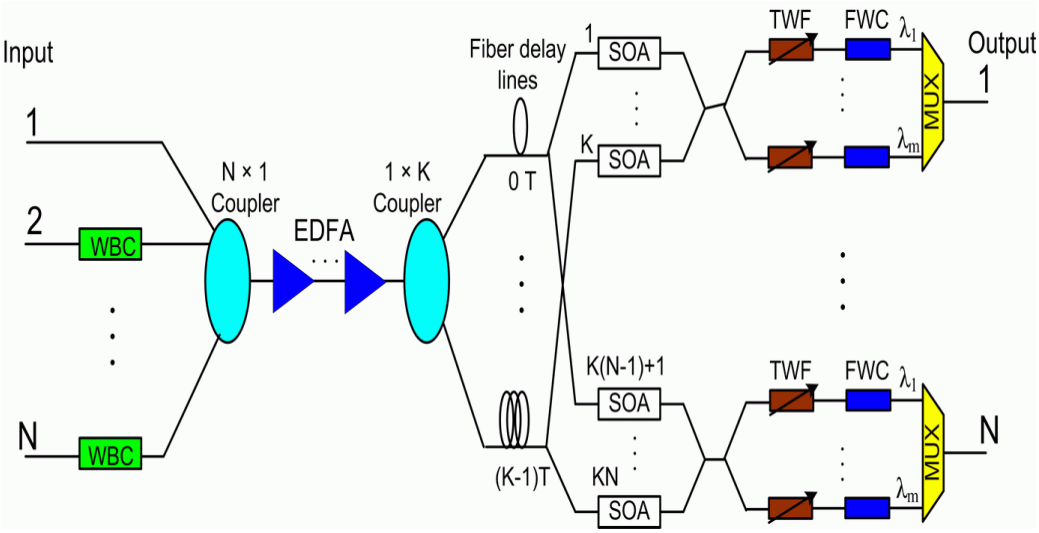

Figure 5-17: Improved switch architecture using the Couple-Amplify-Couple scheme

5.7 Summary

This chapter presented a multi-wavelength multicast packet switch based on the broadcast-and-select architecture. The switch employed the multi-timeslot replication scheme to realize packet multicasting, by which a multicast packet was allowed to be replicated in multiple timeslot to substantially reduce the output contention. An analytical model of the multi-wavelength multicast switch was developed to study its multicast traffic performance in terms of packet loss probability, mean delay and normalized throughput of the switch, and then verified through computer simulation. Both of the analytical and simulation results showed that the multi-wavelength packet switch could achieve much better multicast performance in comparison with single wavelength packet switches. The traffic performance of the multi-wavelength multicast packet switch with and without the multi-timeslot replication scheme was compared under different traffic models. It was found that without the multi-timeslot replication, the packet loss probability and mean delay of the switch would be deteriorated with the multicast traffic ratio increasing; in contrast, the switch with the multi-timeslot replication could achieve a much lower packet loss probability and mean delay, which were independent of the multicast traffic ratio, leading to a higher throughput. Moreover, the discussion on the scalability showed that the power loss for the switch to achieve a fixed packet loss probability could be considerably reduced by increasing the number of wavelengths per fiber. Finally, an improved scheme of the switch architecture was also presented to reduce the number of EDFAs for compensating for power loss of the switch.

Chapter 6
Conclusions and Future Research

6.1 Conclusions

Optical packet switching technologies are believed to be the key for vastly increasing the throughput of future optical packet-switched networks. Switching and multicasting in the optical layer is anticipated to significantly reduce the cost and complexity for the optical packet-switched network by taking full advantage of the huge fiber bandwidth to support the increasing amount of multicast packet-based applications such as IPTV, video conferencing, high definition TV, VoD, and VoIP. Optical packet switching systems with multicast capability are very promising, and have attracted much interest of research due to their cost-effective and efficient provisioning of multicast applications.

This thesis focuses on optical multicast packet switching systems in terms of the switch architecture design, optical multicast technologies, packet contention resolution schemes, and traffic performance analysis and evaluation. This section summarizes the main works carried out in this thesis.

Chapter 2 gives an overview of optical packet switching technologies and reviews the existing technologies for optical packet multicasting. The light splitting and multi-wavelength conversion are the two primary schemes of implementing multicast functionary in an optical packet switch. The former is a simple way but requires a large number of optical components to perform the broadcast-and-select processing to achieve packet multicast, which has a potentially high implementation cost, thereby limiting the scalability of the switching systems. The latter achieves packet multicast by converting an optical packet into multiple copies with different wavelengths and using a wavelength router such as AWG to route the copies to desired outputs, which is desirable for large switching systems and compatible with wavelength-sensitive optical networks. Various technologies of multi-wavelength converter are also reviewed and discussed.

In Chapter 3, a wavelength-routed multicast packet switch utilizing multicast modules has been proposed and examined. By means of the multicast modules, the switch allows the copies of a multicast packet to be made in multiple timeslots to reduce the output contention and switched to desired outputs without going through any more tunable wavelength converters. In addition, a packet scheduling technique has been designed for contention resolution for the modified switch. The physical performance such as the bit-error-rate, extinction ratio, and spectral characteristic of the multicast module has been examined by computer simulation. It is found that a tolerant bit-error-rate performance can be maintained if a multicast packet is being stored by no more than 16 timeslots in a multicast module. However, a multicast module cannot concurrently store two or more multicast packets from the same input of the switch

due to wavelength collision. In order to address this restriction, an improvement scheme is then presented by modifying the multicast modules in the switch. The traffic performance of the switch before and after modified by the improvement scheme is evaluated by simulation. The study shows that the improved scheme can considerably reduce the multicast packet loss probability for the switch without increasing the number of multicast modules, leading to a significant reduction in the implementation cost for the optical multicast packet switch. Nevertheless, this type of switch architecture can handle only a small proportion of multicast traffic, as the traffic performance would be deteriorated with the increase of multicast traffic.

To address the issue of performance deterioration caused by a large volume of multicast traffic, a shared-buffer-based wavelength-routed multicast packet switch has been proposed in Chapter 4. This switch allows unicast and multicast packets to share a set of fiber delay lines for buffering, and more importantly, the copies of a multicast packet can be made in multiple timeslots by multi-wavelength conversion in a single timeslot, instead of storing the multicast packet in a loop buffer for multiple timeslots which is more efficient in reducing the packet contention. Moreover, a packet scheduling technique is designed to assist contention resolution for the switch. The traffic performance and the complexity in terms of component counts of the shared-buffer-based wavelength-routed multicast packet switch have been investigated through simulation. Results show that the shared-buffer-based wavelength-routed multicast packet switch in conjunction with the packet scheduling technique can not only effectively reduce the performance deterioration caused by the increase of multicast traffic, but also exhibit cost-effective configuration over other switch architectures.

In Chapter 5, a multi-wavelength broadcast-and-select packet switch has been proposed and its multicast traffic performance has been investigated analytically and by computer simulation. The switch employs the broadcast-and-select architecture to realize packet multicasting. It enables to concurrently transmit multiple optical packets to the same output fiber of the switch. An analytical model of the switch using the multi-timeslot replication scheme has been developed to study the traffic performance in terms of packet loss probability, mean delay and normalized throughput of the switch, and verified through computer simulation. Both analytical and simulation results show that the multi-wavelength broadcast-and-select packet switch can achieve much better multicast performance in comparison with the single wavelength multicast packet switch. Moreover, it is shown that the traffic performance of the switch would be considerably deteriorated as the multicast traffic increases without using the multi-timeslot replication scheme. However with the multi-timeslot replication scheme, the switch can achieve a much lower packet loss probability and mean delay performance, irrespective of multicast traffic ratio, and thus a higher throughput. Scalability analysis shows that the switch with more wavelengths per fiber can achieve a fixed packet loss probability with less power loss. A cost-effective improved scheme is suggested for compensating the power loss of the switch.

The three multicast packet switches proposed in this thesis have their own advantages and weaknesses. From the traffic performance point of view, the multi-wavelength broadcast-and-select switch outperforms the other two wavelength-routed multicast switches, but the requirement of a large number of optical components restricts its practical implementation and also limits its scalability. The switch utilizing multicast

modules and the switch with shared FDLs have advantages in component counts, and both are scalable to large size. However, the former is only applicable to packet multicasting with a small multicast traffic ratio, while the latter can handle a large multicast traffic ratio and achieve traffic performance close to that of the broadcast-and-select switch.

6.2 Recommendations for Future Research

This thesis mainly contributes to the design, modeling and analysis of optical packet switching systems with multicast capability. In the following, we give some of interesting topics that deserve further study in the future research.

In Chapter 3 and Chapter 4, we focused on wavelength-routed optical multicast packet switches because of their scalability and less power loss. Both of the switch architectures presented in Chapter 3 and Chapter 4 employed multi-wavelength converters that were realized by XPM in SOA-based MZI. Although we have carried out simulation to examine the physical performance of the multi-wavelength converter, in order for the switches to be implemented, it is very important to study the multi-wavelength converter by experimental verification, such as the bit-error-rate, extinction ratio and nonlinear effects.

One shortcoming of XPM-based multi-wavelength converter is that it can be only applied to the packet data of on-off keying (OOK) format. As a result, to support more data formats, a multi-wavelength converter that is fully transparent to various data formats such as QPSK, DQPSK, and QAM is desirable for the wavelength-routed

multicast packet switches. FWM-based wavelength converter could be a solution to this issue, while the number of the converted wavelengths of FWM-based wavelength converter is quite small. To convert a large number of wavelengths, one possible solution is a combination of FWM and XPM to achieve a hybrid multi-wavelength converter. This topic is worth further studying both experimentally and analytically.

In Chapter 5, a multi-wavelength broadcast-and-select architecture switch was presented and studied with special focus on its multicast traffic performance. Though the results showed that the switch could achieve excellent multicast traffic performance by using the multi-timeslot replication scheme, the huge power loss and component counts would be the major concerns limiting the scalability of the switch. The scalability of the switch was only discussed from the traffic performance (packet loss probability) point of view in the present work. To examine this problem in its entirety, it is very important to study this issue from the point of view of physical performance such as the equivalent power loss induced by the second order transmission impairments (excess loss, crosstalk, and polarization dependent loss). Therefore, experimental verification of the physical performance of the switch will be included in the future research.

Most of the multicast traffic in current and future optical transport networks is anticipated to be video and voice streams, which could be regarded as flows that have a steady throughput within a certain time period. In most of the reported optical multicast packet switches, however, each packet is treated independently as a loose data entity. Each packet goes through the Store-and-forward process, by which contending packets are stored in the optical buffer through a queuing manager. Due to

the lack of mature all-optical processing logic, optical memory, and synchronization technologies, such operation mode will result in substantial packet loss, nonuniform delay and large power consumption when the traffic is heavy. In our future work, to effectively address this issue, it is interesting to integrate flow technologies into optical multicast packet switches. By use of flow management, all optical packets that contain the same identification of a flow will be switched in an effective way. The optical packet switch only needs to route the first packet of a flow and record the routing parameters of the first packet, then the subsequent packets of the same flow can be directed to the output, avoiding the time delay induced by the fussy queuing process.

Author's Publications

Journal Papers

[1] **Qirui Huang**, and Wen-De Zhong, "An optical wavelength-routed multicast packet switch based on multitimeslot multiwavelength conversion," *IEEE Photonics Technology Letters*, vol. 20, no. 18, pp. 1518-1520, Sept. 2008. (related to Chapter 3)

[2] **Qirui Huang,** and Wen-De Zhong, "Traffic performance evaluation of an optical packet switch with multicast operation," *IEEE Communications Letters*, vol. 12, no. 12, pp. 894-896, Dec. 2008. (related to Chapter 3)

[3] **Qirui Huang**, and Wen-De Zhong, "Wavelength-routed optical multicast packet switch with improved performance," *IEEE/OSA Journal of Lightwave Technology*, vol. 27, no. 24, pp. 5657-5664, Dec. 2009. (related to Chapter 3)

[4] **Qirui Huang**, and Wen-De Zhong, "A multi-wavelength multicast packet switch: performance analysis and evaluation," *IEEE/OSA Journal of Optical Communications and Networking*, vol. 2, no. 9, pp. 678-688, Sept. 2010. (related to Chapter 5)

[5] **Qirui Huang**, and Wen-De Zhong, "A wavelength-routed multicast packet switch with a shared-FDL buffer," *IEEE/OSA Journal of Lightwave Technology*, Vol. 28, no. 19, 2822-2829, Oct. 2010. (related to Chapter 4)

Conference Papers

[1] **Qirui Huang,** and Wen-De Zhong, "Multicast-enabled optical packet switch architecture utilizing multicast modules," in *Proc. OFC 2008*, San Diego, CA, 2008, Paper OMG4. (related to Chapter 3)

[2] **Qirui Huang,** and Wen-De Zhong, "Performance of an multicast-enabled optical packet switch using a prioritized packet scheduling scheme," in *Proc. Photonics Global Conference 2008*, Singapore, 2008, Paper Conf195a87. (related to Chapter 3)

[3] **Qirui Huang,** Wen-De Zhong, and Wen Chen, "Performance evaluation of a WDM optical packet switch with multicast capability," in *Proc. ICICS' 2009*, Macau, P. R. China, , 2009, Paper P0500. (related to Chapter 5)

[4] **Qirui Huang,** and Wen-De Zhong, "A Wavelength-routed multicast packet switch with a shared fiber delay lines buffer," in *Proc. OECC 2010*, Sapporo, Japan, pp 410-411. (related to Chapter 4)

[5] **Qirui Huang,** and Wen-De Zhong, "An optical multicast packet switch using multi-wavelength converters and shared fiber delay lines," in *Proc. Photonics Global Conference 2010*, Singapore, 2010, Paper Conf10a530. (related to Chapter 4)

[6] Wen-De Zhong, and **Qirui Huang**, "Wavelength-routed optical multicast packet switches," in *Proc. ICCS 2010*, Singapore, Invited Paper. (related to Chapter 3 and Chapter 4)

References

[1] B. Mukherjee, *Optical communications networks*, McGraw-Hill, New York, 1997.

[2] G. Keiser, *Optical fiber communications*, McGraw-Hill, 3rd ed., 2000.

[3] G. P. Agrawal, "Fiber-optic communications systems.." John Wiley & Sons, Inc., 3rd ed., 2002, Ch. 1, pp. 1.

[4] J. P. Jue, and V. M. Vokkarane, *Optical burst switched networks*, Springer, 2005.

[5] S. S. Dixit, *IP over WDM: building the next generation optical Internet*, John Wiley &Sons, 2003.

[6] J.-P. Laude, *DWDM fundamentals, components, and applications*, USA: Artech House, 2002.

[7] H. G. Weber, S. Ferber, M. Kroh, C. Schmidt-Langhorst, R. Ludwig, V. Marembert, C. Boerner, F. Futami, S. Watanabe, and C. Schubert, "Single channel 1.28 Tbit/s and 2.56 Tbit/s DQPSK transmission," in *31st European Conference on Optical Communication (ECOC' 05)* 2005, vol. 6, pp. 3-4.

[8] L. Leng, S. Stulz, B. Zhu, L. E. Nelson, B. Edvold, L. Gruner-Nielsen, S. Radic, J. Centanni, and A. Gnauck, "1.6-Tb/s (160x10.7Gb/s) transmission over 4000 km of nonzero dispersion fiber at 25-GHz channel spacing," *IEEE Photon. Technol. Lett.,* vol. 15, no. 8, pp. 1153-1155, Aug. 2003.

[9] B. Zhu, X. Liu, S. Chandrasekhar, D. W. Peckham, and R. Lingle, "Ultra-Long-Haul Transmission of 1.2-Tb/s Multicarrier No-Guard-Interval CO-OFDM Superchannel Using Ultra-Large-Area Fiber," *IEEE Photon. Technol. Lett.,* vol. 22, no. 11, pp. 826-828, June, 2010.

[10] T. Chaney, J. A. Fingerhut, M. Flucke, and J. S. Turner, "Design of a gigabit ATM switch," in *INFOCOM '97. Sixteenth Annual Joint Conference of the IEEE Computer and Communications Societies. Proceedings IEEE*, 1997, vol. 1, pp. 2-11.

[11] K. Genda, Y. Doi, K. Endo, T. Kawamura, and S. Sasaki, "A 160-Gb/s ATM switching system using an internal speed-up crossbar switch," in *Global*

Telecommunications Conference, 1994. GLOBECOM '94. Communications: The Global Bridge., IEEE, 1994, vol. 1, pp. 123-133.

[12] N. Yamanaka, R. Kawano, E. Oki, S. Yasukawa, and K. Okazaki, "640-Gb/s high-speed ATM switching system based on 0.25 μm CMOS, MCM-C, and optical WDM interconnection," *IEEE Transactions on Advanced Packaging,* vol. 25, no. 1, pp. 65-72, 2002.

[13] Web page of Juniper T Series Router. [Online]. Available: http://www.juniper.net/us/en/products-services/routing/t-tx-series/.

[14] S. Yao, S. J. B. Yoo, B. Mukherjee, and S. Dixit, "All-optical packet switching for metropolitan area networks: opportunities and challenges," *IEEE Communications Magazine,* vol. 39, no. 3, pp. 142-148, 2001.

[15] T. S. El-Bawab and S. Jong-Dug, "Optical packet switching in core networks: between vision and reality," *IEEE Communications Magazine,* vol. 40, no. 9, pp. 60-65, 2002.

[16] G. I. Papadimitriou, C. Papazoglou, and A. S. Pomportsis, "Optical switching: switch fabrics, techniques, and architectures," *IEEE/OSA J. Lightw. Technol.,* vol. 21, no. 2, pp. 384-405, Feb. 2003.

[17] "IPTV Global Forecast - 2009 to 2013: Semiannual IPTV Global Forecast Report," Multimedia Research Group, Inc. 2009 [Online]. Available: http://www.mrgco.com/iptv/gf1109.html.

[18] G. N. Rouskas, "Optical layer multicast: rationale, building blocks, and challenges," *IEEE Network,* vol. 17, no. 1, pp. 60-65, 2003.

[19] B. Mukherjee, "WDM optical communication networks: progess and challenges," *IEEE J. Select. Areas Commun.,* vol. 18, no. 10, pp. 1810-1824, Oct. 2000.

[20] G. Charlet, E. Corbel, J. Lazaro, A. Klekamp, R. Dischler, P. Tran, W. Idler, H. Mardoyan, A. Konczykowska, F. Jorge, and S. Bigo, "WDM transmission at 6-Tbit/s capacity over transatlantic distance, using 42.7-Gb/s differential phase-shift keying without pulse carver," *IEEE/OSA J. Lightw. Technol.,* vol. 23, no. 1, pp. 104-107, 2005.

[21] G. Charlet, J. Renaudier, H. Mardoyan, P. Tran, O. B. Pardo, F. Verluise, M. Achouche, A. Boutin, F. Blache, J. Y. Dupuy, and S. Bigo, "Transmission of 16.4-bit/s Capacity Over 2550 km Using PDM QPSK Modulation Format and Coherent Receiver," *IEEE/OSA J. Lightw. Technol.,* vol. 27, no. 3, pp. 153-157, 2009.

[22] Web page of Cisco Cisco XR 12000 Series Router. [Online]. Available: http://www.cisco.com/en/US/products/ps6342/index.html.

[23] S. Banerjee and C. Chien, "Design of wavelength-routed optical networks for circuit switched traffic," in *Global Telecommunications Conference, 1996.*

GLOBECOM '96. 'Communications: The Key to Global Prosperity, 1996, vol. 1, pp. 306-310.

[24] C. Qiao and M. Yoo, "Optical burst switching - a new paradigm for an optical Internet," *Journal of High Speed Networks, Special Issue on Optical Networks,* vol. 8, no. 1, pp. 69-84, 1999.

[25] F. Callegati, G. Corazza, and C. Raffaelli, "Design of a WDM optical packet switch for IP traffic," in *Global Telecommunications Conference, 2000. GLOBECOM '00. IEEE*, 2000, vol. 2, pp. 1283-1287.

[26] Y. Shun, S. J. B. Yoo, B. Mukherjee, and S. Dixit, "All-optical packet switching for metropolitan area networks: opportunities and challenges," *IEEE Commun. Mag.,* vol. 39, no. 3, pp. 142-148, 2001.

[27] M. J. O'Mahony, D. Simeonidou, D. K. Hunter, and A. Tzanakaki, "The application of optical packet switching in future communication networks," *IEEE Commun. Mag.,* vol. 39, no. 3, pp. 128-135, Mar. 2001.

[28] R. S. Tucker and W. D. Zhong, "Photonic packet switching: an overview," *IEICE Trans. Commun.,* vol. E82-B, no. 2, pp. 254-264, Feb. 1999.

[29] A. Misawa, Y. Yamada, M. Tsukada, K. Sasayama, K. Habara, T. Matsunaga, and K. i. Yukimatsu, "A prototype broadcast-and-select photonic ATM switch with a WDM output buffer," *IEEE/OSA J. Lightw. Technol.,* vol. 16, no. 12, pp. 2202-2211, 1998.

[30] C. Guillemot, M. Henry, F. Clerot, A. Le Corre, J. Kervaree, A. Dupas, and P. Gravey, "KEOPS optical packet switch demonstrator: architecture and testbed performance," in *Optical Fiber Communication Conference*, 2000, vol. 3, pp. 204-206.

[31] P. Gambini, M. Renaud, C. Guillemot, F. Callegati, I. Andonovic, B. Bostica, D. Chiaroni, G. Corazza, S. L. Danielsen, P. Gravey, P. B. Hansen, M. Henry, C. Janz, A. Kloch, R. Krähenbühl, C. Raffaelli, M. Schilling, A. Talneau, and L. Zucchelli, "Transparent optical packet switching: network architecture and demonstrators in the KEOPS project," *IEEE J. Select. Areas Commun.,* vol. 16, no. 7, pp. 1245-1259, Sept. 1998.

[32] C. Guillemot, M. Renaud, P. Gambini, C. Janz, I. Andonovic, R. Bauknecht, B. Bostica, M. Burzio, F. Callegati, M. Casoni, D. Chiaroni, F. Clerot, S. L. Danielsen, F. Dorgeuille, A. Dupas, A. Franzen, P. B. Hansen, D. K. Hunter, A. Kloch, R. Krahenbuhl, B. Lavigne, A. Le Corre, C. Raffaelli, M. Schilling, J. C. Simon, and L. Zucchelli, "Transparent optical packet switching: the European ACTS KEOPS project approach," *IEEE/OSA J. Lightw. Technol.,* vol. 16, no. 12, pp. 2117-2134, 1998.

[33] M. J. O'Mahony, K. M. Guild, D. K. Hunter, I. Andonovic, I. H. White, and R. V. Penty, "The WASPNET optical packet switching node and its testbed realization," in *Photonics in Switching*, Monterey, California, 2001, p. JWB3.

[34] D. K. Hunter, M. H. M. Nizam, M. C. Chia, I. Andonovic, K. M. Guild, A. Tzanakaki, M. J. O'Mahony, J. D. Bainbridge, M. F. C. Stephens, R. V. Penty, and I. H. White, "WASPNET: a wavelength switched packet network," *IEEE Commun. Mag.,* vol. 37, no. 3, pp. 120-129, Mar. 1999.

[35] L. Dittmann, "Optical packet networks - conclusions from the IST DAVID project," in *Optical Fiber Communication Conference (OFC 2004)* 2004, vol. 1, p. TuQ1.

[36] L. Dittmann, C. Develder, D. Chiaroni, F. Neri, F. Callegati, W. Koerber, A. Stavdas, M. Renaud, A. Rafel, J. Solé-Pareta, W. Cerroni, N. Leligou, L. Dembeck, B. Mortensen, M. Pickavet, N. L. Sauze, M. Mahony, B. Berde, and G. Eilenberger, "The European IST project DAVID: a viable approach toward optical packet switching," *IEEE J. Select. Areas Commun.,* vol. 21, no. 7, pp. 1026-1040, Sept. 2003.

[37] J. Gripp, D. Stiliadis, J. E. Simsarian, P. Bernasconi, J. D. L. Grange, L. Zhang, L. Buhl, and D. T. Neilson, "IRIS optical packet router," *Journal of Optical Networking,* vol. 5, no. 8, pp. 589-597, 2006.

[38] Web page of LASAGNE Project [Online]. Available: http://ist-lasagne.org/.

[39] F. Ramos, E. Kehayas, J. M. Martinez, R. Clavero, J. Marti, L. Stampoulidis, D. Tsiokos, H. Avramopoulos, J. Zhang, P. V. Holm-Nielsen, N. Chi, P. Jeppesen, N. Yan, I. T. Monroy, A. M. J. Koonen, M. T. Hill, Y. Liu, H. J. S. Dorren, R. Van Caenegem, D. Colle, M. Pickavet, and B. Riposati, "IST-LASAGNE: towards all-optical label swapping employing optical logic gates and optical flip-flops," *IEEE/OSA J. Lightw. Technol.,* vol. 23, no. 10, pp. 2993-3011, 2005.

[40] R. Urata, T. Nakahara, H. Takenouchi, T. Segawa, H. Ishikawa, A. Ohki, H. Sugiyama., S. Nishihara, and R. Takahashi, "4x4 optical packet switching of asynchronous burst optical packets with a prototype, 4x4 label processing and switching sub-system," *Optics Express,* vol. 18, no. 15, pp. 15283-15288, 2010.

[41] M. Maier, *Optical switching networks*, Cambridge University Press, 2008.

[42] Web page of Center for Integrated Photonics (CIP) [Online]. Available: http://www.ciphotonics.com/cip_semiconductor.htm.

[43] K. Habara, T. Matsunaga, and K. i. Yukimatsu, "Large-scale WDM star-based photonic ATM switches," *IEEE/OSA J. Lightw. Technol.,* vol. 16, no. 12, pp. 2191-2201, 1998.

[44] F. Masetti, M. Sotom, D. de Bouard, D. Chiaroni, P. Parmentier, F. Callegati, G. Corazza, C. Raffaelli, S. L. Danielsen, and K. E. Stubkjaer, "Design and performance of a broadcast-and-select photonic packet switching architecture," in *22nd European Conference on Optical Communication (ECOC '96)*, 1996, vol. 3, pp. 309-312.

[45] M. J. Karol, "A Shared-Memory Optical Packet (ATM) Switch," in *Proceedings of the 6th IEEE Workshop on Local and Metropolitan Area Networks, 1993.,* 1993, pp. 205-211.

[46] S. L. Danielsen, B. Mikkelsen, C. Joergensen, T. Durhuus, and K. E. Stubkjaer, "WDM packet switch architectures and analysis of the influence of tunable wavelength converters on the performance," *IEEE/OSA J. Lightw. Technol.,* vol. 15, no. 2, pp. 219-227, 1997.

[47] D. K. Hunter, W. D. Cornwell, T. H. Gilfedder, A. Franzen, and I. Andonovic, "SLOB: a switch with large optical buffers for packet switching," *IEEE/OSA J. Lightw. Technol.,* vol. 16, no. 10, pp. 1725-1736, 1998.

[48] M. Renaud, M. Bachmann, and M. Erman, "Semiconductor optical space switches," *IEEE Journal of Selected Topics in Quantum Electronics,* vol. 2, no. 2, pp. 277-288, 1996.

[49] Z. Haas, "The `staggering switch': an electronically controlled optical packet switch," *IEEE/OSA J. Lightw. Technol.,* vol. 11, no. 5, pp. 925-936, 1993.

[50] W. D. Zhong and R. S. Tucker, "Wavelength routing-based photonic packet buffers and their applications in photonic packet switching systems," *IEEE/OSA J. Lightw. Technol.,* vol. 16, no. 10, pp. 1737-1745, Oct. 1998.

[51] W. D. Zhong and R. S. Tucker, "A new wavelength-routed photonic packet buffer combining traveling delay lines with delay-line loops," *IEEE/OSA J. Lightw. Technol.,* vol. 19, no. 8, pp. 1085-1092, Aug. 2001.

[52] Y.-B. Choi, D.-J. Park, and K.-Y. Kim, "A photonic ATM switch based on wavelength routing," in *Proceedings of the IEEE Region 10 Conference TENCON 99.*, 1999, vol. 2, pp. 1411-1414.

[53] F. Masetti, J. Benoit, F. Brillouet, J. M. Gabriagues, A. Jourdan, M. Renaud, D. Bottle, G. Eilenberger, K. Wunstel, M. Schilling, D. Chiaroni, P. Gavignet, J. B. Jacob, G. Bendelli, P. Cinato, P. Gambini, M. Puleo, T. Martinson, P. Vogel, T. Durhuus, C. Joergensen, K. Stubkjaer, R. Baets, P. Van Daele, J. C. Bouley, R. Lefevre, M. Bachmann, W. Hunziker, H. Melchior, A. McGuire, F. Ratovelomanana, and N. Vodjdani, "High speed, high capacity ATM optical switches for future telecommunication transport networks," *IEEE Journal on Selected Areas in Communications,* vol. 14, no. 5, pp. 979-998, 1996.

[54] P. Pavon-Mariño, J. Garcia-Haro, and A. Jajszczyk, "Parallel desynchronized block matching: A feasible scheduling algorithm for the input-buffered wavelength-routed switch," *Computer Networks,* vol. 51, no. 15, pp. 4270-4283, 2007.

[55] P. Pavon-Marino, J. Garcia-Haro, J. Malgosa-Sanahuja, and F. Cerdan, "Maximal matching characterization of optical packet input-buffered wavelength routed switches," in *Workshop on High Performance Switching and Routing, HPSR 2003,* 2003, pp. 55-60.

[56] R. Nejabati, D. Klonidis, D. Simeonidou, and M. O'Mahony, "Demonstration of an agile hybrid IP-optical packet construction mechanism in wavelength routed optical packet switched networks," *IEEE Communications Letters,* vol. 9, no. 6, pp. 552-554, 2005.

[57] J. M. Gabriagues and J. B. Jacob, "Photonic ATM switching matrix based on wavelength routing," in *Proc. Photonic Switching*, 1992, p. 2H2.

[58] S. J. B. Yoo, L. Hyuek Jae, P. Zhong, C. Jing, Z. Yanda, K. Okamoto, and S. Kamei, "Rapidly switching all-optical packet routing system with optical-label swapping incorporating tunable wavelength conversion and a uniform-loss cyclic frequency AWGR," *IEEE Photon. Technol. Lett.,* vol. 14, no. 8, pp. 1211-1213, 2002.

[59] S. Yao, B. Mukherjee, S. J. B. Yoo, and S. Dixit, "A unified study of contention-resolution schemes in optical packet-switched networks," *IEEE/OSA J. Lightw. Technol.,* vol. 21, no. 3, pp. 672-683, 2003.

[60] X. Fei, P. Zhong, Y. Bansal, C. Jing, J. Minyong, K. Okamoto, S. Kamei, V. Akella, and S. J. B. Yoo, "End-to-end contention resolution schemes for an optical packet switching network with enhanced edge routers," *IEEE/OSA J. Lightw. Technol.,* vol. 21, no. 11, pp. 2595-2604, 2003.

[61] S. J. B. Yoo, "Optical packet and burst switching technologies for the future photonic Internet," *IEEE/OSA J. Lightw. Technol.,* vol. 24, no. 12, pp. 4468-4492, Dec. 2006.

[62] A. G. P. Rahbar and O. W. W. Yang, "Contention avoidance and resolution schemes in bufferless all-optical packet-switched networks: a survey," *IEEE Communications Surveys & Tutorials,* vol. 10, no. 4, pp. 94-107, 2008.

[63] S. Debnath, S. Mahapatra, and R. Gangopadhyay, "Analysis of an optical packet switch with partially shared buffer and wavelength conversion," *IET Communications,* vol. 1, no. 4, pp. 810-818, 2007.

[64] L. Xu, H. G. Perros, and G. Rouskas, "Techniques for optical packet switching and optical burst switching," *IEEE Communications Magazine,* vol. 39, no. 1, pp. 136-142, 2001.

[65] D. K. Hunter, M. C. Chia, and I. Andonovic, "Buffering in optical packet switches," *IEEE/OSA J. Lightw. Technol.,* vol. 16, no. 12, pp. 2081-2094, Dec. 1998.

[66] H. J. S. Dorren, M. T. Hill, Y. Liu, N. Calabretta, A. Srivatsa, F. M. Huijskens, H. d. Waardt, and G. D. Khoe, "Optical packet switching and buffering by using all-optical signal processing methods," *IEEE/OSA J. Lightw. Technol.,* vol. 21, no. 1, pp. 2-12, 2003.

[67] M. Cheng, W. Hu, W. Sun, F. Yan, and H. He, "Wavelength converted broadcast-selective buffering contention resolution in synchronous WDM OPS networks," *IEEE/OSA J. Lightw. Technol.,* vol. 28, no. 9, pp. 1356-1362, 2010.

[68] H. Harai and M. Murata, "Optical fiber-delay-line buffer management in output-buffered photonic packet switch to support service differentiation," *IEEE Journal on Selected Areas in Communications,* vol. 24, no. 8, pp. 108-116, 2006.

[69] H. Harai, N. Wada, F. Kubota, and W. Chujo, "Contention resolution using multi-stage fiber delay line buffer in a photonic packet switch," in *IEEE International Conference on Communications, 2002 (ICC 2002)*, vol. 5, pp. 2843-2847.

[70] F. Masetti, P. Gavignet-Morin, D. Chiaroni, and G. Da Loura, "Fiber delay lines optical buffer for ATM photonic switching applications," in *INFOCOM '93 Proceedings. Twelfth Annual Joint Conference of the IEEE Computer and Communications Societies. Networking: Foundation for the Future*, 1993, vol. 3, pp. 935-942.

[71] Y. Liu, M. T. Hill, N. Calabretta, H. de Waardt, G. D. Khoe, and H. J. S. Dorren, "All-optical buffering in all-optical packet switched cross connects," *IEEE Photon. Technol. Lett.,* vol. 14, no. 6, pp. 849-851, 2002.

[72] A. Liu, C. Wu, Y. Gong, and P. Shum, "Dual-loop optical buffer (DLOB) based on a 3×3 collinear fiber coupler," *IEEE Photon. Technol. Lett.,* vol. 16, no. 9, pp. 2129-2131, Sept. 2006.

[73] A. Chowdhury, Y. Yeo, J. Yu, and G. Chang, "DWDM reconfigurable optical delay buffer for optical packet switched networks," *IEEE Photon. Technol. Lett.,* vol. 18, no. 10, pp. 1176-1178, May 2006.

[74] S. Fu, P. Shum, N. Q. Ngo, C. Wu, Y. Li, and C. C. Chan, "An enhanced SOA-based double-loop optical buffer for storage of variable-length packet," *IEEE/OSA J. Lightw. Technol.,* vol. 26, no. 4, pp. 425-431, Feb. 2008.

[75] N. Chi, J. J. V. Olmos, K. Thakulsukanant, Z. Wang, O. Ansell, S. Yu, and D. Huang, "Experimental characteristics of optical crosspoint switch matrix and its applications in optical packet switching," *IEEE/OSA J. Lightw. Technol.,* vol. 24, no. 10, pp. 3646-3653, Oct. 2006.

[76] Y. Liu, M. T. Hill, R. Geldenhuys, N. Calabretta, H. d. Waardt, G. D. Khoe, and H. J. S. Dorren, "Demonstration of a variable optical delay for a recirculating buffer by using all-optical signal processing," *IEEE Photon. Technol. Lett.,* vol. 16, no. 7, pp. 1748-1750, July 2004.

[77] R. Langenhorst, M. Eiselt, W. Pieper, G. Grosskopf, R. Ludwig, L. Kuller, E. Dietrich, and H. G. Weber, "Fiber loop optical buffer," *IEEE/OSA J. Lightw. Technol.,* vol. 14, no. 3, pp. 324-335, 1996.

[78] S. H. G. Chan and H. Kobayashi, "Packet scheduling algorithms and performance of a buffered shufflenet with deflection routing," *IEEE/OSA J. Lightw. Technol.,* vol. 18, no. 4, pp. 490-501, 2000.

[79] S. Lee, K. Sriram, H. Kim, and J. Song, "Contention-Based Limited Deflection Routing Protocol in Optical Burst-Switched Networks," *IEEE Journal on Selected Areas in Communications,* vol. 23, no. 8, pp. 1596-1611, 2005.

[80] S. Yamano, F. Xue, and S. J. B. Yoo, "Load-sensitive deflection routing for contention resolution in optical packet switched networks," in *Proceedings of the 12th International Conference on Computer Communications and Networks (ICCCN 2003)*, 2003, pp. 243-248.

[81] M. Baresi, S. Bregni, A. Pattavina, and G. Vegetti, "Deflection routing effectiveness in full-optical IP packet switching networks," in *IEEE International Conference on Communications (ICC '03)*, 2003, vol. 2, pp. 1360-1364.

[82] S. L. Danielsen, P. B. Hansen, and K. E. Stubkjaer, "Wavelength conversion in optical packet switching," *IEEE/OSA J. Lightw. Technol.,* vol. 16, no. 12, pp. 2095-2108, 1998.

[83] V. Eramo, M. Listanti, and A. Germoni, "Cost Evaluation of Optical Packet Switches Equipped With Limited-Range and Full-Range Converters for Contention Resolution," *IEEE/OSA J. Lightw. Technol.,* vol. 26, no. 4, pp. 390-407, 2008.

[84] P. Zhong, J. Min Yong, Y. Bansal, C. Jing, J. Taylor, V. Akella, S. Kamei, K. Okamoto, and S. J. B. Yoo, "Packet-by-packet wavelength, time, space-domain contention resolution in an optical-label switching router with 2R regeneration," *IEEE Photon. Technol. Lett.,* vol. 15, no. 9, pp. 1312-1314, 2003.

[85] J. J. V. Olmos, N. Chi, G. Zervas, D. Simeonidou, S. Yu, A. Lopez, I. T. Monroy, and A. M. J. Koonen, "Optical node with time-space-and-wavelength domain contention resolution capability," in *32nd European Conference on Optical Communications (ECOC 2006)*, 2006, pp. 1-2.

[86] S. Rangarajan, H. Zhaoyang, L. Rau, and D. J. Blumenthal, "All-optical contention resolution with wavelength conversion for asynchronous variable-length 40 Gb/s optical packets," *IEEE Photon. Technol. Lett.,* vol. 16, no. 2, pp. 689-691, 2004.

[87] J. M. H. Elmirghani and H. T. Mouftah, "All-optical wavelength conversion: technologies and applications in DWDM networks," *IEEE Communications Magazine,* vol. 38, no. 3, pp. 86-92, 2000.

[88] S. J. B. Yoo, "Wavelength conversion technologies for WDM network applications," *IEEE/OSA J. Lightw. Technol.,* vol. 14, no. 6, pp. 955-966, June 1996.

[89] C. Raffaelli and M. Savi, "Cost Comparison of All-Optical Packet Switches with Shared Wavelength Converters," in *9th International Conference on Transparent Optical Networks (ICTON '07)*, 2007, vol. 3, pp. 209-212.

[90] H. J. Chao, C. H. Lam, and E. Oki, "Broadband packet switching technologies: a practical guide to ATM switches and IP routers." John Wiley & Sons, Inc., 2001, Ch. 5, pp. 49.

[91] N. McKeown, "The iSLIP scheduling algorithm for input-queued switches," *IEEE/ACM Transactions on Networking,* vol. 7, no. 2, pp. 188-201, 1999.

[92] N. McKeown, A. Mekkittikul, V. Anantharam, and J. Walrand, "Achieving 100% throughput in an input-queue switch," *IEEE Trans. on Communications,* vol. 48, no. 8, pp. 1260-1266, Aug. 1999.

[93] M. A. Marsan, A. Bianco, P. Giaccone, E. Leonardi, and F. Neri, "Packet scheduling in input-queued cell-based switches," in *Proc. INFOCOM'01*, 2001, vol. 2, pp. 22-26.

[94] D. Chiaroni, "Packet switching matrix: a key element for the backbone and the metro," *IEEE J. Select. Areas Commun.,* vol. 21, no. 7, pp. 1018-1025, Sept. 2003.

[95] X. Li and M. Hamdi, "On scheduling optical packet switches with reconfiguration delay," *IEEE J. Select. Areas Commun.,* vol. 21, no. 7, pp. 1156-1164, July 2003.

[96] K. Kar, D. Stiliadis, T. V. Lakshman, and L. Tassiulas, "Scheduling algorithm for optical packet fabrics," *IEEE J. Select. Areas Commun.,* vol. 21, no. 7, pp. 1143-1155, Sept. 2003.

[97] B. Prabhakar and N. Mckeown, "Designing a multicast switch scheduler," in *Proceedings of the 33rd Annual Allerton Conference on Communication, Control, and Computing*, 1995, pp. 984-993.

[98] B. Prabhakar, N. McKeown, and R. Ahuja, "Multicast scheduling for input-queued switches," *IEEE J. Select. Areas Commun.,* vol. 15, no. 5, pp. 855-866, 1997.

[99] M. Andrews, S. Khanna, and K. Kumaran, "Integrated Scheduling of Unicast and Multicast Traffic in an Input-Queued Switch," in *Proc. IEEE INFOCOM'99*, New York, NY, 1999, pp. 1144-1151.

[100] B. Hu and K. L. Yeung, "Load-balanced optical switch for high-speed router design," *IEEE/OSA J. Lightw. Technol.,* vol. 28, no. 13, pp. 1969-1977, 2010.

[101] L. Zucchelli, M. Burzio, and P. Gambini, "New solutions for optical packet delination and synchronization in optical packet switched networks," in *Proc. ECOC'96*, 1996, vol. 3, pp. 301-304.

[102] D. Chiaroni, B. Lavigne, A. Jourdan, M. Sotom, L. Hamon, C. Chauzat, J. C. Jacquinot, A. Barroso, T. Zami, F. Dorgeuille, C. Janz, J. Y. Emery, E. Grard, and M. Renaud, "Physical and logical validation of a network based on all-optical packet switching systems," *IEEE/OSA J. Lightw. Technol.,* vol. 16, no. 12, pp. 2255-2264, 1998.

[103] T. Sakamoto, A. Okada, M. Hirayama, Y. Sakai, O. Moriwaki, I. Ogawa, R. Sato, K. Noguchi, and M. Matsuoka, "Optical packet synchronizer using wavelength and space switching," *IEEE Photon. Technol. Lett.,* vol. 14, no. 9, pp. 1360-1362, 2002.

[104] J. P. Mack, H. N. Poulsen, and D. J. Blumenthal, "Variable Length Optical Packet Synchronizer," *IEEE Photon. Technol. Lett.,* vol. 20, no. 14, pp. 1252-1254, 2008.

[105] Y. A. Vlasov and S. J. McNab, "Coupling into the slow light mode in slab-type photonic crystal waveguides," *Opt. Lett.,* vol. 31, no. 1, pp. 50-52, Jan. 2006.

[106] Y. Shun, B. Mukherjee, and S. Dixit, "Advances in photonic packet switching: an overview," *IEEE Commun. Mag.,* vol. 38, no. 2, pp. 84-94, 2000.

[107] P. Toliver, I. Glesk, R. J. Runser, K. L. Deng, B. Y. Yu, and P. R. Prucnal, "Routing of 100 Gb/s in a packet-switched optical networking demonstration (POND) node," *IEEE/OSA J. Lightw. Technol.,* vol. 16, no. 12, pp. 2169-2180, Dec. 1998.

[108] M. D. Vaughn, A. Wang, and D. J. Blumenthal, "Simultaneous all-optical wavelength conversion of baseband payload and removal/replacement of subcarrier multiplexed headers," in *Optical Fiber Communications, 1996. OFC '96*, 1996, pp. 128-129.

[109] M. Cerisola, T. K. Fong, R. T. Hofmeister, L. G. Kazovsky, C. L. Lu, P. Poggiolini, and D. I. Sabido, "Subcarrier multiplexing of packet headers in a WDM optical network and a novel ultrafast header clock-recovery technique," in *OFC Tech. Dig. Series. Postconference Edition*, Washington, DC, 1995, vol. 8, pp. 273-274.

[110] L. Chung-Li, D. J. M. I. Sabido, P. Poggiolini, R. T. Hofmeister, and L. G. Kazovsky, "CORD-a WDMA optical network: subcarrier-based signaling and control scheme," *IEEE Photon. Technol. Lett.,* vol. 7, no. 5, pp. 555-557, 1995.

[111] E. Park and A. E. Willner, "Self-routing of wavelength packets using an all-optical wavelength shifter and QPSK subcarrier routing control headers," *IEEE Photon. Technol. Lett.,* vol. 8, no. 7, pp. 938-940, 1996.

[112] L. Hyuek Jae, S. J. B. Yoo, V. K. Tsui, and S. K. H. Fong, "A simple all-optical label detection and swapping technique incorporating a fiber Bragg grating filter," *IEEE Photon. Technol. Lett.,* vol. 13, no. 6, pp. 635-637, 2001.

[113] Y. M. Lin, W. I. Way, and G. K. Chang, "A novel optical label swapping technique using erasable optical single-sideband subcarrier label," *IEEE Photon. Technol. Lett.,* vol. 12, no. 8, pp. 1088-1090, 2000.

[114] H. Tsushima, M. Shabeer, P. Barnsley, and D. Pitcher, "Demonstration of an optical packet add drop with wavelength-coded header," *IEEE Photon. Technol. Lett.,* vol. 7, no. 2, pp. 212-214, Feb. 1995.

[115] A. Okada, "All-optical packet routing in AWG-based wavelength routing networks using an out-of-band optical label," in *Optical Fiber Communication Conference and Exhibit, 2002. OFC 2002*, 2002, pp. 213-215.

[116] G. Cincotti, W. Naoya, and K. Kitayama, "Characterization of a full encoder/decoder in the AWG configuration for code-based photonic routers-part I: modeling and design," *IEEE/OSA J. Lightw. Technol.,* vol. 24, no. 1, pp. 103-112, 2006.

[117] N. Wada and K. I. Kitayama, "Photonic IP routing using optical codes: 10 Gbit/s optical packet transfer experiment," in *Optical Fiber Communication Conference*, 2000, vol. 2, pp. 362-364.

[118] K. I. Kitayama and N. Wada, "Photonic IP routing," *IEEE Photon. Technol. Lett.,* vol. 11, no. 12, pp. 1689-1691, 1999.

[119] W. Naoya, G. Cincotti, S. Yoshima, N. Kataoka, and K. Kitayama, "Characterization of a full encoder/decoder in the AWG configuration for code-based photonic Routers-part II: experiments and applications," *IEEE/OSA J. Lightw. Technol.,* vol. 24, no. 1, pp. 113-121, 2006.

[120] N. Wada, W. Chujo, and K. Kitayama, "1.28 Tbit/s (160 Gbit/s x 8 wavelengths) throughput variable length packet switching using optical code based label switch," in *27th European Conference on Optical Communication (ECOC '01)*, 2001, vol. 6, pp. 62-63.

[121] V. Olmos, J. Zhang, P. V. Holm-Nielsen, I. T. Monroy, V. Polo, A. M. J. Koonen, C. Peucheret, and J. Prat, "Simultaneous optical label erasure and insertion in a single wavelength conversion stage of combined FSK/IM modulated signals," *IEEE Photon. Technol. Lett.,* vol. 16, no. 9, pp. 2144-2146, Sept. 2004.

[122] N. Chi, P. V. Holm-Nielsen, P. Jeppesen, C. Peucheret, J. Zhang, J. J. Vegas Olmos, and I. Tafur Monroy, "Optical label swapping of payloads up to 40 Gb/s using an orthogonally modulated label," in *The 17th Annual Meeting of the IEEE Lasers and Electro-Optics Society (LEOS 2004)*, 2004, vol. 2, pp. 851-852.

[123] N. Chi, J. Zhang, P. V. Holm-Nielsen, L. Xu, I. T. Monroy, C. Peucheret, K. Yvind, L. J. Christiansen, and P. Jeppesen, "Experimental demonstration of cascaded transmission and all-optical label swapping of orthogonal IM/FSK labelled signal," *Electronics Letters,* vol. 39, no. 8, pp. 676-678, 2003.

[124] C. W. Chow and H. K. Tsang, "Orthogonal label switching using polarization-shift-keying payload and amplitude-shift-keying label," *IEEE Photon. Technol. Lett.,* vol. 17, no. 11, pp. 2475-2477, 2005.

[125] X. Lin, N. Chi, L. K. Oxenlowe, J. Mork, Y. Siyuan, and P. Jeppesen, "A new orthogonal labeling scheme based on a 40-Gb/s DPSK payload and a 2.5-Gb/s PolSK label," *IEEE Photon. Technol. Lett.,* vol. 17, no. 12, pp. 2772-2774, 2005.

[126] X. Lei, W. Ting, O. Matsuda, M. Cvijetic, I. Glesk, and P. R. Prucnal, "Wavelength-shift-keying (WSK) encoded pulses for optical labeling applications," *IEEE Photon. Technol. Lett.,* vol. 17, no. 12, pp. 2775-2777, 2005.

[127] H. Wai, C. Chun-Kit, and C. Lian-Kuan, "A novel optical packet labeling scheme using interleaved low-speed DPSK labels," *IEEE Photon. Technol. Lett.,* vol. 16, no. 2, pp. 698-700, 2004.

[128] R. Malli, X. Zhang, and C. Qiao, "Benefit of multicasting in all-optical networks," in *Proc. SPIE*, 1998, vol. 3531, pp. 209-220.

[129] D. Thaker and G. N. Rouskas, "Multi-destination communication in broadcast WDM networks: a survey," *Optical Networks,* vol. 3, no. 1, pp. 34-44, 2002.

[130] W.-D. Zhong and Q. Huang, "Wavelength-routed optical multicast packet switches," in *ICCS 2010*, Singapore, 2010, p. Invited Paper.

[131] X. Zhang, J. Y. Wei, and C. Qiao, "Constrained multicast routing in WDM networks with sparse light splitting," *IEEE/OSA J. Lightw. Technol.,* vol. 18, no. 12, pp. 1917-1927, 2000.

[132] Y.-K. Yeo, J. Yu, and G.-K. Chang, "A broadcast and multicast-enabled switch architecture utilizing a gateless channel selection scheme," in *Optical Fiber Communication Conference/National Fiber Optic Engineers Conference (OFC/NFOEC 2006)*, 2006, p. OTuG7.

[133] W. S. Hu and Q. J. Zeng, "Multicasting optical cross connects employing splitter-and-delivery switch," *IEEE Photon. Technol. Lett.,* vol. 10, no. 7, pp. 970-972, July 1998.

[134] Q. Huang and W.-D. Zhong, "Multiwavelength Multicast Packet Switch: Performance Analysis and Evaluation," *IEEE/OSA J. Opt. Commun. Netw.,* vol. 2, no. 9, pp. 678-688, 2010.

[135] C. P. Lai and K. Bergman, "Network architecture and test-bed demonstration of wavelength-striped packet multicast," in *Optical Fiber communication/National Fiber Optic Engineers Conference (OFC/NFOEC 2010)*, 2010, p. OW14.

[136] C. P. Lai and K. Bergman, "Demonstration of programmable broadband packet multicasting in an optical switching fabric test-bed," in *Optical Fiber communication/National Fiber Optic Engineers Conference (OFC/NFOEC 2009)*, 2009, p. OTuA5.

[137] R. Varrazza, T. Bricheno, and Y. Siyuan, "A fully packaged 4 x 4 integrated optical switch matrix," *IEEE Journal of Selected Topics in Quantum Electronics,* vol. 11, no. 6, pp. 1248-1254, 2005.

[138] S.-C. Lee, R. Varrazza, O. Ansell, C. Born, and S. Yu, "Optical packet multicast operation using active vertical coupler (AVC) based 4 x 4 optical

crosspoint switch matrix," in *17th Annual Meeting of the IEEE Lasers and Electro-Optics Society (LEOS 2004)*, 2004, vol. 2, pp. 915-916.

[139] S.-C. Lee, R. Varrazza, O. Ansell, and S. Yu, "Highly flexible 4 x 4 optical crosspoint packet switch matrix for optical multicast operations," *IEEE Photon. Technol. Lett.,* vol. 17, no. 4, pp. 911-913, 2005.

[140] S. Yu, S.-C. Lee, O. Ansell, and R. Varrazza, "Lossless optical packet multicast using active vertical coupler based optical crosspoint switch matrix," *IEEE/OSA J. Lightw. Technol.,* vol. 23, no. 10, pp. 2984-2992, 2005.

[141] K. Lau, S. H. Wang, X. Lixin, L. F. K. Lui, P. K. A. Wai, C. Lu, and H. Y. Tam, "All-Optical Multicast Switch based on Raman-Assisted Four-Wave Mixing in Dispersion-shifted Fiber," in *Conference on Lasers and Electro-Optics - Pacific Rim (CLEO/Pacific Rim 2007)*, 2007, pp. 1-2.

[142] B. Wu, S. Fu, J. Wu, P. Shum, N. Q. Ngo, K. Xu, X. Hong, and J. Lin, "40 Gb/s Multifunction Optical Format Conversion Module With Wavelength Multicast Capability Using Nondegenerate Four-Wave Mixing in a Semiconductor Optical Amplifier," *IEEE/OSA J. Lightw. Technol.,* vol. 27, no. 20, pp. 4446-4454, 2009.

[143] M. Presi, G. Contestabile, and E. Ciaramella, "6x10 Gbit/s WDM multicast by means of FWM in DS fibers," in *Conference on Lasers and Electro-Optics (CLEO 2004)*, 2004, vol. 1, p. CTuV3.

[144] N. Yan, T. A, T. Silveira, I. T. Monroy, P. Monteiro, G. T. Beleffi, and A. M. J. Koonen, "Optical Multicasting Performance Evaluation using Multi-Wavelength Conversion by Four-Wave Mixing in DSF at 10/20/40 Gb/s," in *Proc. IEEE Int. Conf. on Photonics in Switching (PS'06)*, Herakleion, Crete, Greece, 16-18 Oct. 2006, pp. 1-3.

[145] G. Contestabile, M. Presi, and E. Ciaramella, "Multiple wavelength conversion for WDM multicasting by FWM in an SOA," *IEEE Photon. Technol. Lett.,* vol. 16, no. 7, pp. 1775-1777, July 2004.

[146] C. Gosset and D. Guang-Hua, "Multi-wavelength conversion and resynchronization of wavelength division multiplexed signals by use of four-wave mixing in a semiconductor optical amplifier," in *Optical Fiber Communication Conference and Exhibit (OFC 2002)*, 2002, pp. 706-707.

[147] A. L. J. Teixeira, R. Nogueira, M. J. N. Lima, P. S. B. Andre, J. L. Pinto, and J. R. F. da Rocha, "Multi-wavelength conversion based on a semiconductor optical amplifier self pumped converter," in *10th International Conference on Telecommunications (ICT 2003)*, 2003, vol. 1, pp. 661-664.

[148] C. Politi, D. Klonidis, and M. J. O'Mahony, "Waveband converters based on four-wave mixing in SOAs," *IEEE/OSA J. Lightw. Technol.,* vol. 24, no. 3, pp. 1203-1217, 2006.

[149] C.-S. Brès, N. Alic, E. Myslivets, and S. Radic, "Scalable multicasting in one-pump parametric amplifier," *IEEE/OSA J. Lightw. Technol.,* vol. 27, no. 3, pp. 356-363, 2009.

[150] C.-S. Brès, A. O. J. Wiberg, B. P.-P. Kuo, N. Alic, and S. Radic, "Wavelength multicasting of 320-Gb/s channel in self-seeded parametric amplifier," *IEEE Photon. Technol. Lett.,* vol. 21, no. 14, pp. 1002-1005, 2009.

[151] X. Zhang, D. Huang, J. Sun, and D. Liu, "Single to 16-channel wavelength conversion at 10 Gb/s based on cross-gain modulation of ASE spectrum in SOA," *J. Optical and Quantum Electronics,* vol. 36, no. 7, pp. 627-634, 2004.

[152] D. Liu, H. Ng Jun, and C. Lu, "Wavelength conversion based on cross-gain modulation of ASE spectrum of SOA," *IEEE Photon. Technol. Lett.,* vol. 12, no. 9, pp. 1222-1224, 2000.

[153] K. K. Y. Wong, L. Guo-Wei, L. Kwan-Chi, P. K. A. Wai, and C. Lian-Kuan, "All-optical wavelength conversion and multicasting by cross-gain modulation in a single-stage fiber optical parametric amplifier," in *Optical Fiber Communication and the National Fiber Optic Engineers Conference, (OFC/NFOEC 2007)*, 2007, pp. 1-3.

[154] B. H. L. Lee, R. Mohamad, and K. Dimyati, "Performance of All-Optical Multicasting Via Dual-Stage XGM in SOA for Grid Networking," *IEEE Photon. Technol. Lett.,* vol. 18, no. 21, pp. 2215-2217, 2006.

[155] G. Contestabile, N. Calabretta, R. Proietti, and E. Ciaramella, "Simultaneous multi-wavelength conversion by double stage XGM in SOAs," in *18th Annual Meeting of the IEEE Lasers and Electro-Optics Society (LEOS 2005)*, 2005, pp. 155-156.

[156] G. Contestabile, N. Calabretta, R. Proietti, and E. Ciaramella, "Double-stage cross-gain modulation in SOAs: an effective technique for WDM multicasting," *IEEE Photon. Technol. Lett.,* vol. 18, no. 1, pp. 181-183, Jan. 2006.

[157] K. K. Chow and C. Shu, "All-optical wavelength conversion with multicasting at 6×10 Gbit/s using electroabsorption modulator," *Electron. Lett.,* vol. 39, no. 19, pp. 1395-1397, Sept. 2003.

[158] K. K. Chow and C. Shu, "All-optical signal regenration with wavelength multicasting at 6x10 Gb/s using a single electroabsorption modulator," *Optics Express,* vol. 12, no. 13, pp. 3050-3054, 2004.

[159] L. Xu, N. Chi, K. Yvind, L. J. Christiansen, L. K. Oxenløwe, J. Mørk, P. Jeppesen, and J. Hanberg, "8×40 Gb/s RZ all-optical broadcasting utilizing an electroabsorption modulator," in *Proc. OFC 2004*, Los Angeles, CA, 2004, p. MF71.

[160] L. Xu, N. Chi, K. Yvind, L. J. Christiansen, L. K. Oxenløwe, J. Mørk, P. Jeppesen, and J. Hanberg, "7×40 Gb/s base-rate RZ all-optical broadcasting

utilizing an electroabsorption modulator," *Optics Express,* vol. 12, no. 3, pp. 416-420, 2004.

[161] S. Fu, W.-D. Zhong, S. P., C. Wu, and Z. J. Q., "Nonlinear Polarization Rotation in Semiconductor Optical Amplifiers With Linear Polarization Maintenance," *IEEE Photon. Technol. Lett.,* vol. 19, no. 23, pp. 1931-1933, 2007.

[162] F. Songnian, Z. Wen-De, S. Ping, W. Yang Jing, and T. Ming, "Simultaneous Multichannel Photonic Up-Conversion Based on Nonlinear Polarization Rotation of an SOA for Radio-Over-Fiber Systems," *IEEE Photon. Technol. Lett.,* vol. 21, no. 9, pp. 563-565, 2009.

[163] F. Songnian, W. Minxue, Z. Wen-De, P. Shum, W. Yang Jing, W. Jian, and L. Jintong, "SOA Nonlinear Polarization Rotation With Linear Polarization Maintenance: Characterization and Applications," *IEEE Journal of Selected Topics in Quantum Electronics,* vol. 14, no. 3, pp. 816-825, 2008.

[164] J. Huan, W. He, H. Liuyan, G. Yili, and Z. Hanyi, "All-Optical NRZ-OOK to BPSK Format Conversion in an SOA-Based Nonlinear Polarization Switch," *IEEE Photon. Technol. Lett.,* vol. 19, no. 24, pp. 1985-1987, 2007.

[165] G. Contestabile, N. Calabretta, M. Presi, and E. Ciaramella, "Single and multicast wavelength conversion at 40 Gb/s by means of fast nonlinear polarization switching in an SOA," *IEEE Photon. Technol. Lett.,* vol. 17, no. 12, pp. 2652-2654, Dec. 2005.

[166] M. Weiming, P. A. Andrekson, and J. Toulouse, "All-optical wavelength conversion based on sinusoidal cross-phase modulation in optical fibers," *IEEE Photon. Technol. Lett.,* vol. 17, no. 2, pp. 420-422, 2005.

[167] L. Rau, B. E. Olsson, and D. J. Blumenthal, "Wavelength multicasting using an ultra high-speed all-optical wavelength converter," in *Optical Fiber Communication Conference and Exhibit (OFC 2001)*, 2001, vol. 3, p. WDD52.

[168] B. E. Olsson, P. Ohlen, L. Rau, and D. J. Blumenthal, "A simple and robust 40-Gb/s wavelength converter using fiber cross-phase modulation and optical filtering," *IEEE Photon. Technol. Lett.,* vol. 12, no. 7, pp. 846-848, 2000.

[169] J. L. Pleumeekers, J. Leuthold, M. Kauer, P. Bernasconi, C. A. Burrus, M. Cappuzzo, E. Chen, L. Gomez, and E. Laskowski, "All-optical wavelength conversion and broadcasting to eight separate channels by a single semiconductor optical amplifier delay interferometer," in *Optical Fiber Communication Conference and Exhibit (OFC 2002)*, 2002, pp. 596-597.

[170] H. S. Chung, R. Inohara, K. Nishimura, and M. Usami, "All-optical multi-wavelength conversion of 10 Gbit/s NRZ/RZ signals based on SOA-MZI for WDM multicasting," *Electron. Lett.,* vol. 41, no. 7, pp. 432-433, Mar. 2005.

[171] N. Yan, T. Silveira, A. Teixeira, A. Ferreira, E. Tangdiongga, P. Monteiro, and A. M. J. Koonen, "40 Gb/s all-optical multi-wavelength conversion via a single

SOA-MZI for WDM wavelength multicast," in *Proc. OECC 2007*, Yokohama, Japan, July 2007, pp. 530-531.

[172] N. Yan, E. Tangdiongga, H.-D. Jung, I. T. Monroy, H. d. Waardt, and A. M. J. Koonen, "Regenerative all-optical wavelength multicast for next generation WDM network and system applications," *Photon. Network Comm.,* vol. 15, no. 1, pp. 1-6, Sept. 2007.

[173] N. Yan, H. Jung, I. T. Monroy, H. D. Waardt, and T. Koonen, "All-optical multi-wavelength conversion with negative power penalty by a commercial SOA-MZI for WDM wavelength multicast," in *Proc. OFC 2007*, Anaheim, CA, 2007, Paper. JWA36.

[174] N. Yan, T. Silveira, A. Teixeira, A. Ferreira, E. Tangdiongga, P. Monteiro, and A. M. J. Koonen, "40 Gbit/s wavelength multicast via SOA-MZI and applications," *Electron. Lett.,* vol. 43, no. 23, pp. 1300-1301, Nov. 2007.

[175] D. Reading-Picopoulos, F. Wang, Y. J. Chai, R. V. Penty, and I. H. White, "10Gb/s and 40Gb/s WDM multi-casting using a hybrid integrated Mach-Zehnder interferometer," in *Proc. OFC 2006*, Anaheim, CA, 2006, p. OFP2.

[176] R. Ramamurthy and B. Mukherjee, "Fixed-alternate routing and wavelength conversion in wavelength-routed optical networks," *IEEE/ACM Transactions on Networking,* vol. 10, no. 3, pp. 351-367, 2002.

[177] G. Shen, S. K. Bose, T. H. Cheng, C. Lu, and T. Y. Chai, "Operation of WDM networks with different wavelength conversion capabilities," *IEEE Communications Letters,* vol. 4, no. 7, pp. 239-241, 2000.

[178] A. I. Al-Fuqaha, G. M. Chaudhry, M. Guizani, and G. B. Brahim, "Routing in all-optical DWDM networks with sparse wavelength conversion capabilities," in *Global Telecommunications Conference, 2003. GLOBECOM '03. IEEE*, 2003, vol. 5, pp. 2569-2574.

[179] J. Dong, X. Zhang, J. Xu, D. Huang, S. Fu, and P. Shum, "40 Gb/s all-optical NRZ to RZ format conversion using single SOA assisted by optical bandpass filter," *Optics Express,* vol. 15, no. 6, pp. 2907-2914, 2007.

[180] Y. Liu, E. Tangdiongga, Z. Li, S. Zhang, H. de Waardt, G. D. Khoe, and H. J. S. Dorren, "80 Gbit/s wavelength conversion using semiconductor optical amplifier and optical bandpass filter," *Electronics Letters,* vol. 41, no. 8, pp. 487-489, 2005.

[181] B. Mikkelsen, M. Vaa, H. N. Poulsen, S. L. Danielsen, C. Joergensen, A. Kloch, P. B. Hansen, K. E. Stubkjaer, K. Wunstel, K. Daub, E. Lach, G. Laube, W. Idler, M. Schilling, and S. Bouchoule, "40 Gbit/s all-optical wavelength converter and RZ-to-NRZ format adapter realised by monolithic integrated active Michelson interferometer," *Electronics Letters,* vol. 33, no. 2, pp. 133-134, 1997.

[182] L. Christen, I. Fazal, O. F. Yilmaz, X. Wu, S. Nuccio, A. E. Willner, C. Langrock, and M. M. Fejer, "Tunable 105-ns Optical Delay for 80-Gbit/s RZ-DQPSK, 40-Gbit/s RZ-DPSK, and 40-Gbit/s RZ-OOK Signals using Wavelength Conversion and Chromatic Dispersion," in *Optical Fiber communication/National Fiber Optic Engineers Conference (OFC/NFOEC 2008)*, 2008, pp. 1-3.

[183] Y. Kuo, H. Rong, V. Sih, S. Xu, M. Paniccia, and O. Cohen, "Demonstration of wavelength conversion at 40 Gb/s data rate in silicon waveguides," *Optics Express,* vol. 14, no. 24, pp. 11721-11726, 2006.

[184] Y. Liu, E. Tangdiongga, Z. Li, H. d. Waardt, A. M. J. Koonen, G. D. Khoe, X. Shu, I. Bennion, and H. J. S. Dorren, "Error-free 320-Gb/s all-optical wavelength conversion using a single semiconductor optical amplifier," *IEEE/OSA J. Lightw. Technol.,* vol. 25, no. 1, pp. 103-108, 2007.

[185] M. Galili, B. Huettl, C. Schmidt-Langhorst, A. Gual i Coca, R. Ludwig, and C. Schubert, "320 Gbit/s DQPSK All-Optical Wavelength Conversion using Four Wave Mixing," in *Optical Fiber Communication and the National Fiber Optic Engineers Conference (OFC/NFOEC 2007)*, 2007, pp. 1-3.

[186] Y. Liu, E. Tangdiongga, Z. Li, H. d. Waardt, A. M. J. Koonen, G. D. Khoe, and H. J. S. Dorren, "Error-free 320 Gb/s SOA-based wavelength conversion using optical filtering," in *Proc. OFC 2006*, Anaheim, CA, 2006, p. PDP28.

[187] A. Bogoni, W. Xiaoxia, I. Fazal, and A. E. Willner, "320 Gb/s nonlinear operations based on a PPLN waveguide for optical multiplexing and wavelength conversion," in *Conference on Optical Fiber Communication - incudes post deadline papers (OFC 2009)*, 2009, pp. 1-3.

[188] M. C. Chia, D. K. Hunter, I. Andonovic, P. Ball, I. Wright, S. P. Ferguson, K. M. Guild, and M. J. O'Mahony, "Packet loss and delay performance of feedback and feed-forward arrayed-waveguide gratings-based optical packet switches with WDM inputs-outputs," *IEEE/OSA J. Lightw. Technol.,* vol. 19, no. 9, pp. 1241-1254, 2001.

[189] N. Yan, J. del Val Puente, T. G. Silveira, A. Teixeira, A. Ferreira, E. Tangdiongga, P. Monteiro, and A. Koonen, "Simulation and Experimental Characterization of SOA-MZI-Based Multiwavelength Conversion," *IEEE/OSA J. Lightw. Technol.,* vol. 27, no. 2, pp. 117-127, 2009.

[190] P. Zhong, Y. Haijun, Y. Jinqiang, H. Junqiang, Z. Zuqing, C. Jing, K. Okamoto, S. Yamano, V. Akella, and S. J. B. Yoo, "Advanced optical-label routing system supporting multicast, optical TTL, and multimedia applications," *IEEE/OSA J. Lightw. Technol.,* vol. 23, no. 10, pp. 3270-3281, 2005.

[191] Q. Huang and W.-D. Zhong, "Multicast-Enabled Optical Packet Switch Architecture Utilizing Multicasting Modules," in *Optical Fiber communication/National Fiber Optic Engineers Conference (OFC/NFOEC 2008)*, 2008, pp. 1-3.

[192] Q. Huang and W.-D. Zhong, "Traffic performance evaluation of an optical packet switch with multicast operation," *IEEE Communications Letters,* vol. 12, no. 12, pp. 894-896, 2008.

[193] Q. Huang and W.-D. Zhong, "An Optical Wavelength-Routed Multicast Packet Switch Based on Multitimeslot Multiwavelength Conversion," *IEEE Photon. Technol. Lett.,* vol. 20, no. 18, pp. 1518-1520, 2008.

[194] Q. Huang and W.-D. Zhong, "Wavelength-Routed Optical Multicast Packet Switch With Improved Performance," *IEEE/OSA J. Lightw. Technol.,* vol. 27, no. 24, pp. 5657-5664, 2009.

[195] K. K. Y. Wong, G. W. Lu, K. C. Lau, P. K. A. Wai, and L. K. Chen, "All-optical wavelength conversion and multicasting by cross-gain modulation in a single-stage fiber optical parametric amplifier," in *Proc. OFC 2007*, Anaheim, CA, 2007, Paper. OTuI4.

[196] T. G. Silveira, A. Teixeira, G. T. Beleffi, D. Forin, P. Monteiro, H. Furukawa, and N. Wada, "All-Optical Conversion From RZ to NRZ Using Gain-Clamped SOA," *IEEE Photon. Technol. Lett.,* vol. 19, no. 6, pp. 357-359, 2007.

[197] D. T. Schaafsma, E. Miles, and E. M. Bradley, "Comparison of conventional and gain-clamped semiconductor optical amplifiers for wavelength-division-multiplexed transmission systems," *IEEE/OSA J. Lightw. Technol.,* vol. 18, no. 7, pp. 922-925, July 2000.

[198] Web page of Optiwave System Inc. [Online]. Available: http://www.optiwave.com/.

[199] M. G. Hluchyj and M. J. Karol, "Queueing in high-performance packet switching," *IEEE Journal on Selected Areas in Communications,* vol. 6, no. 9, pp. 1587-1597, 1988.

[200] A. Y. M. Lin and J. A. Silvester, "On the performance of an ATM switch with multichannel transmission groups," *IEEE Transactions on Communications,* vol. 41, no. 5, pp. 760-770, 1993.

[201] W. De Zhong, Y. Onozato, and J. Kaniyil, "A copy network with shared buffers for large-scale multicast ATM switching," *IEEE/ACM Transactions on Networking,* vol. 1, no. 2, pp. 157-165, 1993.

[202] T. T. Lee, "Nonblocking copy networks for multicast packet switching," *IEEE Journal on Selected Areas in Communications,* vol. 6, no. 9, pp. 1455-1467, 1988.

[203] X. Liu and H. T. Mouftah, "Design of a high performance nonblocking copy network for multicast ATM switching,"*, IEE Proceedings Communications,* vol. 141, no. 5, pp. 317-324, 1994.

[204] Web page of USC/ISI, Los Angeles, CA. The NS simulator and documentation [Online]. Available: http://www.isi.edu/nsnam/ns/.

[205] Q. Huang and W.-D. Zhong, "An optical multicast packet switch using multi-wavelength converters and shared fiber delay lines," in *IEEE Photonics Global Conference 2010*, Singapore, 2010, p. Conf10a530.

[206] Q. Huang and W.-D. Zhong, "A Wavelength-routed multicast packet switch with a shared fiber delay lines buffer," in *Proc. OECC'2010*, 2010, pp. 410-411.

[207] Q. Huang and W.-D. Zhong, "A wavelength-Routed multicast packet switch with a shared-FDL buffer," *IEEE/OSA J. Lightw. Technol.,* vol. 28, no. 19, pp. 2822-2829, 2010.

[208] Q. Huang, W.-D. Zhong, and W. Chen, "Performance evaluation of a WDM optical packet switch with multicast capability," in *Processing of 7th International Conference on Information, Communications and Signal (ICICS 2009)*, 2009, pp. 1-4.

[209] V. Eramo and M. Listanti, "Packet loss in a bufferless optical WDM switch employing shared tunable wavelength converters," *IEEE/OSA J. Lightw. Technol.,* vol. 18, no. 12, pp. 1818-1833, 2000.

[210] J. Yamawaku, H. Takara, T. Ohara, K. Sato, A. Takada, T. Morioka, O. Tadanaga, H. Miyazawa, and M. Asobe, "Simultaneous 25 GHz-spaced DWDM wavelength conversion of 1.03 Tbit/s (103 x 10 Gbit/s) signals in PPLN waveguide," *Electronics Letters,* vol. 39, no. 15, pp. 1144-1145, 2003.

[211] J. Yamawaku, H. Takara, T. Ohara, A. Takada, T. Morioka, O. Tadanaga, H. Miyazawa, and M. Asobe, "Low-crosstalk 103 channel x 10 Gb/s (1.03 Tb/s) wavelength conversion with a quasi-phase-matched LiNbO3 waveguide," *IEEE Journal of Selected Topics in Quantum Electronics,* vol. 12, no. 4, pp. 521-528, 2006.

[212] T. Segawa, S. Matsuo, T. Ishii, Y. Ohiso, Y. Shibata, and H. Suzuki, "High-speed wavelength-tunable optical filter using cascaded Mach-Zehnder interferometers with apodized sampled gratings," *IEEE Journal of Quantum Electronics,* vol. 44, no. 10, pp. 922-930, 2008.

[213] S. L. Danielsen, C. Joergensen, B. Mikkelsen, and K. E. Stubkjaer, "Analysis of a WDM packet switch with improved performance under bursty traffic conditions due to tuneable wavelength converters," *IEEE/OSA J. Lightw. Technol.,* vol. 16, no. 5, pp. 729-735, 1998.

[214] R. Gaudino, G. A. Gavilanes Castillo, F. Neri, and J. M. Finochietto, "Simple Optical Fabrics for Scalable Terabit Packet Switches," in *IEEE International Conference on Communications (ICC '08), 2008*, pp. 5331-5337.